CHEMOKINE RECEPTORS AS THERAPEUTIC

TARGETS IN LIVER DISEASE

by

Richard Parker

A thesis submitted to the University of Birmingham for the degree of DOCTOR OF

PHILOSOPHY

Centre for Liver Research

School of Immunity and Infection

College of Medical and Dental Sciences

University of Birmingham

July 2015

Chemokine Receptors as Therapeutic Targets in Liver Disease

There is an urgent need for new insights into the pathology of liver disease to underpin new therapeutic approaches. Chemokines and their receptors are central to the development of liver inflammation. I investigated liver disease using *ex-vivo* human tissue to analyse gene and protein expression in liver and the nature of inflammation. Animal models of liver disease were used to investigate the effects of manipulating the chemokine system.

In Non-Alcoholic Fatty Liver Disease (NAFLD) expression of CCL2 is increased. A subset of monocytes expressed CD11c and CD206, and maintained CCR2 expression in NAFLD. The frequency of this subset was associated with insulin resistance. In animal models of NAFLD, antagonism of CCR2 improved liver disease. In mouse models of acute liver failure (ALF), expression of CCL25 was an early response after injury, a phenomenon also seen in human ALF. Influx of CCR9$^+$ monocytes was a corresponding early event in murine liver. Prophylactic administration of a CCR9 antagonist reduced liver injury and macrophage infiltration. CXCR6 has contrasting effects in murine liver injury: damaging in acute injury but protective in chronic injury. In human liver CXCR6 promotes infiltration Natural Killer cells, particularly in primary biliary cirrhosis, but may also promote regeneration of hepatocytes.

Acknowledgements

I would not have been able to undertake this work without the patient help and advice of many individuals. The patience and tolerance of Dr Chris Weston and Professor David Adams has been invaluable. Help, suggestions and coffee from my fellow fellows in the liver labs has been gratefully received. The support of my wife Ellen and my son George has been unwavering.

Chemokine Receptors as Therapeutic Targets in Liver Disease

List of contents

List of figures

List of tables

List of abbreviations

7 AAD	7-aminoactinomycin
ACLF	Acute on chronic liver failure
ALD	Alcoholic Liver Disease
ALF	Acute liver failure
ALT	Alanine transaminase
ANOVA	Analysis of variance
AST	Aspartate aminotransferase
BSA	Bovine serum albumin
CCL2	CC chemokine ligand 2
CCL25	CC chemokine ligand 25
CCl_4	Carbon tetrachloride
CCR2	CC chemokine receptor 2
CCR9	CC chemokine receptor 9
CLD	Chronic liver disease
CXCL16	CXC chemokine ligand 16
CXCR6	CXC chemokine receptor 6
DMEM	Dulbecco's modified eagle medium
DMSO	Dimethyl sulfoxide
DNA	Deoxyribonucleic acid
EDTA	Ethylenediaminetetraacetic acid
ELISA	Enzyme linked immunosorbant assay
FC	Flow cytometry

g	Gram
HCC	Hepatocellular carcinoma
HFD	High fat diet
IFN-γ	Interferon gamma
IQR	Interquartile range
kg	Kilogram
L	Litre
LEAN	Liraglutide Efficacy and Actions in NASH (study)
MCD	Methionine and choline deficient (diet)
mg	Milligram
mL	Millilitre
NAFLD	Non-alcoholic fatty liver disease
NAS	NAFLD activity score
NASH	Non-alcoholic steatohepatitis
NK	Natural killer
NKT	Natural killer T
nL	Nanolitre
PBC	Primary Biliary Cirrhosis
PBS	Phosphate buffered saline
pg	picogram
PSC	Primary Sclerosing Cholangitis
qRT-PCR	Quantitative real time Polymerase chain reaction
RNA	Ribonucleic acid
RPMI	Roswell Park Memorial Institute medium

SEM	Standard error of mean
TNFα	Tumour necrosis factor alpha
Treg	T regulatory
UK	United Kingdom
USA	United States of America
μg	Microgram
μL	Microlitre

CHAPTER 1: Chemokine Receptors as Therapeutic Targets in Liver Disease

Introduction

The liver is the largest organ in the body with diverse roles in the metabolism of proteins, carbohydrate and lipids (Sherlock's Diseases of the Liver and Biliary System 12th Ed. Dooley *et al.*, 2011). It is the site of metabolism of many drugs and toxins. The anatomical position of the liver, receiving blood draining from the gut via the portal vein (Bismuth, 2013), requires a condition of immune tolerance to prevent catastrophic reaction to harmless proteins derived from the diet (Tiegs and Lohse, 2010). In contrast, many liver diseases are characterised by infiltration of the liver by immune cells leading to chronic inflammation (Colombat *et al.*, 2002, Boisvert *et al.*, 2003, Gadd *et al.*, 2014), which disrupts the normal function of the liver. Overwhelming acute inflammation of the liver, or chronic inflammation and increasing hepatic fibrosis, can cause liver failure. The chemokine system plays a critical role in the trafficking of immune cells from blood into the liver is activated in disease to promote inflammation (Oo and Adams, 2010). This system is an attractive therapeutic target in in inflammatory liver diseases where, with the exception of viral hepatitis, there are few effective treatments.

The Liver

The liver lies in the upper right quadrant of the abdomen, sheltered by the lower ribcage. In adults it weighs 1000-1500g. It is formed of two large left and right lobes and a smaller caudate lobe (Bismuth, 2013). The lobes are subdivided into segments, each supplied by a single artery and single branch of the portal vein. The liver is unique in that it has a dual blood supply: the hepatic artery carries 25-30% of inflowing blood, a much larger proportion is carried though the portal vein which transports substances from the gut to the liver.

The functional unit of the liver is the lobule. Here blood drains from portal venules into hepatic sinusoids (**figure 1.1**), a specialised environment distinguished by a layer of fenestrated endothelium interspersed with Kupffer cells (KC, liver-resident macrophages) and overlying pericytes (hepatic stellate cells, HSC) but without a basement membrane. Plates of hepatocytes lie beneath the sinusoids and are in contact with particulate matter in blood via microvilli extended through endothelial fenestrations. This is an area of low shear stress, where hepatocytes, KC and hepatic sinusoidal endothelial cells (HSEC) can all take up substances from blood. Hepatic sinusoids drain to a central vein and then to right or left hepatic veins, which unite to form the hepatic vein. This drains into the inferior vena cava close to the right atrium. Blood from central vein, derived from the portal vein, drains into hepatic sinusoids and eventually to small branches of the hepatic veins at the portal triads.
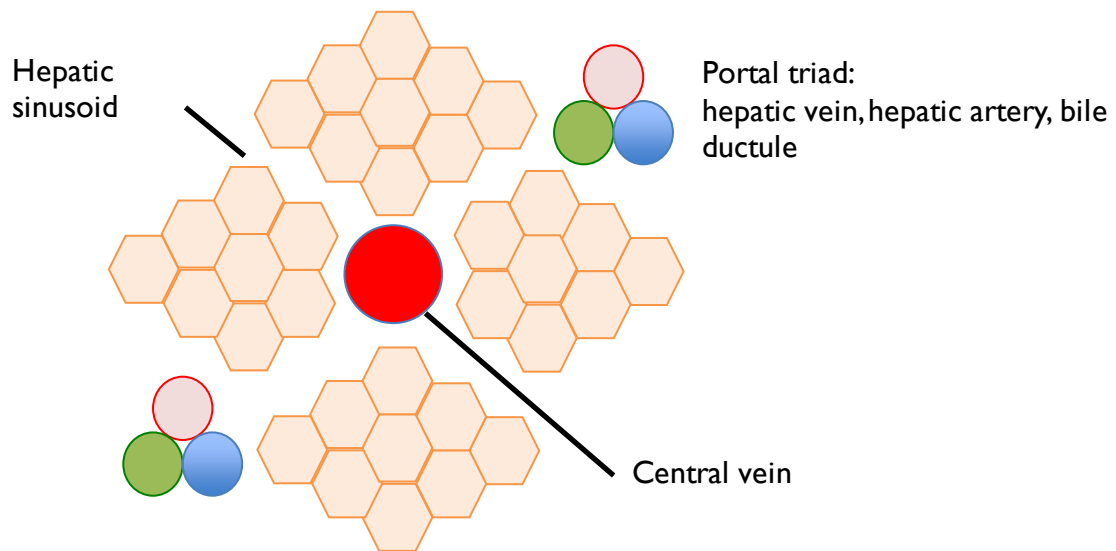
Figure 1.1: Schematic of hepatic lobule
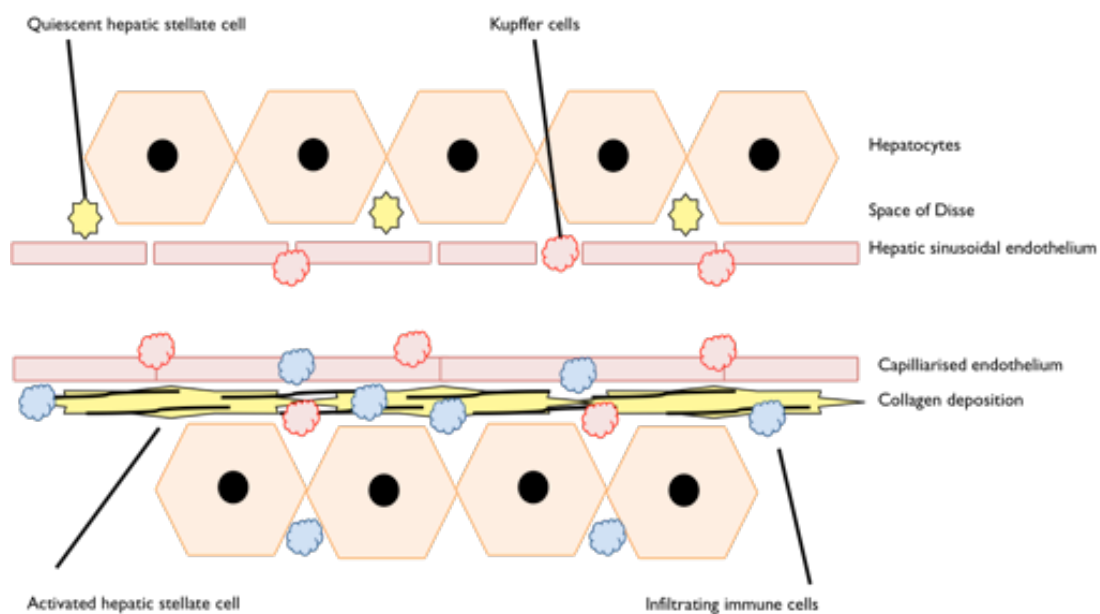
Figure 1.2: the hepatic sinusoid in health and disease

Above: The hepatic sinusoid is lined by specialised endothelium characterised by fenestrae and a lack of a basement membrane. Fenestrae allow sampling of the sinusoid by hepatocytes and Kupffer cell patrol the sinusoids. Below: in disease, activation of stellate cells by inflammation and infiltrating immune cells causes deposition of collagen. This expands the space of Disse and creates a functional basement membrane, a process referred to as capilliarisation of the sinusoid (DeLeve, 2007, Kubes and Mehal, 2012)

A layer of unique endothelium lines the hepatic sinusoids. HSEC differ from other endothelial cell populations by expression of particular cell surface molecules, notably scavenger receptors, and the presence of fenestrations (Lalor *et al.*, 2006). There is a functional space between endothelial cells and hepatocytes, the Space of Disse. This space is occupied by KC and HSC which act as pericytes to modulate sinusoidal blood flow and endothelial integrity (DeLeve, 2007). The hepatic endothelial layer is further characterised by the lack of a basement membrane (**figure 1.2**). These features allow constant sampling of hepatic blood flow by hepatocytes, KC as well as HSEC, which have potent scavenging functions (Elvevold *et al.*, 2004). In cirrhosis, the endothelial layer becomes capiliarised (Schaffner and Poper, 1963), a process of deposition of collagen in the space beneath HSEC effectively forming a basement membrane as a consequence of inflammation and stellate cell activation (Urashima *et al.*, 1993) (Xu *et al.*, 2003). Capillarisation restricts the normal function of the scavenging function of cells of the sinusoid and contributes to hepatic dysfunction (Le Couteur *et al.*, 2005).

Bile canaliculi form from grooves in the surface of hepatocytes, and receive substances excreted through active and passive processes from hepatocytes. Bile drains from here into ductules lined with specialised epithelium, which drain in turn into bile ducts. These coalesce to a major duct in each lobe of the liver, which unite outside the liver at the porta hepatis to form the common bile duct. Lymphatic drainage from the liver is mainly to coeliac axis lymph nodes. There is minor lymph drainage to mediastinal nodes and lymph nodes associated with the inferior vena cava.

Liver disease

Chronic liver disease is increasing in prevalence in the UK (Leon and McCambridge, 2006) (Fleming *et al.*, 2008), due to trends in alcohol consumption, prevalence of viral hepatitis and obesity. In addition, mortality due to liver disease has risen, in contrast to other common causes of mortality, which have fallen over recent decades (Trust, 2008). This reflects advances in many areas of medicine, and the paucity of effective treatment for many chronic liver diseases (**figure 1.3**). Acute liver injury, most often caused by drugs is common (Sgro *et al.*, 2002) but is usually mild and self-limiting, acute liver failure is rare (Bretherick *et al.*, 2011).

Movements in mortality 1971-2008
Deaths per million of population
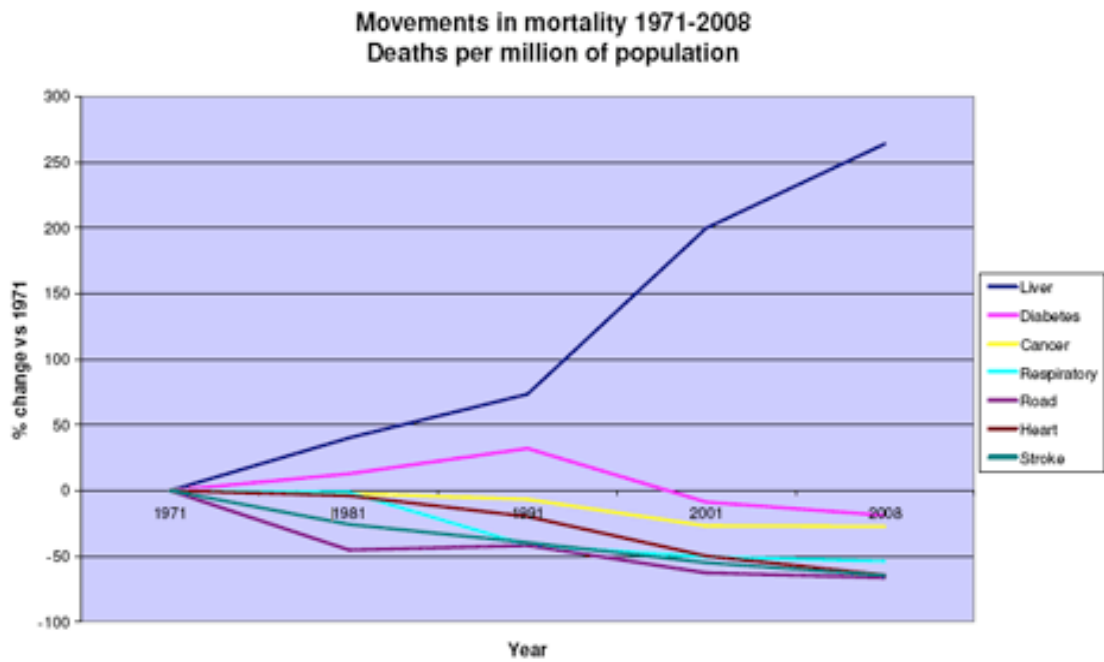
Figure 1.3: mortality from liver disease has risen compared to other common causes of death in the UK

Mortality from common conditions relative to 1971 showing large increase in deaths due to liver disease relative to 1971, in contrast to other common causes of mortality in the UK (Williams et al., 2014)

In the UK common causes of chronic liver disease include alcoholic and non-alcoholic fatty liver disease, viral hepatitis and autoimmune liver disease. Fatty liver disease, caused by alcohol or the metabolic syndrome is the most common cause of liver disease in the UK accounting for approximately half of all liver disease (Armstrong *et al.*, 2011). The causes of cirrhotic liver disease differ slightly to the aetiology of liver disease *per se*: alcohol is implicated in 38% of cases of cirrhosis, viral hepatitis 5.3%, and autoimmune disease 7.1% (Fleming *et al.*, 2008).

Hepatitis B infection causes both acute and chronic disease, largely dependent on the mode of transmission: vertical transmission in the peri-natal period or childhood is associated with greatly increased risk of chronic disease (Liver, 2012b). Hepatitis C is more common than Hepatitis B in Europe (Blachier *et al.*, 2013) and almost always causes chronic infection. Improved detection since the discovery of Hepatitis C in the 1980s has established Hepatitis C as a major cause of liver-related morbidity and mortality, however better screening and infection control methods have limited new infections (Esteban *et al.*, 2008, Lavanchy, 2011). Intense research efforts have yielded powerful anti-viral drugs that effectively control Hepatitis B infection and new agents that can cure Hepatitis C are entering clinical practice (Liver, 2014).

Autoimmune hepatitis (AIH), primary biliary cirrhosis (PBC) and primary sclerosing cholangitis (PSC) are rarer autoimmune liver diseases that may progress to end-stage cirrhosis and require liver transplantation. Most cases of AIH and some cases of PBC will respond to medical treatment, whilst PSC has no universally effective treatment.

Liver diseases that are directly relevant to this project are now discussed in more detail.

Non-Alcoholic Fatty Liver Disease

Non-alcoholic fatty liver disease (NAFLD) describes a spectrum of disease, ranging from simple hepatic steatosis (non-alcoholic fatty liver, NAFL), through more advanced non-alcoholic steatohepatitis (NASH) to cirrhosis (Chalasani *et al.*, 2012). NAFLD is common: hepatic steatosis is present in up to one-third of individuals (Browning *et al.*, 2004) in the US, and NASH is seen in approximately 10% (Williams *et al.*, 2011). The earlier stages of NAFLD are not associated with liver-related outcomes, whereas the presence of advanced fibrosis incurs greater risk morbidity and mortality (Adams *et al.*, 2005b, Ekstedt *et al.*, 2014). NAFLD is closely associated with the metabolic syndrome up to 75% of people with Diabetes Mellitus (DM) have NAFLD (Targher *et al.*, 2007, Leite *et al.*, 2009, Vernon *et al.*, 2011) and NALFD is almost universal in morbidly obese individuals (Reha *et al.*, 2014)

NASH is associated with a chronic inflammatory cell infiltrate (Gadd *et al.*, 2014) largely around portal tracts (Itoh *et al.*, 2013, Wehr *et al.*, 2014). Monocyte infiltration of the liver is a feature of both alcoholic and non-alcoholic steatohepatitis (Liaskou *et al.*, 2013). KC are activated by multiple pathways in NAFLD and promote hepatic steatosis and insulin resistance (Baffy, 2009) (Huang *et al.*, 2010, Lanthier *et al.*, 2011).

Treatment is desirable for patients with NASH to decrease the risk of progressive liver disease, and to reduce risk of liver-related morbidity. Many pharmaceutical treatments have been investigated, none have shown categorical benefit in NASH (Musso *et al.*, 2010). Weight loss is beneficial, but patients must lose 7% of their body mass to gain benefit in

terms of liver histology (Promrat *et al.*, 2010). Many patients are unable to achieve or maintain such significant weight loss. Given the prevalence of NAFLD, there is an urgent need for effective treatments to prevent or treat end-stage liver disease.

Acute liver failure

Acute liver failure (ALF) is a rare syndrome with an incidence of approximately 6 per 100,000 people/year (Bower *et al.*, 2007, Bretherick *et al.*, 2011). ALF, characterized by jaundice and encephalopathy, is most commonly caused by drugs but may also be caused by viral infection and rarely autoimmune disease (Bower *et al.*, 2007, Marudanayagam *et al.*, 2009, Hadem *et al.*, 2012).

Paracetamol is the most common cause of drug-induced ALF in the UK (Bower *et al.*, 2007, Bretherick *et al.*, 2011, Gulmez *et al.*, 2013). Paracetamol-induced ALF has a significant associated mortality – 29% at three weeks in a large US cohort (Larson *et al.*, 2005).

Paracetamol induced acute liver failure is characterised by infiltration of liver tissue by a mixed infiltrate where macrophages are prominent (Antoniades *et al.*, 2012, Nakamoto *et al.*, 2012) as well as lymphocytes and neutrophils (Tuncer *et al.*, 2013) (Marques *et al.*, 2012). The infiltration of macrophages and neutrophils into liver tissue in ALF is regulated in part by chemokines many of which are over-expressed in the acutely injured liver (Tuncer *et al.*, 2013). The patterns of chemokine expression differs quantitatively and qualitatively between aetiologies of ALF, for example work from our laboratory shows greater CCL4 expression in paracetamol-induced ALF compared to seronegative hepatitis (Tuncer *et al.*, 2013).

Paracetamol-induced ALF is further distinguished from fulminant auto-immune hepatitis (AIH) by the pattern of infiltrating cells, where a predominance of lymphocytes and plasma cells is seen in AIH (Czaja, 2013).

Acute liver failure of any cause has few treatment options. In the case of paracetamol-induced liver failure, the only current available treatment is intravenous N-actylcysteine (Lee *et al.*, 2011) to replace hepatic stores of glutathione exhausted by the metabolism of excess paracetamol. Liver transplantation remains the only treatment option for the minority not responding to medical treatment.

Primary Biliary Cirrhosis

In PBC small intrahepatic bile ducts within the liver become inflamed often associated with a characteristic granulomata (Selmi *et al.*, 2011). PBC is a rare condition affecting up to 200 people in a million (Myers *et al.*, 2009, Boonstra *et al.*, 2012) and the incidence may be increasing. It is far more common in women than in men and tends to present in middle age. The strong association of PBC with auto-antibodies against mitochondria (anti-mitochondrial antibody, AMA) and the presence of auto-reactive T cell in liver tissue and draining lymph nodes (Kita *et al.*, 2002) show PBC to be an autoimmune disease. However, AMA are not universally found in individuals with PBC and most people with AMA do not develop PBC (Michieletti *et al.*, 1994, Mattalia *et al.*, 1998). In addition to alterations of T cell phenotype, an increase in the presence of activated NK cells has been observed in PBC (Björkland *et al.*, 1991). Shimoda *et al* demonstrated the cytotoxicity of NK cells against autologous biliary epithelial cells under certain pro-inflammatory conditions (Shimoda *et al.*, 2011).

Treatment with ursodeoxycholic acid slows progression of disease and improves overall survival (Lindor *et al.*, 2009) but those who do not respond to treatment have a poor prognosis. This group of patients will often require liver transplantation.

Hepatocellular carcinoma

HCC had an annual incidence of 4.9/100,000 people in the USA in 2005, a three-fold rise since 1975 (Altekruse *et al.*, 2009), although incidence of HCC varies depending on the prevalence of risk factors such as viral hepatitis (Ferenci *et al.*, 2010). In the west most HCC occur on a background of liver cirrhosis (Altekruse *et al.*, 2009). In cirrhosis, loco-regional therapy of smaller lesions is occasionally curative but larger lesions require transplantation to offer curative treatment (Liver, 2012a).

Multiple aberrations in cell signalling pathways have been described in HCC including cell cycle dysregulation, increased angiogenesis and evasion of apoptosis (Calvisi *et al.*, 2007, Hoshida *et al.*, 2010, Whittaker *et al.*, 2010). None of these are unique to HCC. The CXC chemokine receptor CXCR6 has been reported to be overexpressed in HCC (Gao *et al.*, 2012), where knock-out of CXCR6 reduced growth, angiogenesis and metastasis of hepatoma cells implanted into mice.

Immunology of the liver

The liver is a unique immunological environment. The influx of blood draining the gut carries multiple antigens derived from food and gut bacteria, many of which will be harmless

(Crispe, 2009). To prevent immune activation in response to benign particles the liver has multiple mechanisms by which tolerance is maintained. Under normal circumstances KC and HSEC express anti-inflammatory compounds such as IL-10, PGE_2 and TGF-β in response to LPS and other antigens, rendering liver resident naïve DCs tolerogenic (Knolle and Gerken, 2000). In addition, vitamin A secreted by HSC prompt naïve $CD4^+$ to differentiate towards a regulatory phenotype (Tiegs and Lohse, 2010). Liver-resident non-T cell lymphoid cells such as NK and NKT cells also play a role in maintaining tolerance (Doherty and O'Farrelly, 2000) in part through recruitment and activation of T regulatory cells (Santodomingo-Garzon and Swain, 2011).

The normal liver contains a large population of lymphocytes, the distribution of which differs from that of blood with more NKT and NK cells and proportionally fewer $\alpha\beta$ T lymphocytes (Norris *et al.*, 1998, Norris *et al.*, 1999) (Hata *et al.*, 1990). These cells are found throughout the parenchyma and within portal tracts. Kupffer cells reside in the space of Disse and actively patrol the sinusoids. Liver resident dendritic cells are potent APCs and take up antigen and migrate via lymphatics and the sinusoids to draining lymph nodes where they activate T cells. HSEC, HSC and hepatocytes can under some circumstances also present antigens to lymphocytes and this usually results in tolerance (Racanelli and Rehermann, 2006, Tay *et al.*, 2014).

Immune cells in liver disease

Monocyte/macrophages

Monocytes circulate in blood for a short period after leaving bone marrow before entering tissue and differentiating further into macrophages and also dendritic cells (Ziegler-Heitbrock *et al.*, 2010). Monocytes in humans can be classified on the basis of CD14 and CD16 expression (**figure 3.5**) into classical $CD14^{++}CD16^{-}$ monocytes that predominate in blood; non-classical $CD14^{-}CD16^{++}$ monocytes that are expanded under inflammatory conditions and an intermediate $CD14^{++}C16^{+}$ population of monocytes which also expand under inflammatory conditions. Previous reports from our laboratory have shown that diseased liver tissue in NASH and ALD is enriched for monocytes compared to normal tissue (Liaskou *et al.*, 2013) due to increases in the non-classical $CD14^{-}CD16^{++}$ and intermediate $CD14^{++}CD16^{+}$ monocytes. Recent work has demonstrated that $CD16^{+}$ and $CD16^{-}$ cells behave differently after transmigration through hepatic endothelium *in vitro*: $CD14^{++}CD16^{-}$ cells mainly remained sub-endothelial and demonstrated high phagocytic capacity whereas $CD14^{++}CD16^{+}$ and $CD14^{-}CD16^{++}$ cells often gave rise to DC precursors with T-cell inducing properties (Zimmermann *et al.*, 2015).

Tissue resident macrophage populations – Kupffer cells in the case of the liver - are established before birth and are able to self-replenish without requiring addition of blood-borne monocytes (Hashimoto *et al.*, 2013, Yona *et al.*, 2013). These two distinct populations have different functions – KC detect liver injury and initiate inflammatory responses which are perpetuated and amplified by infiltrating monocytes (Tacke and Zimmermann, 2014).

Natural killer cells

Natural killer (NK) cells are cells of the innate immune system of lymphoid lineage that are directly cytotoxic and have cytokine secreting effector functions (Vivier *et al.*, 2008). Through prompt recognition of non-self cells NK cells have potent antimicrobial properties and also anti-tumour capability. More recently research has demonstrated a regulatory role for NK cells through inhibition of macrophages, as well as through modulation of dendritic cell actions.

CD56 expression is the hallmark of NK cells in humans and NK cells can be subdivided based on their relative expression of CD56 (Vivier *et al.*, 2008). The CD56^{dim} subset is more common in peripheral blood whereas CD56^{hi} cells predominate in tissue. Expression of CD56 is inverse to CD16 expression (Cooper *et al.*, 2001) where the expression of CD16 is required for antibody-mediated cytotoxity through binging of antibody. Accordingly, CD56^{hi} NK cells show lower levels of antibody mediated cell killing than CD56^{dim}. CD56^{hi} subsets produce more cytokines e.g. IFNγ than cd56^{dim} subset (Cooper *et al.*, 2001) (Poli *et al.*, 2009).

Chemokines

Chemokines are small cytokines (8-12kDa). They are a phylogenetically ancient feature of the immune system with origins around 650 million years ago and found in fish, amphibians and birds as well as mammals (DeVries *et al.*, 2006). The human chemokine superfamily

comprises 46 known chemokines, which bind to 18 chemokine receptors (Zlotnik *et al.*, 2006). Chemokine ligands are defined by the arrangement of N-terminal cysteine residues (Zlotnik and Yoshie, 2000). Chemokine ligands bind to receptors in defined pairings. Some receptors bind more than one ligand, some ligands bind to more than one receptor whilst other receptor-ligand pairs are monogamous, i.e. interact only with each other.

Chemokine receptors have seven trans-membrane regions and are G-protein coupled (Allen *et al.*, 2007a). Binding of chemokine ligand to it's receptor generally results in activation of multiple intracellular pathways through activation of G-protein coupled receptors (Allen *et al.*, 2007b) although binding to decoy chemokine receptors does not elicit an overt signalling response but instead internalise, transport or degrade chemokines (Bonecchi *et al.*, 2010).

Activation of chemokine receptor causes activation of the Gα subunit of the associated G-intracellular protein, leading to separation of both the Gα subunit and the G$\beta\gamma$ (Allen *et al.*, 2007b). Both of these have signalling effects inside the cell although the G$\beta\gamma$ subunit may be of greater importance in the context of cell migration (Thelen and Stein, 2008). A variety of intracellular pathways are activated including activation of phospholipase lading to calcium mobilisation, cell polarisation and integrin mobilisation and activation, (Kinashi, 2005, Thelen and Stein, 2008), activation of phosphoinositide 3-kinases leading to cytoskeleton rearrangements (Curnock *et al.*, 2002, Rot and von Andrian, 2004). The canonical role of chemokines is to exert effects on immune cell trafficking. These effects are fundamental at all stages of leukocyte development from positioning within the thymus and bone marrow, egress into blood, to recruitment and positioning in sites of inflammation and secondary lymphoid tissue (Rot and von Andrian, 2004). Chemokines also have a role in other

biological functions for example angiogenesis and embryology (Mehrad *et al.*, 2007, Raz and Mahabaleshwar, 2009).

Chemokines in liver disease

Infiltration of inflammatory cells is a common feature of liver injury (Björkland *et al.*, 1991, Boisvert *et al.*, 2003). Differing types of liver disease are associated with distinct patterns of infiltration characteristic to differing types of injury (Susca *et al.*, 2001, Lalor *et al.*, 2002). Chemokines are produced in the liver by multiple cell types (Afford *et al.*, 1998, Shields *et al.*, 1999). The combination of chemokines secreted and presented in the liver will contribute to the nature of inflammation by driving adhesion and positioning of immune cells within liver (Oo and Adams, 2010). In this thesis I have focussed on the role of specific chemokine receptors CCR2, CCR9 and CXCR6. These receptors where investigated on the basis of previous reports from our laboratory and others suggesting roles for CCR2, CCR9 and CXCR6 in fatty liver disease, acute liver failure and biliary disease respectively. In addition the role of CXCR6 in HCC was investigated in view of results examining CXCR6 in hepatic leukocyte trafficking.

CCR2

CCR2 is widely expressed on monocytes and T cells in humans (Charo *et al.*, 1994) (Frade *et al.*, 1997) and mice (Mack *et al.*, 2001). CCR2 has several ligands CCL2, CCL7, CCL8, CCL13 and CCL16 which are expressed by diverse cell types (Zlotnik and Yoshie, 2000), as well as CCL11, which is an antagonist of CCR2 (Ogilvie *et al.*, 2003).

Investigations in obesity showed macrophage infiltration of adipose and hepatic tissue to be mediated by CCR2 (Kanda *et al.*, 2006, Weisberg *et al.*, 2006). Particular CCR2$^+$ monocyte/macrophage subsets have been shown to contribute to insulin resistance: in mice CD11b$^+$CD11c$^+$ F4/80$^+$ macrophages contribute to chronic inflammation and insulin resistance in mice (Patsouris *et al.*, 2008) and a functionally similar pro-inflammatory CD11c$^+$CD206$^+$ monocyte subset are found in human adipose tissue associated with insulin resistance (Wentworth *et al.*, 2010). In light of these data most attention in liver disease has focused on CCR2/CCL2 in NAFLD.

Individuals with NAFLD have higher serum concentrations of CCL2 than age and gender-matched controls (Haukeland *et al.*, 2006), and serum CCL2 levels are greater in patients with more advanced NASH than those with simple steatosis. Serum CCL2 also correlates with levels of ALT, a marker of liver injury and inflammation (Kirovski *et al.*, 2010). In mice, a high fat diet increases hepatic and serum CCL2 (Kirovski *et al.*, 2011). Over-expression of CCL2 increases hepatic steatosis whereas its lack or reduced activity decreases hepatic steatosis (Kanda *et al.*, 2006) (Nio *et al.*, 2012). CCR2 knockout animals also demonstrate reduced steatosis (Weisberg *et al.*, 2006) associated with a reduction in myeloid cell infiltration - defined histologically as F4/80$^+$ cells (Miura *et al.*, 2012) or with flow cytometry as CD11b$^+$ F4/80^{dim} (Obstfeld *et al.*, 2010). CCR2 knockout mice are also protected against carbon tetrachloride-induced fibrosis, attributed to expression of CCR2 by hepatic stellate cells (Seki *et al.*, 2009).

The CCR2/CCL2 axis has been targeted with a variety of pharmaceutical agents in animal models of fatty liver disease. In addition to confirming a role in the pathogenesis of disease,

these studies have demonstrated improved disease when either CCR2 or CCL2 is antagonised. Yang *et al* showed that administration of a CCR2 inhibitor in transgenic mice prone to lipotoxicity (Yang *et al.*, 2009) reduced liver weight (as proportion of body mass), hepatic pro-inflammatory gene expression and macrophage accumulation. Miura used a CCR2 antagonist therapeutically (i.e. once disease was established) in a model of fatty liver induced by choline deficient diet (Miura *et al.*, 2012). Again, macrophages were reduced in number in the livers of treated animals, assessed by identifying $Ly6C^+$ cells by immunohistochemistry. ALT and fibrosis were also reduced.

Baeck and colleagues (Baeck *et al.*, 2012) used an L-RNA oligonucleotide (or Speigelmer) to inhibit CCL2, with a non-functional molecule as a control. In mice fed a methionine-choline deficient (MCD) diet to induce steatohepatitis, inhibition of CCL2 throughout the dietary period reduced accumulation of hepatic fat and infiltration of the liver by $F4/80^+CD11b^+$ macrophages, without any difference in measures of fibrosis. Therapeutic application of the L-RNA olignonucleotide for the final two weeks of an eight-week experiment also reduced fat accumulation.

CCR9

Chemokine-C-receptor 9 (CCR9) is a chemokine receptor with a single ligand, CCL25, in both human and mouse (Zaballos *et al.*, 1999). CCR9 expression defines a population of gut-homing T lymphocytes (Johansson-Lindbom *et al.*, 2003), that migrate to the small bowel epithelium in response to locally expressed CCL25 (Svensson *et al.*, 2002, Johansson-Lindbom *et al.*, 2003) and a population of thymocytes that use CCR9 to enter the thymus.

Pro-inflammatory myeloid cells expressing CCR9 have been reported in inflammatory bowel disease (Linton *et al.*, 2012) and rheumatoid arthritis (Schmutz *et al.*, 2010) in humans.

CCR9$^+$ macrophages have recently been reported as playing a key role in a mouse model of acute liver injury (Nakamoto *et al.*, 2012). In concanavalin A (ConA) induced hepatitis, CCR9$^+$ macrophages were increased in number in injured liver tissue, expressed TNFα and induced differentiation of naïve CD4 T-cells towards a Th1 phenotype. In CCR9$^{-/-}$ mice adoptive transfer of CCR9$^+$ macrophages from wild type mice was required for hepatitis to occur after ConA administration. In peripheral blood samples from four human subjects with acute liver injury (due to hepatitis B in two patients, and autoimmune hepatitis in two patients) CCR9 was up regulated on CD14$^+$CD16$^+$ macrophages, compared to chronic liver injury or healthy controls. The same group went on to show that CCR9$^+$ macrophages could activate hepatic stellate cells and promote fibrosis in acute and chronic liver injury in mice (Chu *et al.*, 2013).

Chemokines are over-expressed in acute liver failure: serum concentration and liver expression of CCL2, CCL3, CCL4 and CCL5 were increased in human fulminant hepatic failure (26 cases predominantly due to viral hepatitis) compared to healthy controls and also chronic liver disease (Leifeld *et al.*, 2003). Antoniades *et al* showed that CCL2 and CCL3 are increased in paracetamol-induced acute liver injury, and associated with necrotic areas within ALF liver tissue (Antoniades *et al.*, 2012). Serum CXCL8, CXCL9 and CXCL10 are all markedly up regulated in human acute liver failure (Marques *et al.*, 2012) (Tuncer *et al.*, 2013).

CXCR6

CXCR6 was first described as a G-protein coupled receptor that functioned as a co-receptor for simian immunodeficiency virus (SIV) and human immunodeficiency virus (HIV) (Deng *et al.*, 1997, Liao *et al.*, 1997, Loetscher *et al.*, 1997). CXCL16 is the only ligand for CXCR6 (Matloubian *et al.*, 2000). CXCR6 was subsequently shown to be a chemotactic receptor for several lymphocyte subsets and to be involved in the patrolling of NKT cells in the hepatic sinusoid (Geissmann *et al.*, 2005).

$CXCR6^+$ lymphocytes are enriched in human liver tissue (Kim *et al.*, 2001, Billerbeck *et al.*, 2010). CXCR6 is expressed by both $CD4^+$ and $CD8^+$ lymphocytes (Unutmaz *et al.*, 2000, Kim *et al.*, 2001, Boisvert *et al.*, 2003, Tabata *et al.*, 2005). CXCR6 expression on T lymphocytes is linked to markers indicating an effector, tissue-infiltrating phenotype (Northfield *et al.*, 2008, Billerbeck *et al.*, 2010). CXCR6 is highly expressed on $CD56^+$ lymphoid cells, both NK and NKT cells (Campbell *et al.*, 2001). $CD14^+$ monocytes express CXCR6 (Ruth *et al.*, 2006, Huang *et al.*, 2008) as do neutrophils (Gaida *et al.*, 2008). CXCL16 is expressed in liver by hepatic vascular endothelium, hepatocytes and biliary epithelium (Heydtmann *et al.*, 2005). Adhesion of human lymphocytes to biliary epithelial cells *ex vivo* is a CXCL16-dependent process (Heydtmann *et al.*, 2005).

$CXCR6^{-/-}$ mice exhibit a reduced number of NKT cells in sinusoids and are protected against T-cell mediated hepatitis, a phenomenon attributed to reduced NKT cell survival (Geissmann *et al.*, 2005). In mice, preventing CXCL16/CXCR6 interactions with anti-

CXCL16 antibodies reduced infiltration of CD3^{+} lymphocytes in BCG-mediated liver injury and protected against liver necrosis (Xu *et al.*, 2005). More recent work (Wehr *et al.*, 2013) found that CXCR6^{-/-} mice demonstrated lower serum ALT and fewer infiltrating NKT cells compared to wild type mice in carbon tetrachloride-induced acute liver injury. In chronic liver injury, CXCR6^{-/-} mice showed less fibrosis and reduced macrophage accumulation. The fibrotic response was restored when CXCR6^{+} NKT cells were adoptively transferred to CXCR6^{-/-} mice.

CXCR6 expression in cancer

The direction of cell trafficking may be seen as the classical role of chemokines, but other roles are well reported particularly in embryology, angiogenesis and carcinogenesis (Horuk, 1998, Bernardini *et al.*, 2003, Spring *et al.*, 2005, Lazennec and Richmond, 2010). CXCR6 is expressed in a variety of tumour cell lines and in tumour tissue, often associated with a more aggressive phenotype (Porta, 2012). Conversely, CXCR6 knockout mice show increased metastasis of melanoma cells to the liver that was ameliorated by activating NKT cells (Cullen *et al.*, 2009).

In liver disease, cirrhosis is often complicated by hepatocellular carcinoma (HCC). HCC specimens show higher protein expression of CXCR6 in tumour tissue compared to distal, non-cancerous liver tissue (Gao *et al.*, 2012). This was variable, with particularly increased expression in tumours showing evidence of vascular invasion. In keeping with this CXCR6 protein expression was inversely correlated with recurrence free survival. In hepatoma cell lines, knock down of CXCR6 and of CXCL16 reduced migration in a transwell assay. When

CXCR6 deficient hepatoma cells or control hepatoma cells were transplanted into nude mice, CXCR6 knockdown tumours grew more slowly. These effects were attributed to reduced membrane expression of caveolin-1 and β-catenin, analysed by western blotting. Although caveolin-1 is linked to cell cycle progression, no data were shown to describe cell proliferation although the authors report that no effects were seen.

Hepatocyte expression of other CXC chemokine receptors has been documented (Hogaboam *et al.*, 1999, Bone-Larson *et al.*, 2001, Clarke *et al.*, 2011). CXCR4 and its ligand CXCL12 have been reported to influence metastasis of hepatocellular carcinoma (Liu *et al.*, 2008). Other CXC-chemokine receptors have been implicated in hepatic regeneration including CXCR1 (Clarke *et al.*, 2011) and CXCR2 (Hogaboam *et al.*, 1999, Bone-Larson *et al.*, 2001) at least under some circumstances (Kuboki *et al.*, 2008).

Potential for therapeutic manipulation of chemokine system

The chemokine system has been identified as amenable to pharmaceutical manipulation for many years. There has been some scepticism regarding this approach, and evidence of binding of multiple ligands to a single receptor that suggests redundancy within the chemokine system has been held as a particular barrier. This implies that inhibition of a single receptor or ligand may be ineffective if another ligand/receptor interaction will provide the same biological effect (Schall and Proudfoot, 2011). This does not reflect more nuanced differences in receptor behaviour after activation by different ligands, or differences in spatial or temporal expression of receptors (Corbisier *et al.*, 2015). Indeed, drugs that target chemokine receptors have been approved for use: maraviroc is a CCR5 antagonist used in

the treatment of HIV, and a CXCR4 antagonist plerixafor has recently been approved for the mobilisation of haematopoietic stem cells from bone marrow.

In the field of liver medicine, in addition to experiments in pre-clinical animal models with pharmaceutical agents targeting the chemokine system, described above, novel agents are being studied in early-phase human trials. The efficacy of CCR2 inhibition in humans has been studied in various diseases. Whilst there has been considerable interest in targeting CCR2 in the treatment of disease associated with insulin resistance (Pirow, 2012, Di Prospero *et al.*, 2014). Cencriviroc, a dual CCR2/CCR5 inhibitor initially examined in HIV infection is being used in NAFLD (02217475, 2014).

Aims of project

Liver disease is common in the UK but has few therapeutic options. A common feature of most acute and chronic liver disease is the infiltration of liver tissue by inflammatory cells, a process mediated in part by chemokines and their receptors. Non-haematopoietic cells also express chemokine receptors and signalling through CXC receptors on hepatocytes may be protective in injury but pathological in the context of hepatocellular carcinoma. The chemokine system is thus implicated in the development of many liver diseases. It is complex system but offers potential targets for the treatment of liver disease. The aim of this project was to understand the role of chemokines and their receptors in pathogenesis of liver disease. In view of previous reports from our laboratory and others, the objectives were to focus on chemokine receptors CCR2, CCR9 and CXCR6. These chemokine receptors were investigated on the basis of existing data from our group and others suggesting they were

involved in the aetiology of liver disease, as discussed in detail above. Where possible disease processes were modelled in mice to evaluate the effect of inhibition or knock out of chemokine receptors on disease.

CHAPTER 2: Methods

Human tissue

Human liver tissue used for experiments was collected at University Hospitals Birmingham NHS Foundation Trust (UHB). All liver tissue was obtained through the hepatobiliary surgical programme where research Ethics Committee approval has been granted for the consensual use of resected or explanted liver tissue. Experimental data were related to clinical parameters collected routinely through clinical practice at UHB.

Blood obtained through the haemochromatosis venesection programme at University Hospitals Birmingham, or taken from patients at the time of transplantation was used with appropriate informed consent and research ethics approval. Serum from patients with NAFLD was obtained through the LEAN and NOBLES studies. LEAN is a randomised controlled trial of liraglutide in patients with NAFLD (Armstrong *et al.*, 2013), where the serum samples used were taken before randomisation. NOBLES are an observational study of patients with liver disease that aims to correlate serum markers with histological evidence of fibrosis. In both cases serum was separated from whole blood samples and frozen to -80°C within 1 hour of collection. Collaborators at Kings College, London in accordance with local ethics approval, obtained serum from patients with ALF. Control samples were sourced from healthy volunteers with informed consent.

Isolation and culture of non-parenchymal cells

Human sinusoidal endothelial cells (HSEC) and biliary epithelial cells (BEC) were isolated from explanted human livers by Mrs Gill Muirhead at the Centre for Liver Research. Liver was finely chopped before being digested with collagenase and strained through sterile mesh. The resulting homogenate, after washing, was layered over 33% and 77% percoll gradients and centrifuged at 2000rpm for 25 minutes. The band of cells at the interface of the 33% and 77% percoll was removed and washed. HSEC and BEC were separated by magnetic bead separation using antibodies to human embryonic antigen (HEA) to separate HSEC.

Hepatoma cell lines were used to investigate hepatocyte function. HuH-7.5 and HepG2 cells were used from cell lines maintained in the Centre for Liver Research. Primary hepatocytes were purchased from Bioreclaimation. They were delivered in aliquots stored in liquid nitrogen and immediately transferred to a freezer at -80°C. These hepatocytes were defrosted and cultured in collagen-coated T25 Falcon flasks, with a 24-hour period between defrosting and any experimental procedure.

Media for culture

The media used to culture various cell types are detailed in **table 2.1**. These media were supplemented for some experiments, described in the relevant chapter. Cells were serum-starved before experiments with additional factors to allow for a pure effect of that factor to be analysed. In this case, serum without the addition of bovine or human serum or growth factors was used.

Culture medium	Constituents per 200mL
BEC medium	√mL Dulbeco's Modified Eagle's Medium (DMEM) 90mL Hams F12 nutrient mixture 2mL 0.2M penicillin/streptomycin 2mL (2μg/mL) hydrocortisone 2ml (1μg/mL) cholera toxin 2mL Tri-ido-thyronine 20uL hepatocyte growth factor (HGF) (100μg/mL) 248μL insulin
Hepatoma/hepatocyte medium	180mL DMEM 20uL heat inactivated bovine serum albumin (BSA)
HSEC medium	177.92 mL endothelium serum free medium 20mL heat inactivated human serum (HIHS) 2mL 0.2M penicillin/streptomycin 40μL(50μg/mL) vascular endothelium growth factor (VEGF) 40μL (50μg/mL) hepatocyte growth factor
Lymphocyte medium	178mL Roswell Park Memorial Institute medium 20mL heat inactivated BSA 2mL 0.2M penicillin/streptomycin

Table 2.1: media used for cell culture
Base media (DMEM, RPMI, SFM) were obtained from Life Technologies (California, USA), and growth factors from Peprotech (New Jersey, USA). BSA and HIHS, hydrocortisone, cholera toxin, tri-ido-thyronine, insulin and penicillin/streptomycin were obtained from Sigma-Aldrich (Missouri, USA)

Immunohistochemistry

Frozen sections

Liver tissue from mice or humans was snap frozen in liquid nitrogen, protected either in plastic tubes (mice tissue) or foil boats (human tissue). After snap freezing, tissue was stored at -80°C. Frozen blocks were cut into 8μm sections, mounted onto glass slides, and fixed by immersion in acetone for 5 minutes. Slides were stored at -20°c wrapped in foil until use.

Paraffin embedded sections

Liver tissue from mice or humans was placed in formalin until use. Tissue was then embedded in paraffin, cut into 8μm sections and mounted onto glass slides.

Immunohistochemistry procedure

Frozen sections were defrosted for ten minutes at room temperature before use. Endogenous peroxidase activity was quenched by 1% hydrogen peroxidase (Sigma Aldrich, Missouri, USA). Non-specific binding was blocked with 2% casein solution for ten minutes and 1% horse serum for 20 minutes. After twice washing in Tris-buffered saline (TBS) for 5 minutes, primary antibodies were diluted to concentrations detailed in **table 7.1** and slides incubated at 4°c for 12 hours with rocking. After washing slides three times in TBS for five minutes each time, secondary antibodies (IMMpress kits, Vector Labs, USA) were applied for 1 hour at room temperature. Slides were washed in TBS for five minutes and NovaRed (Vector Labs, USA) applied as a chromogen. Slides were incubated in Novared for 2 minutes and then washed in tap water. Mayer's haematoxylin was used as a counterstain, and slides were mounted with Immunomount.

Paraffin embedded sections were rehydrated by immersion in clearene (6 minutes) and ethanol (4 minutes). Endogenous peroxidase activity was quenched by immersion in hydrogen peroxidase. Antigen retrieval was performed by incubating slides in high pH antigen retrieval solution (Vector) at 65°C overnight (approximately 16 hours). Sections were washed in TBS, and non-specific binding blocked with casein and horse serum as above. After twice washing in TBS for 5 minutes, primary antibodies were diluted to concentrations detailed in **table 2.2** and slides incubated at 4°c for 12 hours. After washing slides three times in TBS, secondary antibodies (IMMpress kits, Vector Labs, USA) were applied for 1 hour at room temperature. NovaRed was applied for 2 minutes before washing in tap water and counterstaining in filtered Mayer's haematoxylin for 30 seconds. Slides were dehydrated through alcohol (4 minutes incubation) and clearene (6 minutes incubation), and mounted with DPX mountant. Sections were visualised on an Axioskop 40 microscope.

For fluorescent staining, the same process was followed as per staining of paraffin-embedded slides described above. Secondary antibodies were conjugated to fluorochromes as noted in **table 2.2**. After incubation for one hour at room temperature with secondary antibodies diluted in TBS with 0.05% TWEEN-20, slides were washed three times in TBS. 4',6-Diamidine-2'-phenylindole dihydrochloride (DAPI) diluted 1:1000 in water was added to each slide for 1 minute before washing in water, and then filtered Meyer's haematoxylin added for 30 seconds to reduce background fluorescence. Slides were dehydrated with alcohol and clearene, and mounted with ProLong Gold Anti-Fade (Life Technologies, California, USA). Slides were kept in the dark at 4°C prior to imaging with confocal microscopy. Sections were visualised with an Axiovert UV confocal microscope.

Antibody	Isotype	Supplier	Catalogue number	Clone	Concentration used
Anti-human CXCL16	Polyclonal Goat IgG	R&D systems	AF976		10μg/mL
Anti-human CXCR6	Mouse IgG2b	R&D systems	MAB699	56811	10μg/mL
Anti-human CK18	Mouse IgG1	Dako	M7010	DC10	8μg/mL
Anti-mouse-Alexa Fluor 488	Goat IgG	Life Technologies	A28175		2μg/mL
Anti-mouse Alexa Flour 647	Rabbit IgG	Life Technologies	A21239		2μg/mL
Goat IgG isotype control		R&D systems	AB-108-C		10μg/mL
Mouse IgG2b isotype control		Dako	X0944		10μg/mL
Mouse IgG1 isotype control		R&D systems	MAB002		8μg/mL

Table 2.2 antibodies used in immunohistochemistry procedures

Isolation of RNA

Isolation of RNA from whole tissue

RNA was isolated by homogenizing human or murine liver tissue in Trizol (Life Technologies, California, USA). Chloroform was added and samples centrifuged at top speed in a microfuge for 15 minutes. The upper aqueous layer was removed and the lower layer stored for protein retrieval. Isopropanol was added to the aqueous layer and samples centrifuged at 12,000rpm for 15 minutes. The resulting RNA pellet was washed in 70% ethanol and re-suspended in nuclease free water. Concentration of RNA was measured with a Nanophotometer (Implen, Germany) three times and a mean reading recorded. Purity was noted with 260/280 nm ratio.

Isolation of RNA from cell pellets

Qiashredder (Qiagen, USA) was used to disrupt cell pellets and RNA isolated from the resulting homogenate using Qiagen RNeasy kits (Qiagen, USA) according to the manufacturer's instructions. The concentration of RNA was measured using a Nanophotometer (Implen, Germany). Purity was noted with 260/280 nm ratio.

Synthesis of cDNA

cDNA was prepared from RNA using Taqman reagents (Life Technologies, California, USA) according to the manufacturer's instructions: briefly, 2 µL of RNA was combined with random hexamers, reverse transcriptase, RNase inhibitor, magnesium chloride and a buffer solution. This mixture was heated to 25°C for 10 minutes, 37°C for 30 minutes, 95°C for 5 minutes and then cooled to 4°C. cDNA was then stored at -20°C until use.

Polymerase Chain Reaction

Probe/primer mixes for genes of interest and appropriate controls were obtained from Taqman (Life Technologies, California, USA) and made up with Taqman reagents. A 96 well plate was used for reactions, with wells containing cDNA, primer/probe mix (where FAM was used for the probe)(**table 2.5**) and Taqman mastermix. Three replicates were used for the gene of interest and three for housekeeping gene. A water control was used in each experiment, where water was used in place of cDNA. In addition, a reverse-transcriptase control was used, where cDNA synthesis was performed without reverse transcriptase and the resulting, presumed cDNA free, control used to rule out the presence of genomic cDNA in the samples.

PCR experiments were performed using a Roche Lightcycler 480 machine with cycling parameters: 2 minutes at 50°C, 10 minutes at 95oC, followed by 40 cycles of 10 seconds at 95°C and 1 minute at 60°C. A single quantification measurement was taken during each cycle.

Gene	Catalogue number
Human	
CCL2	Hs00234140_m1
CCL25	Hs00608373_m1
CXCL16	Hs00222859_m1
CXCR6	Hs01890898_s1
18S	Hs03003631_g1
Mouse	
Col1a	Mm00801666_g1
Acta-2	Mm00725412_s1
18S	Mm03928990_g1
B-actin	Mm00607939_s1

Table 2.3: Taqman primers used in RT-qPCR reactions

PCR gene expression array

RNA isolated from primary hepatocytes was converted to cDNA using methodology described above. Gene expression for a range of signalling pathways was analysed using a gene expression array (Qiagen, Netherlands). cDNA (150uL for each well) was added to SYBR green mastermix (Qiagen) and RNA free water was added to each well of the 96 well plate. Gene expression was analysed using a Roche Lightcycler 480 machine with the following settings: 95°c 10 minutes, followed by 45 cycles of 15 seconds at 95°c and 1 minute at 60°c. Data were analysed using online tools available from Qiagen to identify genes that were up-regulated or down-regulated between samples. Housekeeping genes were included in the array and the analysis software automatically normalized gene expression between samples.

Enzyme Linked Immunosorbent Assays (ELISA)

Analysis of human serum was performed using commercially available ELISA kits. Serum concentration of CCL25 was measured using a DuoSet ELISA kit from R&D Systems (Cat. No. DY334, R&D systems, Minnesota, US). Serum CCL2 concentration and CXCL16 concentration were measured using R&D Systems Quantikine kits (Minneapolis, USA) (catalogue numbers PDCP00 and DCX160 respectively). In each case ELISA was performed in accordance with manufacturer's instructions. Recombinant human chemokines were used as a positive control (Peprotech, New Jersey USA). Samples were diluted in sample buffer 1:4 and run in duplicate. A standard curve was generated from known concentrations of recombinant chemokine and sample values interpolated from this curve.

Isolation of leukocytes

Isolation of leukocytes from blood

Whole blood was mixed with an equal volume of PBS. Thirty mL of this mixture was layered over 20 mL of Lympholyte (CedarLane Labs, Canada) and centrifuged at 2000rpm/870g for 25 minutes. The resulting mononuclear cell layer was removed and washed a further three times suspending in RPMI and centrigfuing at 2000rpm for 5 minutes. Leukocytes were either used immediately or kept suspended in RPMI with 10% FCS at 37°c until use.

Isolation of leukocytes from human liver tissue

Liver tissue was dissociated mechanically using a GentleMACS and C-tubes (using program Spleen_01_01; Miltenyi, Germany) and the resulting homogenate passed through a fine mesh (70 micron pores). After washing three - five times with PBS (until a clear supernatant was achieved), 30mL of liver tissue homogenate suspended in PBS was layered over 20mL of Lympholyte (CedarLane Labs, Canada), and centrifuged at 2000rpm/870g for 25 minutes. The resulting mononuclear cell layer was removed and washed a further three times in PBS.

Isolation of leukocytes from murine liver tissue

To isolate leukocytes from tissue, mice ▮▮▮▮▮▮▮ CO_2 inhalation ▮▮▮▮▮▮ ▮▮▮▮▮▮▮▮▮▮▮▮ or terminal anaesthesia ▮▮▮▮▮▮▮▮ ▮▮ and organs perfused with sterile PBS via left ventricular puncture before removal of liver or adipose tissue. These samples were immediately placed into ice-cold RPMI. After weighing, tissue was homogenized and passed through a 100um mesh.

Flow Cytometry analysis of leukocytes

Human cells

Isolated immune cells were suspended in 100μL at 1×10^6 cells/ml in MACS buffer (PBS containing 2% FCS and 1mM EDTA) and incubated with antibodies as shown in **table 2.6**. After incubation for 20 minutes at room temperature, cells were washed and re-suspended in PBS and analysed by flow cytometry using a Beckman Coulter Cyan. Cells stained with single colours were analysed for compensation and isotype controls were used to define the negative populations.

Mouse cells

The liver homogenate was washed and re-suspended at 100mg/mL in cold PBS. Next, 100 μL of this suspension was incubated with Fc-block (Trustain, Biolegend, California USA) for 20 minutes at room temperature before incubation with antibodies (**table 2.7**) in PBS for 30 minutes at room temperature. After a further washing step with cold PBS, the cell pellet was re-suspended in 200μL of cold PBS and a dye to detect live cells added (Invitrogen Live/Dead red dye, used at 1:1000 as per manufacturer's instructions). The sample was incubated for a further 15 minutes before a final wash in cold PBS. The cell pellet was re-suspended in 200μL and filtered through a 70μm mesh. Flow cytometry was performed with a BD FACSCanto using BD Diva software and analysed with FlowJo V10.

Antibody	Fluorochrome	Volume used per 100,000 cells	Isotype	Catalogue number	Clone
CD3	FITC	5 μL	Mouse IgG2a	Biolegend 300306	HIT3a
CD3	APC	5 μL	Mouse IgG1	R&D Systems FAB100a	UCHT1
CXCR6	PE	5 μL	Mouse IgG2a	Biolegend 356004	K041E5
CCR2	PE	2.5 μL	Mouse IgG2a	Biolegend 357205	K036C2
CD8	PerCP-Cy5.5	20 μL	Mouse IgG1	BD bioscience 341050	SK1
CD56	V450	5 μL	Mouse IgG1	BD bioscience 560360	B159
CD4	V500	5 μL	Mouse IgG1	BD bioscience 560768	RPA-T4
CD16	V500	5 μL	Mouse IgG1	BD bioscience 561394	3G8
NKp30	APC	5 μL	Mouse IgG1	Biolegend 325209	P30-15
Annexin V	APC	5 μL		Biolegend 640920	
7AAD		5 μL		Biolegend 420404	
CD45	FITC	5 μL	Mouse IgG1	Biolegend 304005	H130
CD14	V450	5 μL	Mouse IgG2b	BD bioscience 560349	MΦP9
CD16	V500	5 μL	Mouse IgG1	BD bioscience 561394	3G8
CD11c	PE-Cy7	5 μL	Mouse IgG1	Biolegend 337215	Bu15
CD206	APC	5 μL	Mouse IgG1	Biolegend 321109	15-2

Table 2.4: Anti-human antibodies used for flow cytometry

Antibody	Fluorochrome	Dilution used (for 100,000 cells)	Isotype	Catalogue number	Clone
CD45.2	FITC	1:200	Mouse IgG2a, κ	BD Biosciences 553772	104
CD45.2	eF450	1:200	Mouse IgG2a, κ	eBioScience 48-0454-82	104
CD11b	PE	1:100	Rat IgG2b	BD Biosciences 557397	M1/70
CD11b	Alexafluor 700	1:200	Mouse IgG2b, κ	eBioScience 56-0112-82	M1/70
CD11c	APC	1:100	Ar Ham IgG 1 λ2	BD biosciences 558079	HL3
CD11c	PerCP-Cy5.5	1:100	Ar Ham IgG	eBioscience 45-0114-82	N418
Ly6C	PE-Cy7	1:100	Rat IgG2b, κ	BD Biosciences 552985	RB68C5
Ly6G	FITC	1:100	Rat IgG2b, κ	eBioScience 11-5931-82	RB6-8C5
CCR9	PE	1:200	Mouse IgG2a,	eBioscience 12-1991-82	CW-1.2
F4/80	BV 605	1:200	Rat IgG2a, κ	Biolegend 123137	BM8

Table 2.5: Anti-mouse antibodies used for flow cytometry

Apoptosis assay

After isolation from liver, leukocytes were depleted of monocytes by plastic adherence to a T75 flask (BD falcon) for 1 hour. Non-adherent cells were washed and re-suspended in 1%FCS in Roswell Park Memorial Institute media (RPMI) and varying concentrations of recombinant CXCL16 (Peprotech, New Jersey USA). Dead and apoptotic cells were identified using flow cytometry with 7AAD (Biolegend, California USA) and APC anti-Annexin V (Biolegend) respectively.

Proliferation assays

Lymphocytes

Immune cells were isolated as described above and monocytes depleted by plastic adhesion. Lymphocytes were washed and stained with $10\mu M$ CFSE Celltrace (Life Technologies, California, USA) at 37°C for 30 minutes. Five volumes of ice-cold media was added to quench staining and cells were incubated on ice for 5 minutes. Cells were then re-suspended at 2×10^6/ml in RPMI/10%FCS with varying concentrations of CXCL16. After 48 hours cells were washed again and stained for CD3, CD56 and 7AAD and analysed by flow cytometry as described above.

Hepatoma Cell Lines

Proliferation of hepatoma cells (HuH7 and HepG2) was assessed using Hoescht staining of DNA, and by FACS analysis using Celltrace (Life Technologies), as described above.

To assess proliferation with Hoescht dye, 100,000 hepatoma cells were added into each well of 24 well plate and left for to adhere 24 hours. Varying concentrations of CXCL16 were

then added to the remaining wells and measurements taken every 24 hours. For measurement of proliferation, cells were fixed with ethanol for 5 minutes and then incubated with Hoescht dye at a concentration of 2.5ug/ml for 5 minutes. After being washed three times with PBS, emission at 460nm with excitation at 560nm was measured using a Biotek plate reader. A baseline reading was taken by fixing adherent cells in 4 wells after 24 hours adherence step. Results were normalized to baseline assays.

Proliferation was assessed using Celltrace by incubating hepatoma cells with 10uM CFSE Celltrace at 37°C for 30 minutes. Five volumes of ice-cold media was added to quench staining and cells were incubated on ice for 5 minutes. After washing, cells were seeded into 12 well plates with varying concentrations of recombinant CXCL16 (Peprotech, New Jersey USA). After 5 days cells were trypsinised and washed before re-suspension in MACS buffer and analysis by flow cytometry.

Flow Based Adhesion Assay

Slides with six microchannels (Ibidi, Germany) were coated with rat-tail collagen (RTC) diluted at 1:100 in sterile water, by adding RTC to each channel for thirty minutes and then removing the remainder. HSEC isolated from explanted livers with a variety of liver diseases and cultured up to 3 passages, were suspended at $1x\ 10^6$ml, and cultured in the channels at 37°C/5% CO_2 until confluent, then stimulated with TNFα and IFNγ (Peprotech, New Jersey, USA, both10ng/mL) for 24 hours.

Isolated mononuclear cells were incubated in a T25 flask for at least an hour to deplete monocytes. Prior to initiating the flow assay lymphocytes were pretreated with either 10uM

CXCR6 inhibitor, $10\mu M$ DMSO or 40ng/mL sCXCL16 for 20 minutes. For CXCR6 blocking experiments, lymphocytes were incubated with a small molecule inhibitor of CXCR6 (C0335224-4B, ⬛⬛⬛⬛⬛⬛⬛⬛⬛⬛⬛⬛⬛⬛) dissolved in Dimethyl sulfoxide (DMSO) or DMSO alone, at 10uM for 20 minutes. Lymphocytes were then washed, re-suspended to 0.5×10^6 cells/mL in lymphocyte media and flowed over confluent HSEC at a rate of 0.28ml/minute to mimic shear stress of the hepatic sinusoid. Images were recorded for two minutes whilst lymphocytes were flowing over HSEC. After 4 minutes, media without lymphocytes was flowed at the same rate, and then further images recorded for 2 minutes. Images were analysed with regard to numbers of cells which were rolling, static, shape changing or transmigrated. Numbers of cells counted were normalised to number of cells/mm2/cells infused using the formula (number cells / (flow * bolus * area)) * (1 / # million cells).
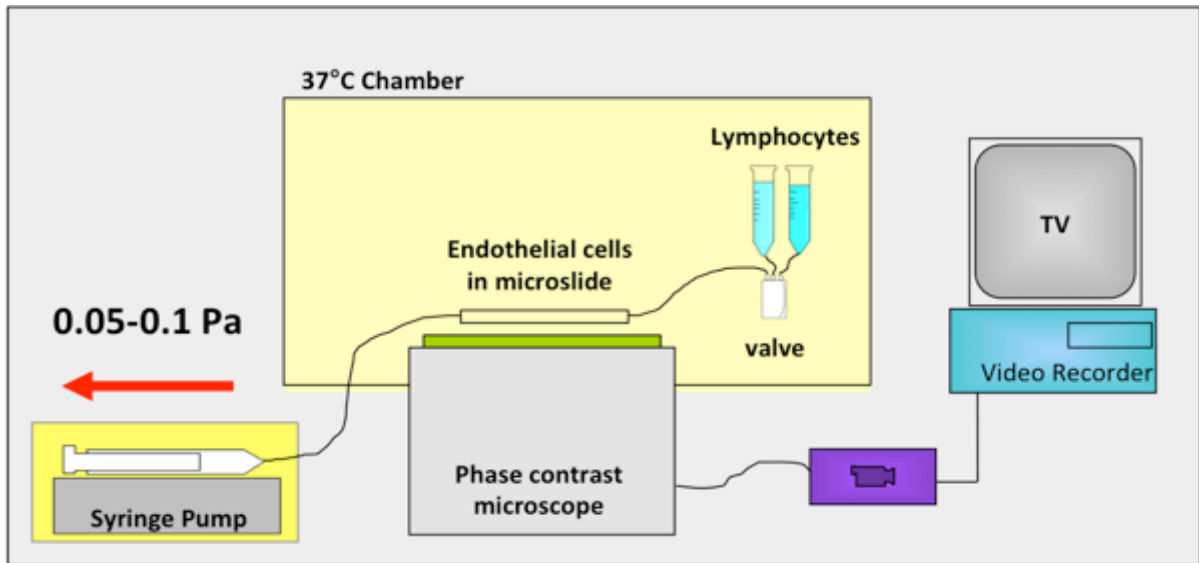
Figure 2.1: flow assay system

Isolated hepatic endothelial cells are grown to confluence in a monolayer in a microslide. Lymphocytes suspended at a known concentration are flowed at physiological shear rate across this endothelial monolayer by a syringe and syringe driver. The interaction of lymphocytes and endothelium is visualised in real time and recorded to DVD for analysis (Lalor et al., 1997).

Animal experiments

Mouse experiments were performed ▮▮▮▮▮▮▮▮▮▮▮▮▮▮▮▮ or at ▮▮▮▮▮ ▮▮▮▮▮▮▮▮▮. In both locations animals were housed according to local and national standards. In the UK and in the US, animal facilities were maintained at 23°c with twelve hour light/dark cycles. Male mice were used for all experiments, and were housed in the research locations for at least three days after delivery before investigations were started.

Animal work in the UK was performed under the auspices of a personal home office licence and under project licences held by senior investigators ▮▮▮▮▮▮▮▮▮▮▮▮ ▮▮▮▮▮▮▮▮▮▮▮.

Unless otherwise stated, mouse experiments used male C57/Black 6 (C57/Bl6) mice bred in controlled clean conditions, aged 6-8 week at the start of experiments. C57/Bl6 mice were obtained from ▮▮▮▮▮▮▮▮.

C57/Bl6 mice in which the *Cxcr6* gene was replaced with a gene expressing green fluorescent protein (GFP) were used in mouse experiments that analysed the role of CXCR6 in liver injury, were purchased from ▮▮▮▮▮▮▮. Animals were genotyped before experiments using end-point PCR.

Animal models of NAFLD

<u>MCD diet</u>

Feeding mice a diet deficient in methionine and choline (methionine-choline deficient diet, MCD diet) produces steatosis through increased hepatic uptake of fatty acids and decreased lipid secretion (Rinella *et al.*, 2008). Methionine and choline are important precursors of phosphatidylcholine, the principal phospholipid comprising the outer coat of VLDL particles (3). When these nutrients are in short supply, VLDL production is impaired and triglycerides accumulate in hepatocytes (2, 4). Inflammation develops through oxidative stress(Anstee and Goldin, 2006) leading to steatohepatitis. Weight loss is a major feature of this diet, in contrast to human NAFLD Mice were fed MCD diet for a period of 5-6 weeks and █████ when 30% of body weight was lost. A control group of littermates were fed a control diet (sufficient in methionine and choline) for the duration of the experiment, without intervention. MCD and control diet were obtained from █████

<u>High fat diet</u>

A high fat diet (HFD) in which 60% of calories are obtained from fat was used to produce a model of steatohepatitis akin to human disease. Male mice were given HFD for 16 weeks. A control group of littermates were fed control diet (10% of calories from fat) for the duration of the experiment, without intervention. HFD and control diet were obtained from █████ ███

Animal models of acute liver injury

Acute liver injury was modelled in mice by using Carbon tetrachloride (CCl_4) or paracetamol.

<u>Acute carbon tetrachloride liver injury</u>

CCl_4 was diluted 1:4 in corn oil (Sigma-Aldrich, Missouri USA) and a single dose of 1 ml/kg was administered to mice by intra-peritoneal (IP) injection. CCl_4 was handled and stored in a fume hood, and animal injections also performed in a fume hood. Corn oil without CCl_4 was used as control.

<u>Paracetamol-induced liver injury</u>

Paracetamol (Sigma-Aldrich, Missouri USA) was dissolved in sterile PBS at 10mg/mL by warming to 30°C with sonication. After initial experiments with non-fasted mice gave wildly divergent results, mice were fasted overnight before paracetamol administration to deplete hepatic glutathione and exaggerate liver injury. Paracetamol was administered by IP injection. Sterile PBS alone was used for sham injection. A maximum volume of 1mL was required.

Chemokine receptor antagonism

Small molecule inhibitors of chemokine receptors were manufactured by ▮▮▮▮▮▮▮▮ ▮▮▮▮▮▮▮▮▮▮▮. Small molecule inhibitors of CCR2 (CCX872) or CCR9 (CCX507) were dissolved in 1% hydroxypropyl methylcellulose (HPMC) and administered to mice by subcutaneous injection. CCX872 was given at a dose of 30mg/kg daily. CCX507 was used at a dose of 30mg/kg as a single injection. An equivalent volume of 1% HPMC was used in control mice. A maximum volume of 350uL was used.

Analysis of animal experiments

███████████████████ ███ ████████████████████████████████████

██

██ Blood

sampling and perfusion of organs with PBS were carried out through cardiac puncture. Blood

was placed into tubes containing citrate or EDTA for isolation of serum or plasma

respectively. After centrifuging in the tubes at 2000rpm/870g for ten minutes, serum or

plasma were frozen at -20°c for later analysis.

Laparotomy was performed and liver, subcutaneous fat, and omental fat removed. Liver

tissue was divided into individual lobes. Some were placed in cold RPMI for subsequent

isolation of immune cells, some snap frozen with liquid nitrogen and a lobe placed in formalin

for subsequent embedding in paraffin. Omental fat samples were placed into ice cold RPMI

for isolation of immune cells or snap frozen. Subcutaneous fat samples were snap frozen.

Triglyceride content of liver tissue

Triglyceride content of murine liver tissue was assessed using a commercially available

colorimetric assay kit (Cayman Chemical Company, Ann Arbor MI USA) according to the

manufacturer's instructions. In short, 400mg of liver tissue was suspended in 2ml of assay

diluent and homogenised. 10ul of homogenate was added to wells of a 96 well plate, each

sample was assayed in triplicate. Triglycerides were enzymatically hydrolysed to free fatty

acids and glycerol using the supplied enzyme mixture. After 15 minutes incubation colour

change was measured with a plate reader (Synergy HT, BioTek, Vermont, USA) measuring

absorbance at 540nm. A standard curve was generated by assaying known concentrations of triglyceride on the same plate as the samples, and the triglyceride concentration of samples interpolated from this curve. Triglyceride content of liver tissue was expressed as milligram per gram of liver tissue.

Glycaemic control

Glucose metabolism in mice was assessed with insulin and glucose challenge experiments. Insulin challenge was performed by administering 0.75U/kg of insulin to non-fasted mice via intra-peritoneal injection. Plasma glucose was measured with an AccuCheck glucometer (Roche, Basel, Switzerland) using a drop of blood from a tail vein. Plasma glucose was measured at baseline and 15, 30, 60, 90 and 120 minutes after insulin.

Mice were fasted overnight before glucose tolerance tests. Glucose was administered at 2g/kg of glucose (as 45% glucose solution), given by gastric lavage. Plasma glucose was measured baseline and 15, 30, 60, 90 and 120 minutes after administration of glucose using an AccuCheck glucometer and drops of blood from tail vein.

Statistical Analysis

Averages are expressed as mean and standard error of mean (SEM) for normally expressed data, and median and interquartile range (IQR) for skewed data. Normality was assessed with the Kolmogorov-Smirnov test. Normally distributed data were compared between groups with student's t-test, and the Mann-Whitney test used for skewed data. Variance across multiple groups, for example over a range of concentrations was analysed with one-

way analysis of variance (ANOVA). Variance between multiple groups across more than one variable, for example lymphocyte subsets was analysed with two-way ANOVA. Survival analysis was analysed by Kaplan-Meier curves with p values assessed with log-rank test. Median time to death in animals that died was also calculated.

Data were analysed using Prism version 5 (Graphpad Inc., California, USA).

CHAPTER 3: The role of CCR2 in Human Non-Alcoholic Fatty Liver Disease

Non-alcoholic fatty liver disease (NAFLD) is common: hepatic steatosis is present in up to one-third of individuals (Browning *et al.*, 2004) whilst the more severe non-alcoholic steatohepatitis (NASH) is seen in approximately 10% (Williams *et al.*, 2011).

Obesity-associated macrophage infiltration of adipose and hepatic tissue is mediated by CCR2 (Kanda *et al.*, 2006, Weisberg *et al.*, 2006, Lumeng *et al.*, 2007, Obstfeld *et al.*, 2010). Experiments in mice confirm that obesity up regulates CCL2 (Kirovski *et al.*, 2011). Absent or reduced CCL2 activity reduces hepatic steatosis (Kanda *et al.*, 2006) (Weisberg *et al.*, 2006, Nio *et al.*, 2012) and inflammation of liver tissue (Obstfeld *et al.*, 2010, Miura *et al.*, 2012). A central role for the CCR2/CCL2 axis has been suggested in human NAFLD (Haukeland *et al.*, 2006, Kirovski *et al.*, 2011).

The CCR2/CCL2 axis has been targeted with a variety of pharmaceutical agents in animal models of fatty liver disease. These studies have demonstrated reduced disease activity when either CCR2 or CCL2 are targeted (Tamura *et al.*, 2008, Yang *et al.*, 2009, Miura *et al.*, 2012) (Tamura *et al.*, 2010)(Baeck *et al.*, 2012) (Cynis *et al.*, 2013)

Despite a large amount of data describing a role for CCR2 and CCL2 in development of obesity and insulin resistance, this axis has not been investigated in depth in human NAFLD. I used *ex vivo* human samples to examine expression of CCL2 in human NAFLD and

correlated this with the expression of CCR2 on liver-infiltrating monocytes in healthy and diseased liver tissue.

Expression of CCL2 in NAFLD

Hepatic *CCL2* gene expression is higher in liver tissue from patients with NASH

To determine whether gene expression of *CCL2* was altered in liver tissue of patients with NASH, RNA was isolated from normal liver (from hepatic resections of malignant lesions - uninvolved tissue distal to the tumour was used), or explanted liver with NASH cirrhosis, and subsequently transcribed to cDNA. *CCL2* gene expression was analysed by quantitative real-time PCR (qRT-PCR) using *18S* as a housekeeping gene. *18S* has been shown to have lowest level of variability across stages of alcoholic liver disease (ALD) suggesting it is reliable as a housekeeping gene in steatohepatitis (Boujedidi *et al.*, 2012). *CCL2* gene expression was significantly up regulated in NASH cirrhosis (Mann Whitney test p=0.009) (**figure 3.1**).
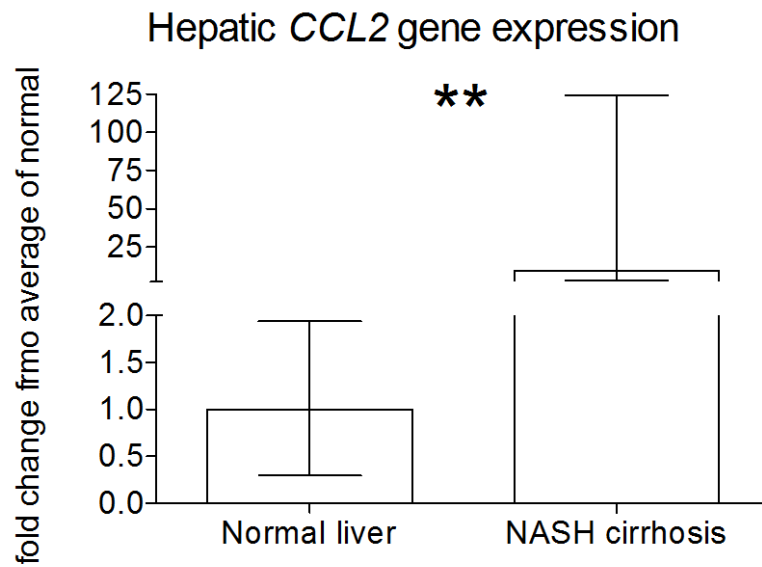
Figure 3.1: CCL2 mRNA expression is elevated in patients with NASH

RNA was isolated from normal liver (n=6) and NASH cirrhosis liver tissue (n=6). CCL2 gene expression was analysed by qRT-PCR, 18S was used as a housekeeping gene. CCL2 expression was normalised to overall median expression of CCL2 in normal liver. Line at median, boxes represent IQR and whiskers represent interquartile range.

Serum concentration of CCL2 is increased in fatty liver disease

After examining gene expression of *CCL2*, I measured CCL2 protein in serum by ELISA in individuals with biopsy-proven NAFLD (n=20), PBC (n=5) or healthy volunteers (n=10). Serum CCL2 concentration was significantly higher in patients with NAFLD compared to healthy controls (median 305.1pg/ml (IQR 211.8 – 385.7) vs. 224.7 (105.2 – 255.4), Mann-Whitney test p=0.021), and individuals with PBC (median 88.67 pg/ml, (IQR 35.9 – 168.5, Mann-Whitney test p=0.002) (**figure 3.2**). This is consistent with previous reports in NAFLD (Haukeland *et al.*, 2006, Kirovski *et al.*, 2011).
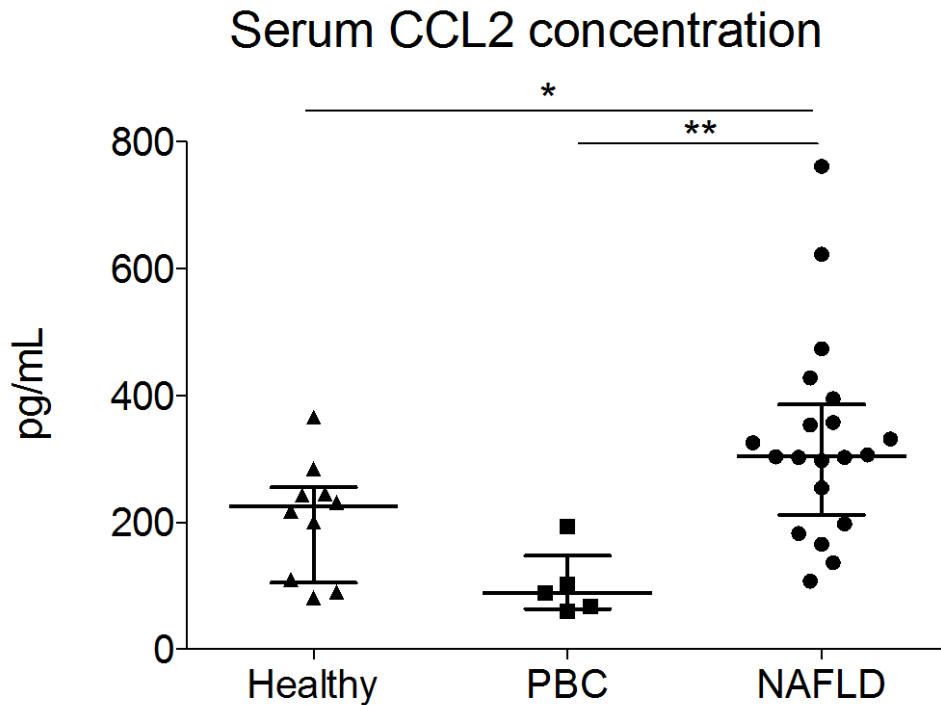
Figure 3.2: Increased serum CCL2 in NAFLD

Serum CCL2 concentration in healthy volunteers (n=10) and patients with PBC (5) or NAFLD (n=20) was measured by ELISA. *p<0.05, **p<0.01 by Mann Whitney test. Each point represents a single patient sample, data are shown with a line at the median and whiskers represent IQR.

Serum CCL2 in patients with NAFLD

 To investigate association between serum CCL2 concentration and disease, the NOBLES study was used to provide a larger dataset of biopsy-proven NAFLD. The NOBLES study was set up by my colleague Dr Chris Corbett to collect serum from patients with a variety of liver diseases who were undergoing liver biopsy, in order to assess serum markers of liver fibrosis and inflammation. All patients undergoing routine liver biopsy at University Hospitals Birmingham were invited to take part in the NOBLES study. Blood samples were taken two-three hours prior to liver biopsy and serum was frozen at -80°C until analysis. Several putative markers of fibrosis were measured and compared to histologically confirmed fibrosis. Dr Chris Corbett collected serum samples and performed the ELISA experiments on these samples. I collected data regarding biopsy characteristics of the group of patients with NAFLD and analysed the association with serum CCL2 concentration. Characteristics of this group are shown in **table 3.1**.

Variable		
Age (years, median)	57	Range 20 - 67
Gender (% female)	60	
BMI (kg/m^2, median)	33.1	Range 24.5 - 49
Platelets (x10^9/L, median)	200	93 – 367
Aspartate aminotransferase (AST) (U/mL, median)	36	15 -149
Alanine transferase (ALT) (U/mL, median)	51	14 - 172

Table 3.1: characteristics of patients with NAFLD included in NOBLES study cohort (n=39)

Fibrosis		Inflammation		
Score	Interpretation	Criteria	Score	Interpretation
0	No fibrosis	Steatosis	0	<5%
			1	5-33%
			2	>33% - 66%
			3	>66%
1	Perisinusoidal or periportal fibrosis	Lobular inflammation	0	No foci of inflammation
			1	< 2 foci per 200x field
			2	2-4 foci
			3	>4 foci
2	Perisinusoidal and portal or periportal	Ballooning	0	No ballooned hepatocytes
			1	Few ballooned hepatocytes
			2	Many ballooned hepatocytes
3	Bridging fibrosis			
4	Cirrhosis			

Table 3.2 Histological grading of NAFLD (Kleiner *et al.*, 2005)

Liver biopsy samples are assessed using the Kleiner-Brunt system which gives a measure of the degree of fibrosis and inflammation.

NAFLD was assessed histologically using the NAFLD activity score (NAS) proposed by Kleiner and Brunt in 2005 (Kleiner *et al.*, 2005), which grades inflammation from 0-8 depending on assessment of steatosis, ballooning degeneration of hepatocytes and lobular inflammation. Under this classification fibrosis is staged from 0 (no fibrosis) to 4 (cirrhosis) (**table 3.2**). Histological scoring was done by Professor Stefan Hubscher, Department of Pathology at University Hospitals Birmingham NHS Foundation Trust.

Serum CCL2 concentration is not associated with body mass index but does correlate with insulin resistance

Serum CCL2 concentration was not correlated with BMI (r^2 0.063, p=0.122), whereas a positive correlation was seen between serum CCL2 and insulin resistance, measured by HbA1c (**figure 3.3**). This is reflects a difference between simple fat mass (i.e. body mass) and inflammation of fat causing insulin resistance and is consistent with CCL2 as a pro-inflammatory chemokine in the metabolic syndrome.

A Serum CCL2 concentration and BMI

B Serum CCL2 concentration and insulin resistance
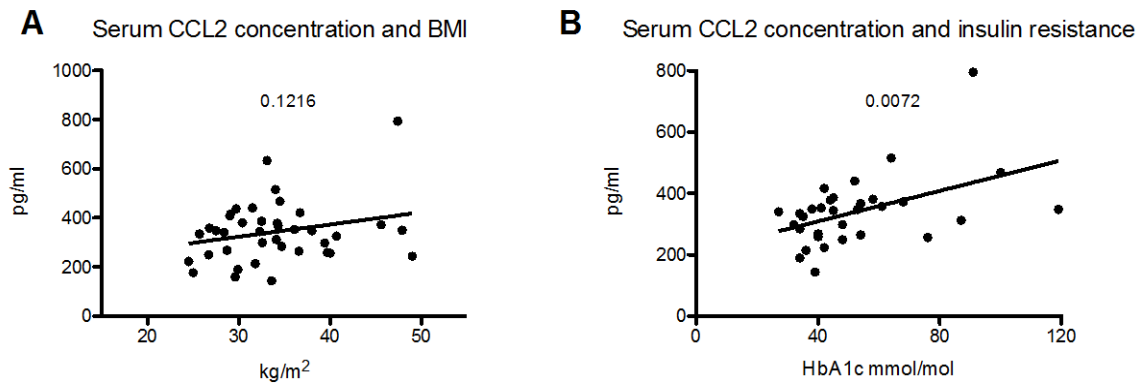
Figure 3.3 Serum CCL2 concentration correlates with insulin resistance but not BMI in patients with NAFLD

Serum concentration of CCL2 from patients with NAFLD in the NOBLES study was compared with **A** body mass index (n=39) and **B** insulin resistance, measured by HbA1c (n=32). No correlation was observed between CCL2 concentration and BMI, whereas a significant correlation was seen between CCL2 concentration and HbA1c.

A Serum CCL2 and overall NAS

B Serum CCL2/fibrosis in NASH
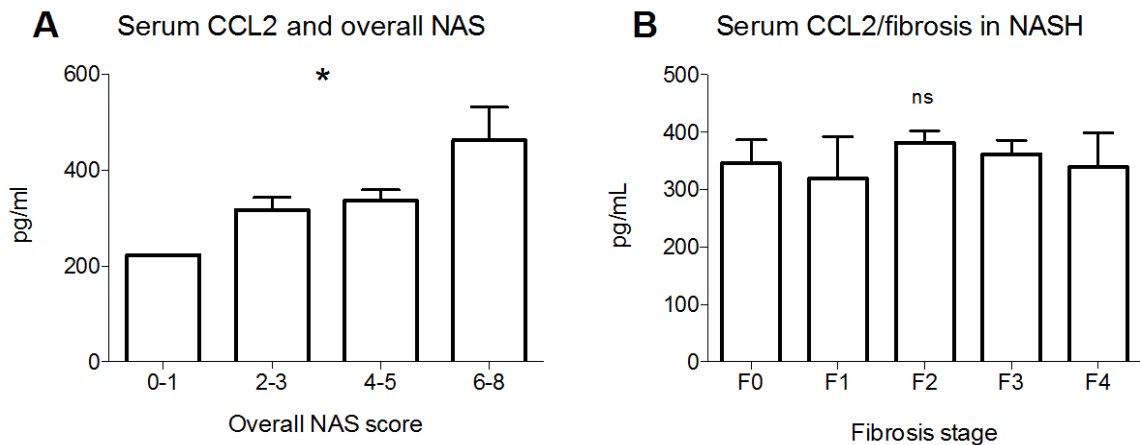
Figure 3.4 Serum CCL2 concentration correlates with inflammation but not fibrosis in NAFLD

Serum CCL2 concentration from patients with NAFLD in the NOBLES study was compared with histological assessment of disease.

A: CCL2 concentration was higher in patients with worse inflammation grade *one-way ANOVA p<0.05. Overall n=39: NAS 0- n=2; NAS 2-3 n=10; NAS 4-5 n=19, NAS 6-8 n=8. **B**: No association was seen between serum CCL2 concentration and fibrosis stage. Overall n=9 8: F0 n=5; F1 n=9; F2 n=4; F3 n=16: F4 n=5

Serum CCL2 concentration is associated with hepatic inflammation but not fibrosis

Serum CCL2 concentration was higher in individuals with worse histological inflammation grade (one way ANOVA p=0.025) but not with fibrosis stage (one way ANOVA p=0.347) (**figure 3.4**), consistent with a previous study demonstrating a correlation between CCL2 and serum ALT (Kirovski *et al.*, 2011). When individual components of the NAS were considered, serum CCL2 concentration was associated with higher lobular inflammation score (one-way ANOVA p=0.043) but not with steatosis or hepatocyte ballooning (**figure 3.5**). This is consistent with the known role of CCL2 as a chemo-attractant, with higher CCL2 expression leading to greater cellular infiltration into injured liver.
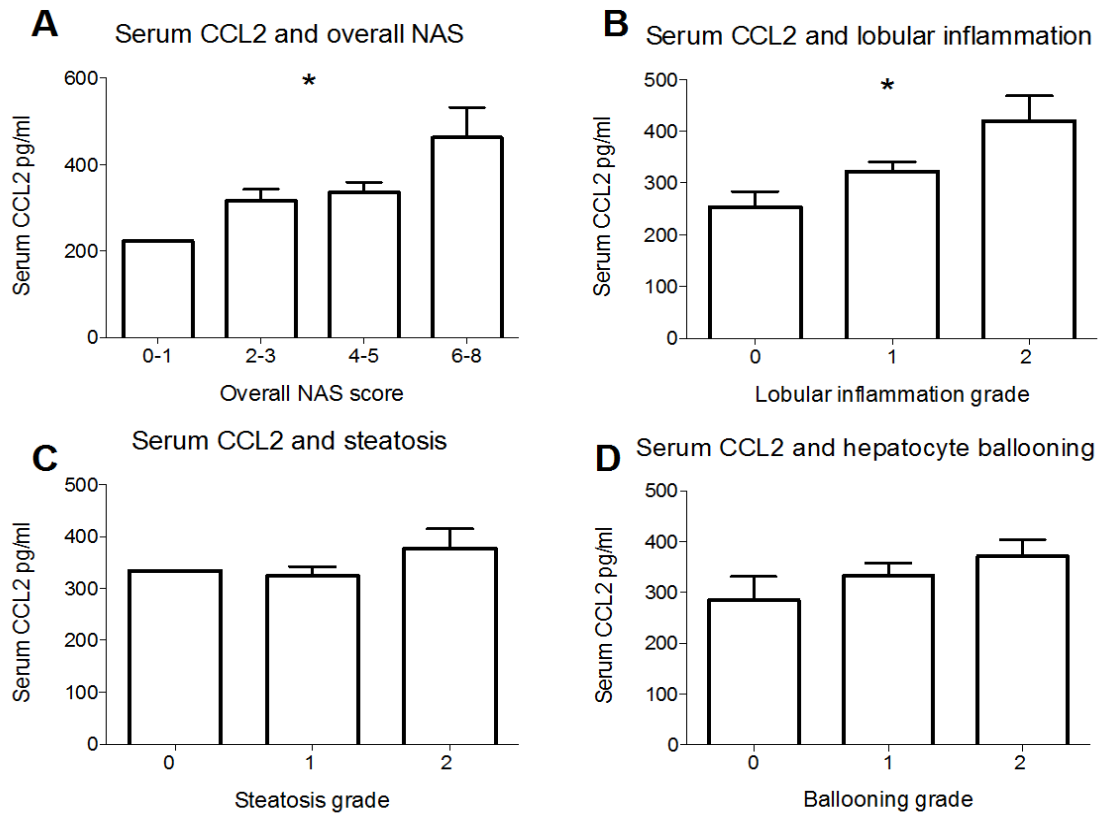
Figure 3.5 Serum CCL2 correlates with lobular inflammation in patients with NAFLD.

*Serum concentration of CCL2 from patients with NAFLD in the NOBLES study was compared to with individual components of NAS. Serum CCL2 was associated with A overall NAS score and B lobular inflammation, but not C steatosis or D hepatocyte ballooning *one way ANOVA p<0.05. Overall n=39:*

Expression of CCR2 on immune cells in NAFLD

In view of data showing up regulation of CCL2 in NAFLD and its correlation with inflammation grade, I went on to investigate expression of CCR2 in liver disease with a focus on NAFLD.

CCR2 is predominantly expressed by CD14$^+$CD16$^-$ monocytes

Monocytes in humans can be classified on the basis of CD14 and CD16 expression (**figure 3.6**) into classical CD14^{++}CD16$^-$ monocytes that predominate in blood; non-classical CD14$^-$CD16^{++} monocytes that are expanded under inflammatory conditions and an intermediate CD14^{++}C16$^+$ population of monocytes which also expand under inflammatory conditions. Previous reports from our laboratory have shown that diseased liver tissue in NASH and ALD is enriched for monocytes compared to normal tissue (Liaskou *et al.*, 2013) due to increases in the non-classical CD14$^-$CD16^{++} and intermediate CD14^{++}CD16$^+$ monocytes.

CD14⁻CD16⁺ non-classical monocytes

CD14⁺CD16⁺ intermediate monocytes

CD14⁺⁺CD16⁻ classical monocytes
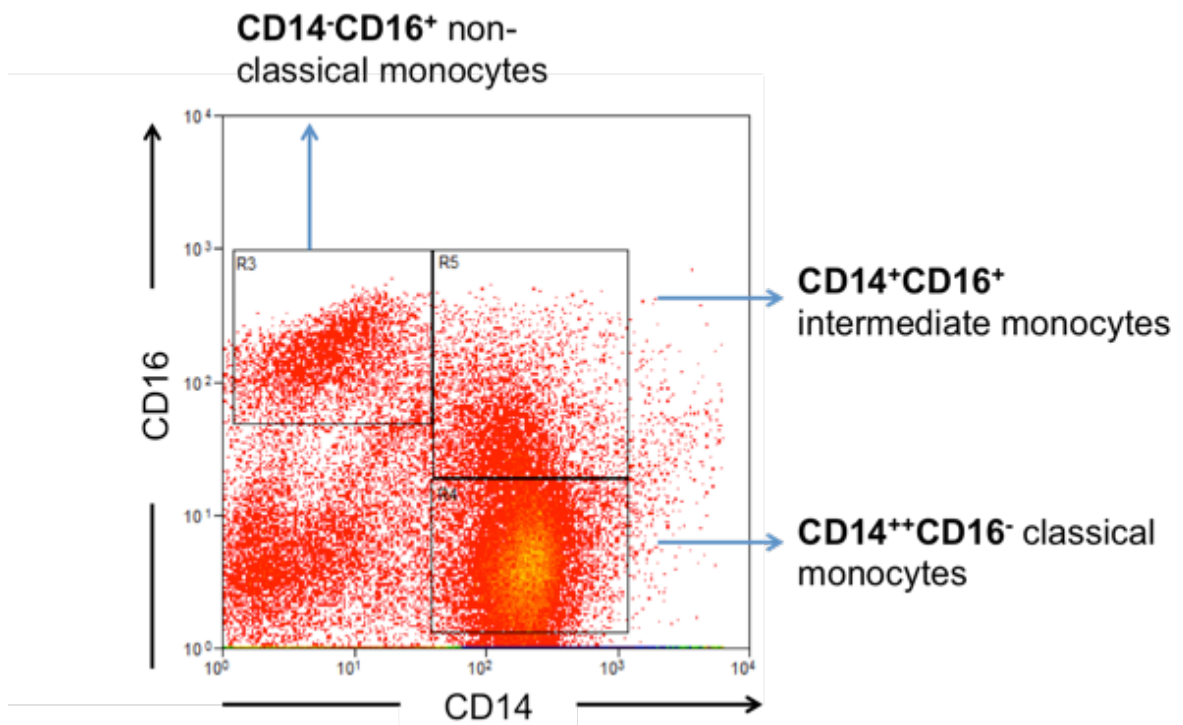
Figure 3.6: monocyte subsets identified by flow cytometry

Monocytes were identified by forward and side scatter and then on the basis of CD14 and CD16 expression. This identifies three subsets of monocytes: CD14⁺⁺CD16⁻ classical monocytes, CD14⁺CD16⁺ intermediate monocytes and CD14⁻CD16⁺ non-classical monocytes.

Monocytes were extracted from liver by non-enzymatic digestion of tissue, avoiding the risk of stripping of CCR2 from cell membranes, and isolated over a gradient and compared by flow cytometry with blood monocytes for CCR2 expression. In both blood and liver, CCR2 expression was predominantly on CD14$^+$ monocytes, with a greater proportion of the classical CD14^{++}CD16$^-$ subset showing CCR2$^+$ expression compared with intermediate CD14$^+$CD16$^+$ cells or non-classical CD14$^-$CD16$^+$ population (**figure 3.6**). Mean fluorescence intensity (MFI) of CCR2 signal was also higher on CD14$^+$CD16$^-$ monocytes but relatively preserved on CD14$^-$CD16$^+$ monocytes indicating fewer CD14$^-$CD16$^+$ cells expressing CCR2 but at a similar intensity to CD14$^+$CD16$^+$ monocytes. There was a trend for lower percentage CCR2 expression on liver-infiltrating monocytes but this was not significant (two-way ANOVA p=0.141), whereas MFI did differ between blood and liver (two-way ANOVA p=0.035).

Monocyte percentage CCR2 expression was similar across all types of liver disease (two-way ANOVA p=0.991), nor did CCR2 MFI differ between disease types (two-way ANOVA p=0.827) (**figure 3.7**).
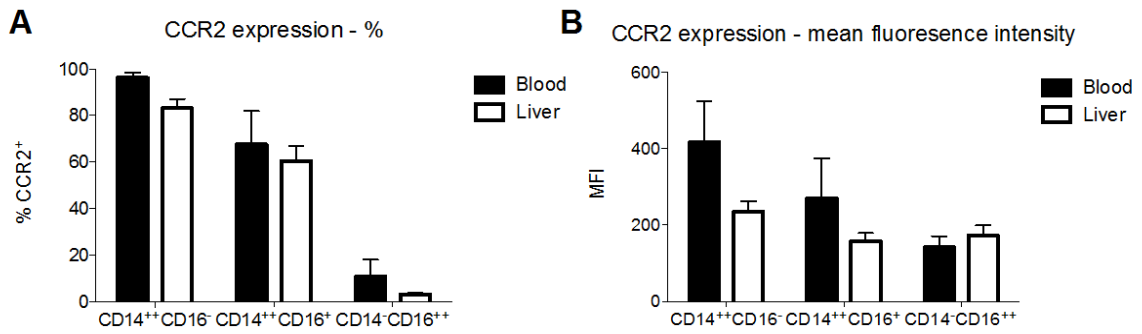
Figure 3.7: CCR2 is predominantly expressed by CD14+CD16- monocytes

Monocytes were isolated from blood or liver tissue and CCR2 expression analysed by flow cytometry. A Percentage expression of CCR2 on monocyte subsets in blood and liver. B CCR2 expression measured by mean fluorescent intensity on intrahepatic monocytes by disease. Data are shown as mean and SEM
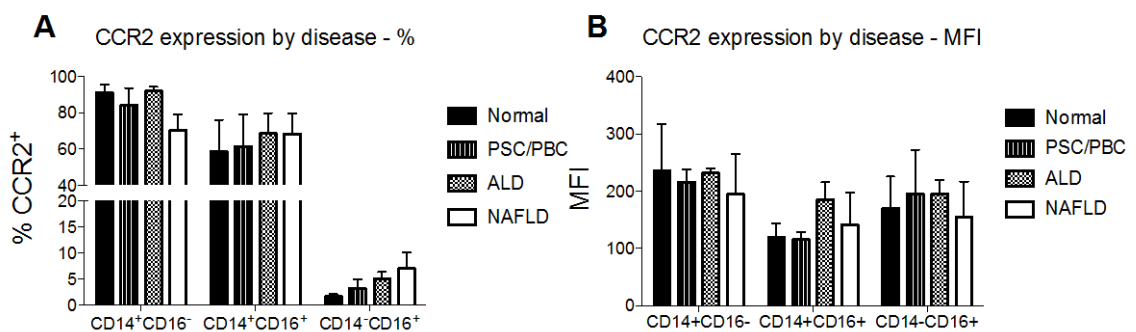
Figure 3.8: CCR2 expression on monocyte subsets across different types of liver disease

Monocytes were isolated from liver tissue and CCR2 expression analysed by flow cytometry. No significant differences in monocyte CCR2 expression was observed between disease types, with regard to either **A** percentage expression or **B** MFI. Data are shown as mean and SEM

CD14$^+$CD11c$^+$CD206$^+$ monocytes are enriched in liver tissue

As CCR2 was widely expressed on monocytes in both blood and liver its use as a sole marker to describe a population of immune cells relevant to a particular disease is limited. Therefore a more focused investigation was undertaken to identify a subset that may be relevant to FLD. A recent paper described of a subset of CD14+ macrophages expressing CD11c and CD206 in human adipose tissue (Wentworth *et al.*, 2010), which were associated with insulin resistance. As insulin resistance is a central feature of NAFLD, I examined this subset in further. Very few CD11c$^+$CD206$^+$ monocytes were observed in peripheral blood, whereas these cells were enriched in liver tissue (**figure 3.9**).
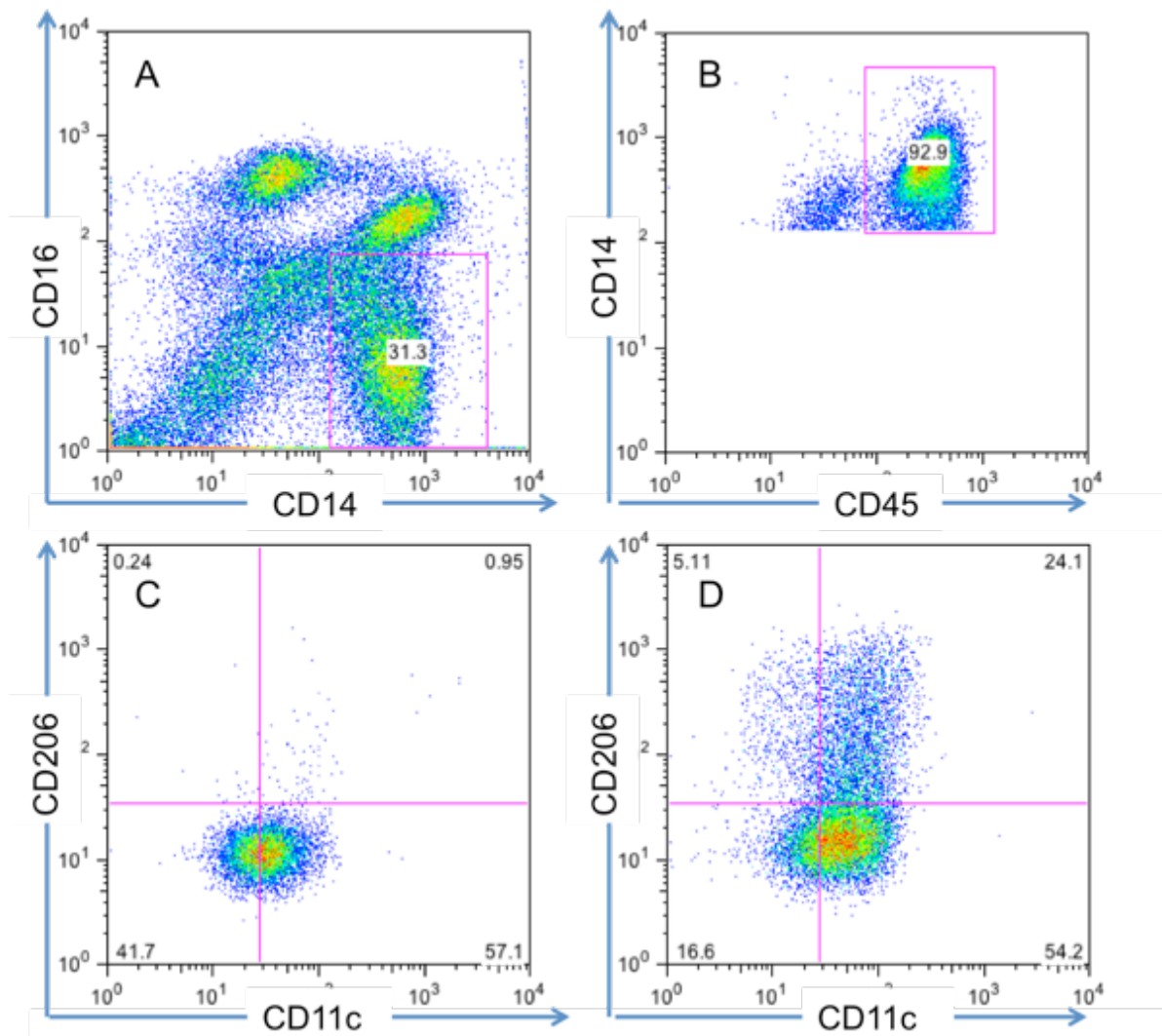
Figure 3.9: CD11c⁺CD206⁺ monocytes are enriched in liver tissue

Monocytes were isolated from blood and liver and analysed by flow cytometry. A and B: gating strategy: A identification of CD14⁺CD16⁻ cells, B CD45⁺CD14⁺ monocytes. Lower panels: CD11c⁺CD206⁺ monocytes in C blood and D liver from the same individual

Frequency of intrahepatic CD14$^+$CD11c$^+$CD206$^+$ monocytes is associated with insulin resistance

To begin to understand the function of CD11c+CD206+ monocytes, clinical parameters were examined. In keeping with previous descriptions of adipose infiltrating cells, a correlation between the number of intrahepatic CD14+CD11c+CD206+ monocytes and insulin resistance (measured with glycosylated haemoglobin (HbA1c)(Rohlfing *et al.*, 2002) was observed (r2 0.562 p=0.0013)(**figure 3.10**). No significant correlation was observed with age, BMI or ALT (**table 3.3**).

	Correlation r^2	p
HbA1c	0.562	0.001
Age	0.1434	0.148
BMI	0.037	0.461
ALT	0.158	0.128

Table 3.3: correlation of clinical markers with frequency of CD11c⁺CD206⁺ monocytes in liver tissue

Monocytes were isolated from liver tissue (both NAFLD and non-NAFLD) and analysed by flow cytometry. Correlation of frequency of intrahepatic CD11c+CD206+ monocytes (as percentage of CD45+CD14+ cells) with clinical markers was investigated
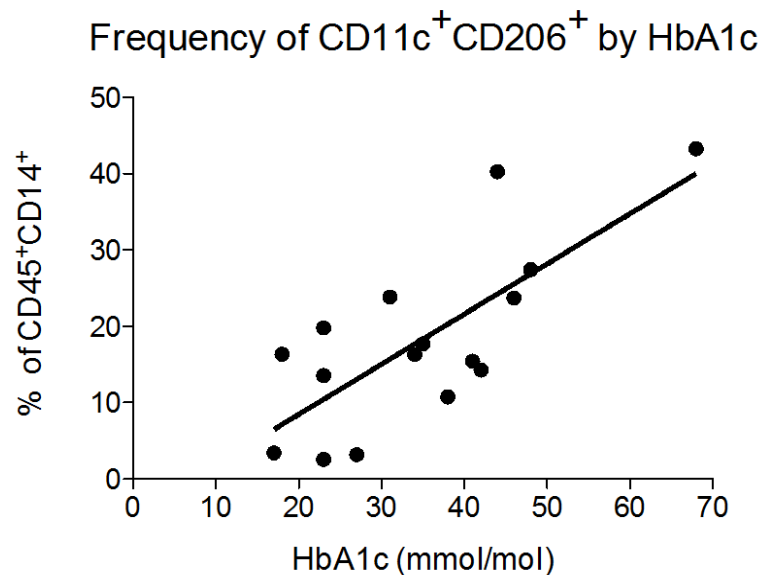
Figure 3.10: The frequency of intrahepatic CD14⁺CD11c⁺CD206⁺ monocytes is associated with insulin resistance

Correlation of the frequency of intrahepatic CD14⁺CD11c⁺CD206⁺ monocytes (as percentage of CD14+cells) and insulin resistance (as assessed by HbA1c fraction) (r2=0.562, p=0.001). Each data point represents an isolate from an individual patient.

CD14+CD11c+CD206+ monocytes are more frequent in NAFLD liver tissue than that from non-NAFLD-related chronic liver disease

The frequency of CD11c$^+$CD206$^+$ monocytes, as a percentage of CD45$^+$CD14$^+$ cells, differed significantly between types of liver disease (one-way ANOVA p=0.034) with highest expression seen in NAFLD (**table 3.4**, **figure 3.11**). Interestingly a high frequency of these monocytes was also seen in alcoholic liver disease (ALD), which has many pathological processes in common with NAFLD.

Liver tissue	CD11c$^+$CD206$^+$ (mean frequency of CD45$^+$CD14$^+$)	SEM
Normal	14.58	3.58
ALD	5.51	5.58
PSC/PBC	15.16	8.90
NAFLD	39.25	10.20

Table 3.4: Frequency of CD11c+CD206+ monocytes by disease

Monocytes were isolated from liver tissue and analysed by flow cytometry. Greater frequency of CD11c+CD206+ monocytes was observed in NAFLD tissue
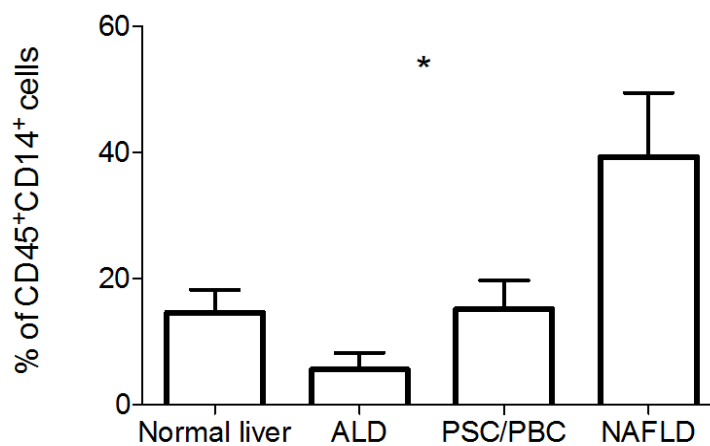
Figure 3.11: frequency of CD11c+CD206+ monocytes in liver tissue differs between type of liver disease.

Monocytes were isolated from liver tissue removed at resection or transplantation and analysed by flow cytometry. The frequency of CD11c$^+$CD206$^+$ monocytes differed significantly between types of liver disease and were more common in NAFLD tissue. Mean and SEM, *$p<0.05$ by one-way ANOVA.

CD14⁺CD11c⁺CD206⁺ monocytes express CCR2 in NAFLD

Intrahepatic CD14$^+$CD11c$^+$CD206$^+$ monocytes expressed higher levels of CCR2 in NAFLD compared to non-NAFLD liver tissue (median non-NAFLD expression 50.6% (IQR 33.8) vs 76.8 (15.6) Mann-Whitney test p=0.008) (**figure 3.12A, 3.13**) although MFI was not significantly different (median MFI Non-NAFLD 201 (IQR 126) vs. 310 (153.9), Mann Whitney p=0.200)(**figure 3.12B**, **figure 3.13**). Interestingly high CCR2 expression on this population was also observed in ALD, although fewer CD11c$^+$CD206$^+$ monocytes were seen overall (**figure 3.11**).
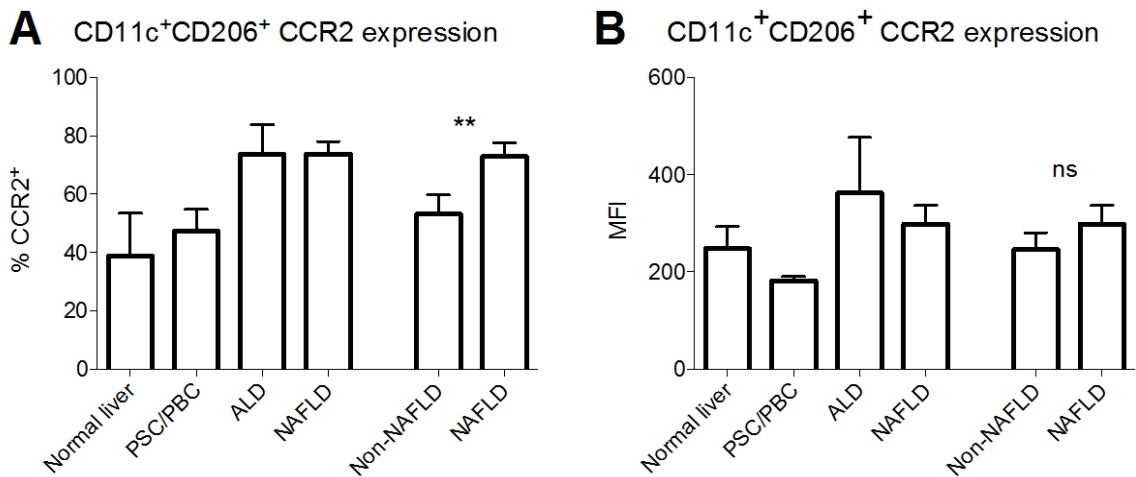
Figure 3.12: CD14⁺CD11c⁺CD206⁺ monocytes express CCR2 more frequently in NAFLD but total CCR2 expression is not significantly different

*Monocytes were isolated from liver tissue removed at resection or transplantation and analysed by flow cytometry. A CD11c+CD206+ monocytes from patients with NAFLD express CCR2 more frequently than non-NAFLD patients B: mean fluorescence intensity of CCR2 was not significantly higher in NAFLD. ** student's t-test p<0.01, ns student's t-test test p>0.05*
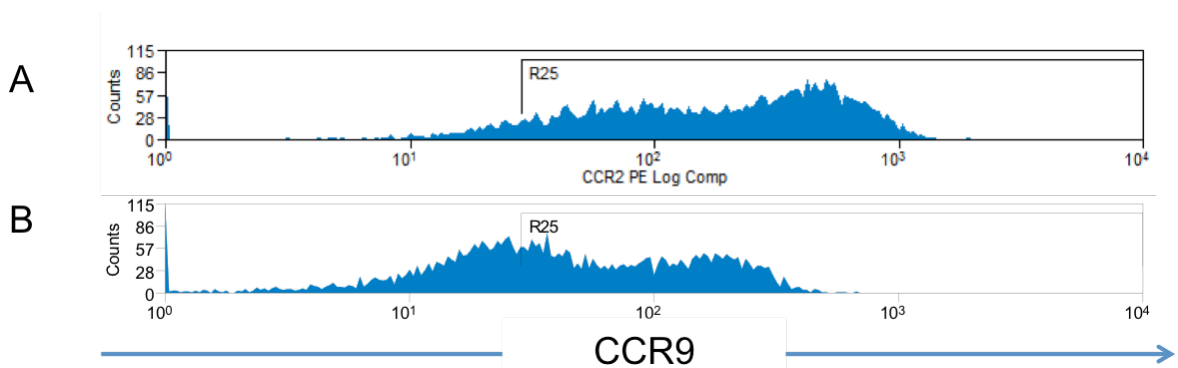
Figure 3.13: CD14+CD11c+CD206+ monocytes express CCR2 more frequently in NAFLD but total CCR2 expression is not significantly different

*Example FACS plots gated on CD11c⁺ CD206⁺ cells from **A** NASH liver and **B** Non-NASH liver (in this case Primary Biliary Cirrhosis) to illustrate greater CCR2 expression in NASH liver tissue*

Discussion

My data show that the CCR2/CCL2 axis is activated in human NAFLD. Greater gene expression of CCL2 was seen in liver tissue from patients with NAFLD, as well as increased serum concentrations of CCL2, which correlated with disease activity on liver biopsy and lobular inflammation in particular. CCR2 expression is common on $CD14^+CD16^-$ monocytes in both blood and liver, and no significant differences were found between liver diseases of varying aetiologies. This was also true of $CD14^+CD16^+$ and $CD14^-CD16^+$ monocyte populations.

A subset of $CD14^+$ monocytes that express CD11c and CD206 have been associated with insulin resistance in adipose tissue, where they secrete pro-inflammatory cytokines and T-cell chemoattrants (Wentworth *et al.*, 2010). I detected few of these cells in blood but found them to be markedly enriched in liver tissue, particularly in patients with NAFLD, and their frequency in liver tissue correlated with insulin resistance. Whilst my data do not provide information on the cells' function they may also promote insulin resistance by secreting inflammatory cytokines as they were shown to in adipose tissue. The finding that few monocytes in blood express CD206 suggests that expression is induced after recruitment of monocytes into liver tissue, a process which may require a pro-inflammatory microenvironment as lower expression was seen in non-diseased liver tissue.

$CD11c^+CD206^+$ monocytes express CCR2, with the highest levels and frequencies observed in NAFLD and ALD, a disease which shows the same histological appearances of steatohepatitis (Diehl *et al.*, 1988). While modest alcohol intake is associated with improved insulin sensitivity (Hendriks, 2007), excessive alcohol intake is associated with insulin

resistance (Iturriaga *et al.*, 1986) and its complications such as diabetes (Holbrook *et al.*, 1990) and cardiovascular disease (Hvidtfeldt *et al.*, 2008). ALD is also associated with increased insulin resistance (Kruszynska *et al.*, 1991). In addition, CCL2 is shown to mediate steatosis and inflammatory infiltration in animal models of ALD although this seemed independent of CCR2 (Mandrekar *et al.*, 2011). There are therefore broad similarities between NAFLD and ALD that can explain the observation of CCR2 expression on CD11c$^+$CD206$^+$ monocytes, however many more CD11c$^+$CD206$^+$ cells were seen in NAFLD liver than ALD liver.

These data support a role for CCR2-mediated infiltration of liver tissue by monocytes that contribute to disease in steatohepatitis.

CHAPTER 4: CCR2 Antagonism in Animal Models of Non-alcoholic Fatty Liver Disease

In the previous chapter I described a role for CCR2 and CCL2 in human NAFLD. In view of these findings I investigated the effect of antagonism of CCR2 in two murine models of NAFLD, using a small molecule CCR2 antagonist (CCX872, ████████████████ ████). I examined the principle features of human NAFLD: steatosis, inflammation and fibrosis together with infiltration of myeloid cells into liver tissue in two animal models o methionine-choline deficient (MCD) diet and high fat diet (HFD).

CCX872 is a small molecule inhibitor of mouse and human CCR2. It is an orally available compound that has been used safely in phase 1 studies where it was tolerated well without significant side effects (Bekker *et al.*, 2013). It is a specific inhibitor of mouse and human CCR2 with a half-life of approximately 24 hours in serum.

Methionine-Choline Deficient diet

A methionine-choline deficient (MCD) diet causes steatohepatitis by inhibition of lipid export from hepatocytes (Anstee and Goldin, 2006) which progresses to fibrosis. Unlike human NAFLD, MCD diet does not cause obesity or insulin resistance and although animals develop fibrosis they do not develop cirrhosis. Thirty male C57/Bl6 mice aged 6 weeks were fed MCD diet for five weeks. Two weeks of diet without intervention was used to establish disease. After two weeks, mice were divided into two groups and given either 30mg/kg/day

of CCX872 or matched volume of vehicle (2% hydroxypropyl methylcellulose, HPMC), administered subcutaneously (**figure 4.1**). A group of five littermates were maintained on a normal diet for the duration of the experiment without intervention.
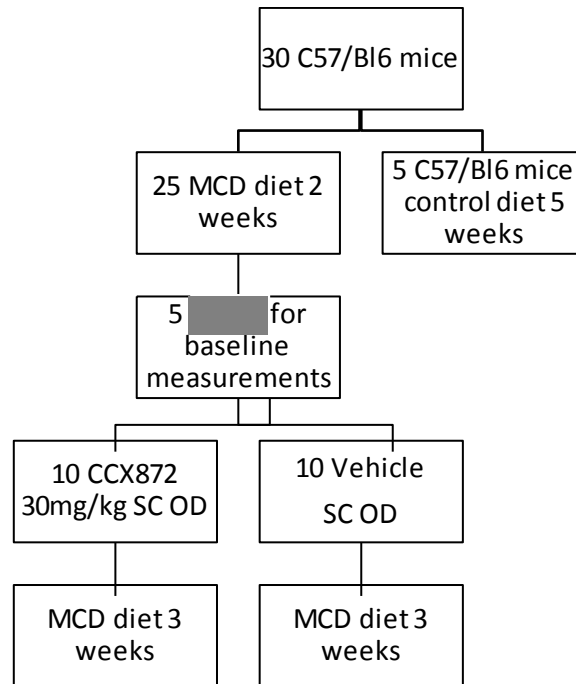
Figure 4.1: Experimental design of MCD experiment

Twenty-five C57/Bl6 mice were fed MCD diet. After two weeks mice were divided into two groups and 30mg/kg of CCX872 or matched volume of vehicle was administered once daily by subcutaneous injection. A further 5 mice were given a control diet without any intervention.
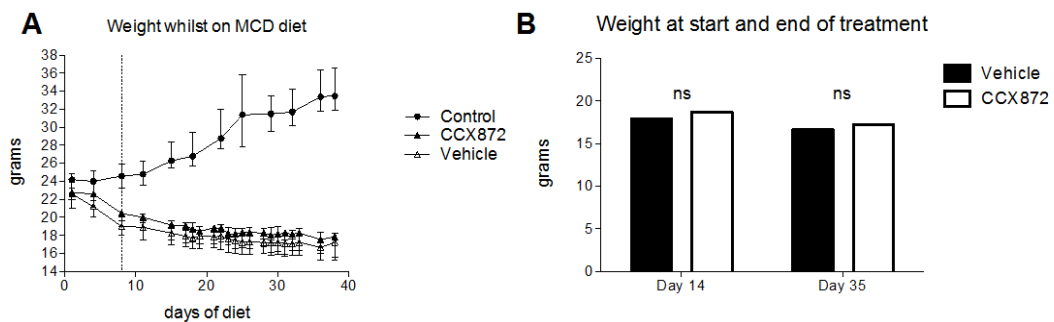
Figure 4.2: CCR2 antagonism does not alter MCD diet-induced weight loss

C57/Bl6 mice were fed an MCD diet or control diet for 5 weeks. After two weeks mice on MCD diet were treated with either CCR2 antagonist CCX872 (n=10), or vehicle (n=10). **A:** Marked weight loss occurred in animals fed an MCD diet: vertical line indicates start of administration of CCX872 or vehicle. Data are shown as median and interquartile range. **B** no difference in weight was observed between vehicle and control groups at the start (day 14) or end (day 35) of treatment. Data shown as mean and SEM, ns=non significant by students t-test

CCR2 antagonism does not alter weight loss on MCD diet

The MCD diet induced marked weight loss, consistent with previous reports (Anstee and Goldin, 2006). No differences in weight loss were observed between mice treated with CCX872 or vehicle (**figure 4.2**).

CCR2 antagonism does not alter hepatic steatosis caused by MCD diet

Steatosis was assessed by measuring the triglyceride content of liver tissue with a commercially available colorimetric assay. Considering the experiment as a whole, there was a significant difference between the three groups (control diet, vehicle-treated and CCX872-treated mice) (one-way ANOVA p=0.038) (**figure 4.3**). Considering comparisons between the groups of mice given MCD, there was no significant difference in the median liver triglyceride content of vehicle and CCX872 treated mice (70.1mg/g (IQR 80.9) vs. 57.9 (61.5), Mann Whitney test p=0.190) (**figure 4.3**). However, mice in the vehicle-treated group had significantly higher liver triglyceride content compared to mice on a control diet (70.1mg/g (IQR 80.9) vs. 36.1mg/g (80.9), Mann Whitney test p=0.003), whereas liver triglyceride content of mice treated with CCX872 did not differ significantly from control diet (Mann Whitney test p=0.371).

Triglyceride content of liver tissue
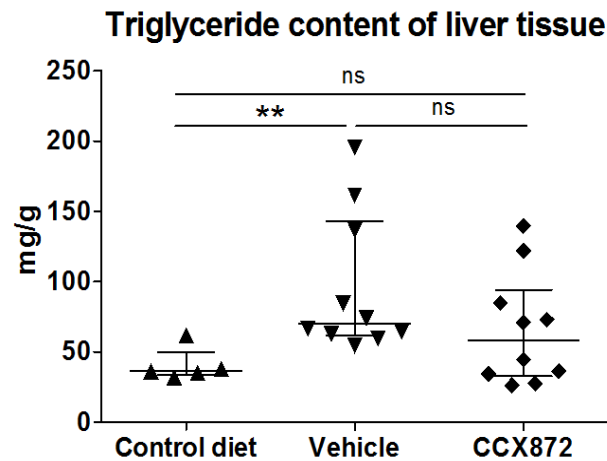
Figure 4.3: CCR2 antagonism does not alter hepatic steatosis caused by MCD diet.

*Triglyceride content of liver tissue was analysed using an enzyme-based colorimetric assay. Hepatic triglyceride content of mice given CCX872 or vehicle was comparable, but only vehicle treated mice differed significantly from control animals **p<0.01 by Mann Whitney test. (Each data point represents a single animal, lines at median, whiskers represent interquartile range).*
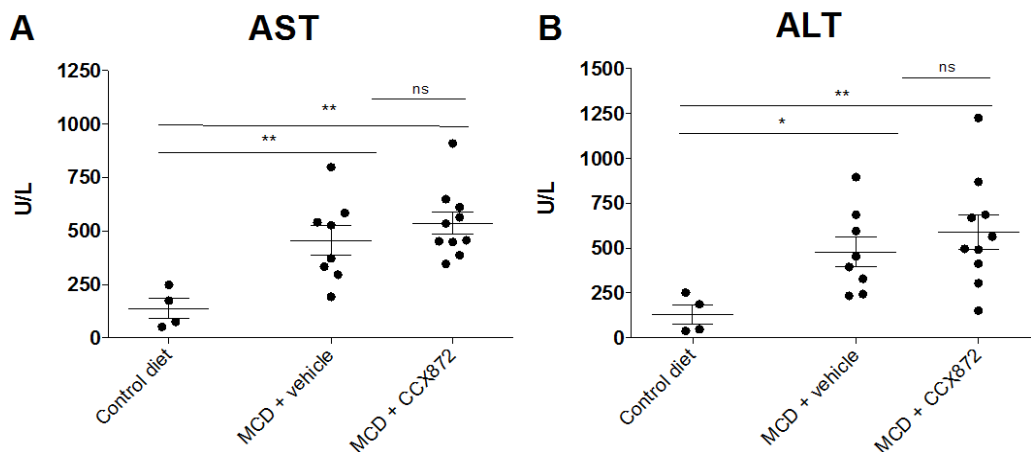
Figure 4.4: CCR2 antagonism does not reduce serum AST or ALT elevation by MCD diet

*C57/Bl6 mice were fed an MCD diet or control diet for 5 weeks. After two weeks mice on MCD diet were treated with a CCR2 antagonist, CCX872, or vehicle. A group of littermates were fed a control diet without intervention for 5 weeks. Liver injury was assessed by serum A AST and B ALT concentration. No differences were observed between CCX872 and vehicle-treated mice. Each point represents an individual mouse, data shown as mean and SEM, *p<0.05 **p<0.001 by student's t-test.*

CCR2 antagonism does not reduce serum AST or ALT elevation by MCD diet

Blood samples were taken by cardiac puncture at the time of ▮▮▮▮▮▮. Serum was analysed for AST and ALT concentrations, as markers of hepatocyte injury and surrogate markers of inflammation. Mice that were fed MCD diet for five weeks had significantly higher serum AST and ALT concentrations than mice on a control diet (**figure 4.4**).

Whilst overall differences between groups were seen by one-way ANOVA for both AST (p=0.003) and ALT (p=0.038), no differences in AST or ALT concentration were seen between vehicle and CCX872-treated mice (**figure 4.4**). No significant differences were seen between mice at baseline (at two weeks) and mice given MCD diet and CCX872 or vehicle for a further three weeks.

CCR2 antagonism reduces infiltration of liver tissue by pro-inflammatory monocytes caused by MCD diet

Inflammation was investigated by flow cytometry of liver tissue to identify sub-groups of infiltrating monocytes. No differences were seen in total infiltrating cells. Monocytes were classified as $CD11b^+F4/80^{lo}$ and further subdivided by Ly6c expression. Fewer infiltrating $Ly6c^{hi}$ monocytes were seen in mice given CCX872 compared to vehicle-treated mice (percentage of $CD45^+$ cells, 5.52 (SEM 0.38) vs. 8.28 (1.17), student's t-test p=0.038) (**figure 4.5A**). No significant differences were seen in $Ly6c^{dim}$ monocytes (**figure 4.5B**).
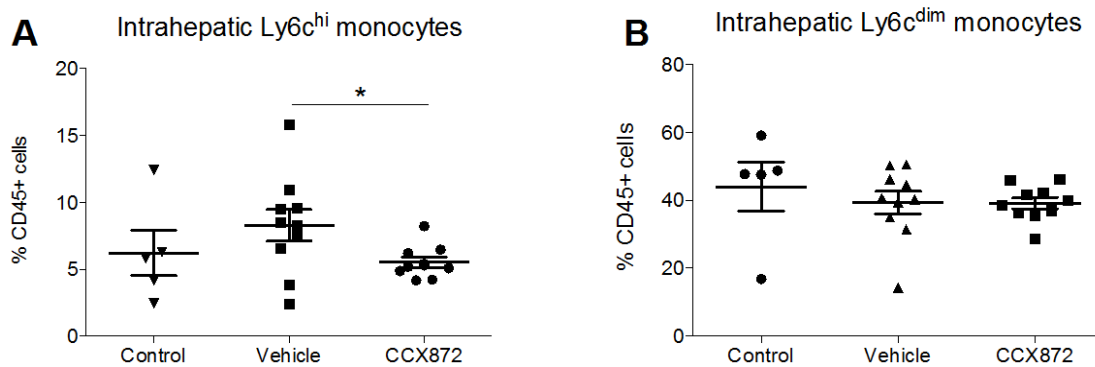
Figure 4.5: CCR2 antagonism reduces infiltration of liver tissue by pro-inflammatory monocytes caused by MCD diet

C57/Bl6 mice were fed an MCD diet or control diet for 5 weeks. After two weeks mice on MCD diet were treated with CCR2 antagonist CCX872, or matched volumes of vehicle. Fewer intrahepatic CD11b⁺Ly6c^{hi} monocytes were observed in mice treated with CCX872 compared to in mice given vehicle **C** No differences in CD11b⁺Ly6c^{lo} monocytes were observed. Each symbol represents one animal, lines represent mean and SEM, *p<0.05 by student's t-test.

High Fat Diet

Steatohepatitis can be induced in mice by feeding a high fat diet (HFD) (Anstee and Goldin, 2006). This has greater relevance to human NAFLD as mice fed HFD exhibit obesity and insulin resistance which is not seen in the MCD diet model (Rinella and Green, 2004). Thirty male C57/Bl6 mice aged 6 weeks at the start of the experiment were given HFD for 16 weeks. This diet delivered 60% of calories from fat. After eight weeks of HFD, four mice were ▮▮▮ to establish presence of liver injury. The remaining mice were divided into two groups: thirteen were treated with CCX872 (30mg/kg/day, administered by subcutaneous injection) and 13 received an equivalent volume of vehicle (1% HPMC). A further 8 littermates were given control diet for the duration of the experiment (**figure 4.6**).
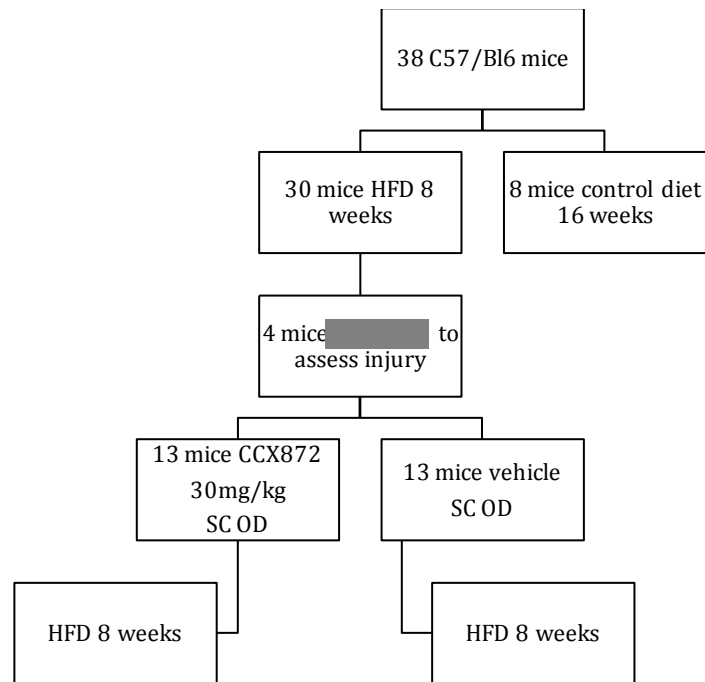
Figure 4.6: Experimental design of HFD experiment

C57/Bl6 mice were fed a high fat diet for eight weeks. After eight weeks mice were divided into two groups and 30mg/kg of CCX872 or matched volume of vehicle was administered once daily by subcutaneous injection and diet continued for a further eight weeks. A further 8 mice were given a control diet, without any intervention for 16 weeks.

CCR2 antagonism reduces weight gain caused by HFD

Bodyweight of mice in vehicle and CCX872 treated groups did not differ at the start of treatment (8 weeks of diet). Over the course of treatment, both groups continued to gain weight but the CCX872 treated mice gained significantly less weight than those treated with vehicle (**figure 4.7A, B**). To investigate possible causes for this, food intake was assessed over the final two weeks of treatment by weighing the food given to mice when it was put into the cage, and then 24 hours later. This gave a crude indication of overall food intake for each cage. No differences were seen between vehicle and CCX872-treated mice (**figure 4.8A**). Concern that reduced weight might be due to side effects of CCX872 prompted an *ad hoc* assessment of wellbeing of mice. Three observers examined each mouse individually without knowing which diet or treatment it was receiving. Mice were given a score for activity, appearance and wellbeing with a maximum score of ten. On this assessment mice in vehicle and CCX872-treated groups did not appear to differ (**figure 4.8B**).
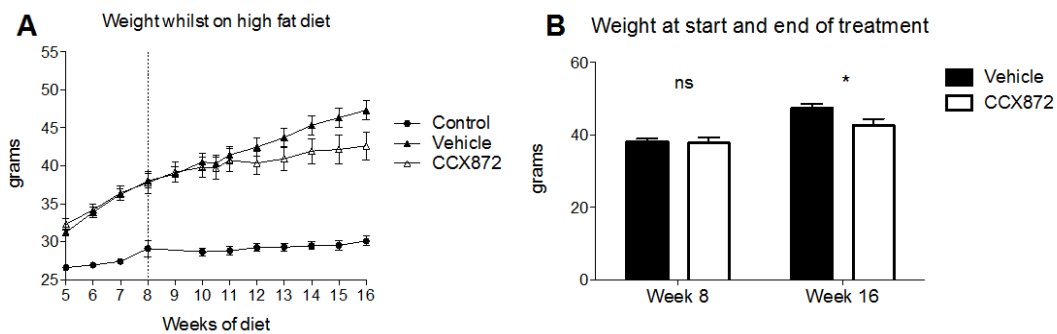
Figure 4.7: CCR2 antagonism reduced weight gain caused by HFD

C57/Bl6 mice were fed HFD (n=30) diet or control diet (n=8) for sixteen weeks. Mice on HFD were treated with a small molecule antagonist of CCR2, CCX872 (n=13), or vehicle (n=13) for the last 8 weeks of diet. Weight was comparable between treatment groups at the start of treatment; both groups gained much more weight than mice fed a control diet. By the end of the experiment mice treated with CC872 had a lower average weight than mice treated with vehicle. Data shown as mean and SEM, vertical line indicates start of treatment with CCX872 or vehicle. ns=non-significant, *p<0.05 by student's t-test
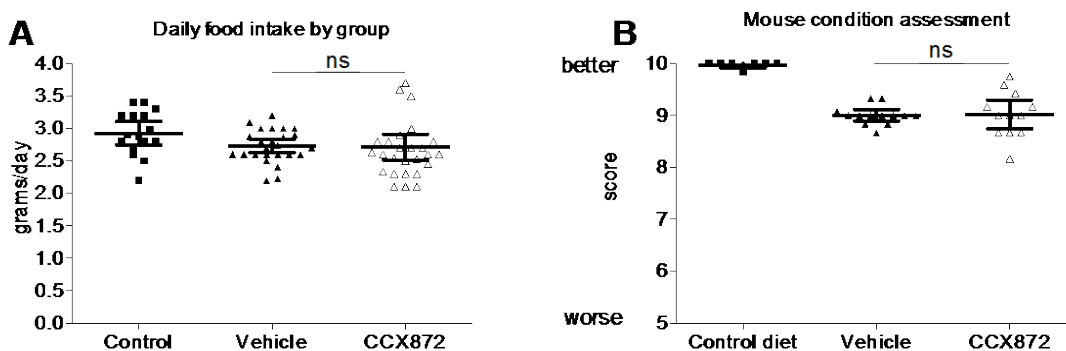
Figure 4.8 No differences were observed in food intake or condition of mice

*A Dietary intake was assessed by weighing food over four 24 hour periods during the final two weeks of treatment. Each data point represents food intake for an individual cage for a single 24 hour period. Food intake appeared comparable between mice treated with vehicle or CCX872. **B** The condition of animals during week 14 (after 6 weeks of treatment) was assessed by three people blinded to which diet or treatment mice were receiving. Mice were given a score between 1 and 10 to indicate the wellbeing of individual animals. Mice treated with vehicle or CCX872 did not differ in appearance.*

CCR2 antagonism reduces hepatic steatosis caused by HFD

Steatosis was assessed by measuring triglyceride content of liver tissue with a commercially available colorimetric assay. After 16 weeks of HFD, there was marked steatosis in all mice on HFD. Mice treated with CCX872 had significantly less triglyceride accumulation in comparison with vehicle treated mice (169.6mg/g ±21.20 vs. 284.2 ±31.9, student's t-test p=0.007) and was not significantly different from animals receiving control diet (**figure 4.9**).

CCR2 antagonism lowers HFD-induced serum ALT concentration

Blood samples were taken by cardiac puncture at the time of ▮▮▮▮ Serum was analysed for AST and ALT concentrations, markers of hepatocyte necrosis. AST concentration was lower in CCX872 treated mice but this was not statistically significant (mean 357.8IU/ml ±68.92 vs. 510.7 ±91.67, student's t-test p=0.210). Serum ALT was lower in CCX872-treated mice and this difference was statistically significant (mean ALT 252.5IU/ml ±56.02 vs. 532.8 ±98.07, student's t-test p=0.028). Serum AST concentration in mice fed a control diet was surprisingly high (**figure 4.10**).

Whilst a similar pattern for AST and ALT was observed, This difference was only of statistical significance for ALT. ALT is a more liver-specific enzyme, whereas AST is also found for example in muscle. The more robust result for ALT may therefore reflect a liver-specific improvement. Conversely an unanticipated effect on muscle function might explain these findings.

HFD: Liver triglyceride content
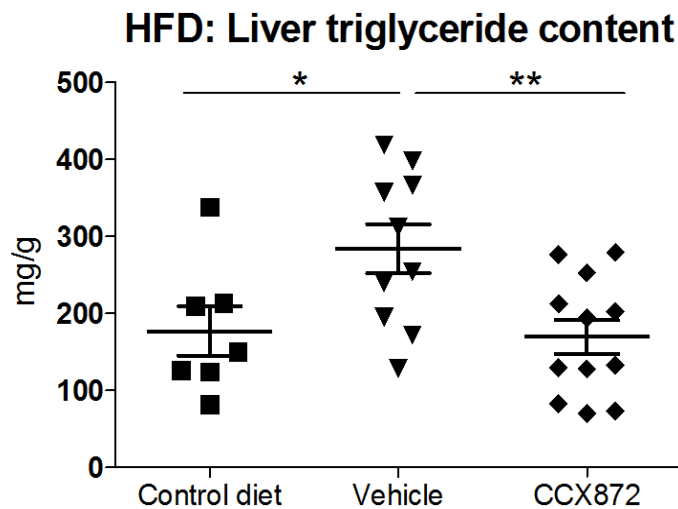
Figure 4.9: CCR2 antagonism reduces hepatic steatosis caused by HFD

C57/Bl6 mice were given HFD diet or control diet for sixteen weeks. Mice on HFD were treated with a small molecule antagonist of CCR2, CCX872 or vehicle for the last 8 weeks of diet. Hepatic steatosis was assessed by measuring triglyceride content of liver tissue. Mice on a HFD treated with CCX872 showed significantly lower triglyceride content than mice given vehicle. Each data point represents one animal, lines at mean and SEM **$p<0.01$ by student's t-test.
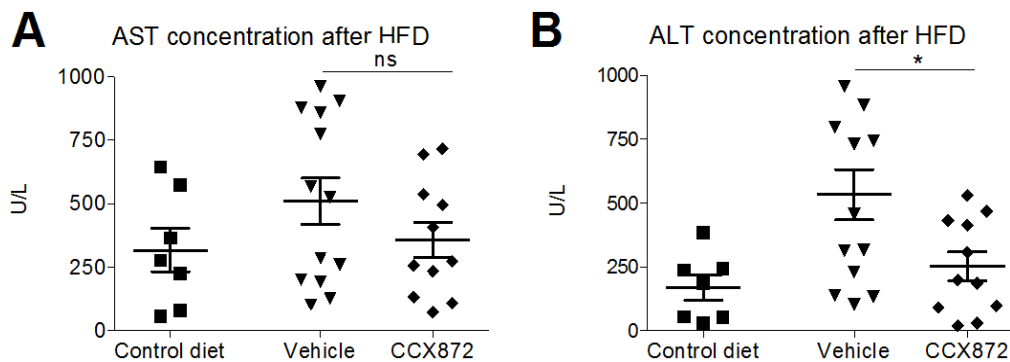
Figure 4.10: CCR2 antagonism lowers HFD-induced serum ALT concentration

C57/Bl6 mice were given HFD diet or control diet for sixteen weeks. Mice on HFD were treated with a small molecule antagonist of CCR2, CCX872 or vehicle for the last 8 weeks of diet. Liver injury was assessed by measuring serum **A** AST and **B** ALT concentration. No differences in AST concentration were seen between CCX872 and vehicle-treated mice, but ALT concentrations were lower in CCX872 treated mice. Each data point represents one animal, data shown as mean and SEM. **$p<0.01$ by student's t-test

CCR2 antagonism does not reduce the proportion of monocytes in liver tissue in HFD

Inflammation caused by HFD was investigated by flow cytometric analysis of isolated liver-infiltrating immune cells. No overall differences were seen in overall cellular infiltrate. No differences were seen between groups of mice with regard to $CD11b^+F4/80^{hi}$ monocytes or $CD11b^+F4/80^{lo}$ Kupffer cells in liver tissue (**figure 4.11**).

A HFD: CD11b$^+$F4/80^{hi} Kupffer Cells

B HFD: CD11b$^+$ F4/80^{lo} intrahepatic monocytes
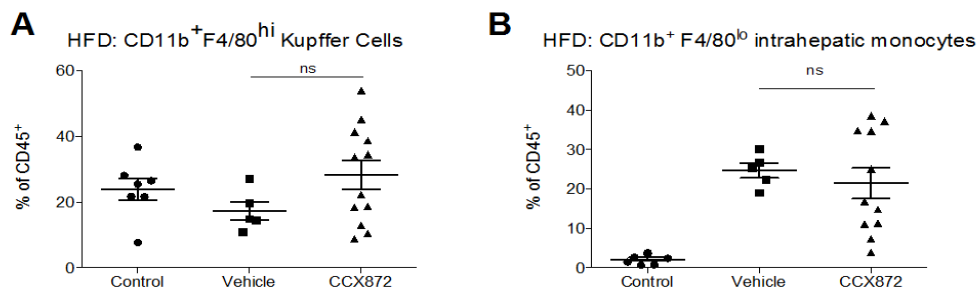
Figure 4.11: CCR2 antagonism does not reduce frequency of intra-hepatic Kupffer cells or monocytes

C57/Bl6 mice were fed HFD diet or control diet for sixteen weeks. Mice on HFD were treated with a small molecule antagonist of CCR2, CCX872 or vehicle for the last 8 weeks of diet. CCR2 antagonism did not alter frequency of **A** CD11b$^+$F4/80^{hi} liver-resident Kupffer cells or **B** CD11b$^+$F4/80^{dim} liver-infiltrating monocytes. Each data point represents an individual animal, data shown as mean and SEM. ns: non-significant by student's t-test

CCR2 antagonism reduces infiltration of adipose and liver tissue by monocytes associated with insulin-resistance

HFD is a model of obesity and insulin resistance comparable to the human syndrome of NAFLD in contrast to the MCD model which is not associated with either obesity or IR. Given the findings that particular monocyte subsets are associated with human obesity (Wentworth *et al.*, 2010) and my data in human fatty liver disease, I examined monocytes associated with insulin resistance in the HFD model. It is difficult to compare directly between subsets of monocytes in mice and humans based purely on expression of surface markers but previously published work indicated that a subset of $CD11b^+$ macrophages that are $CD11c^+F4/80^+$ may be critical in the development of obesity mediated insulin resistance (Lumeng *et al.*, 2007). I thus examined liver and adipose-infiltrating monocytes for the presence of this subset in mice given HFD.

After 16 weeks of HFD, mice treated with CCX872 had fewer $CD11b^+CD11c^+F4/80^+$ cells than mice treated with vehicle, in both visceral adipose tissue and liver tissue (**figures 4.12**).

Adipose tissue was not examined in MCD diet as only HFD is characterised by weight gain and insulin resistance – a phenomenon resulting from adipose tissue inflammation. MCD diet causes weight loss.
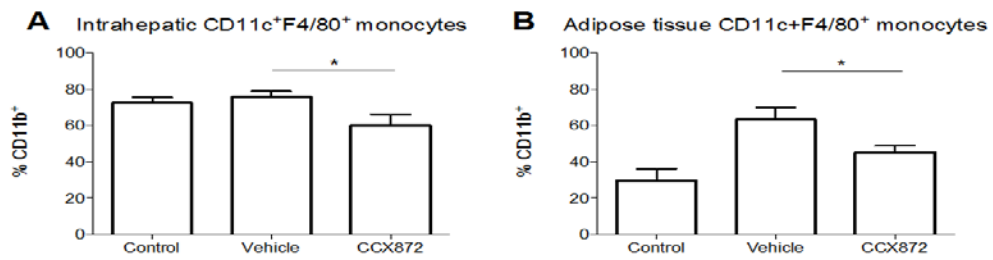
Figure 4.12: CCR2 antagonism reduces infiltration of liver and adipose tissue by CD11c+F4/80+monocytes

C57/Bl6 mice were given HFD diet or control diet for sixteen weeks. Mice on HFD were treated with a small molecule antagonist of CCR2, CCX872 or vehicle for the last 8 weeks of diet. Liver and adipose infiltrating monocytes were analysed by flow cytometry. A subset of $CD11b^+CD11c^+F4/80^+$ cells were observed less frequently (as a percentage of $CD11b)^+$ in both **A** liver and **B** adipose tissue of mice given CCX872 compared to vehicle treated mice and mice given a control diet. Data are shown as mean and SEM, *$p<0.05$ by student's t-test

CCR2 antagonism does not affect hepatic fibrosis caused by sixteen weeks of HFD

Paraffin-embedded liver sections were stained with Van Gieson's stain to detect collagen. This was quantified by analysis with image-j software to calculate percentage collagen area. Modest increases in hepatic fibrosis were seen in HFD fed mice after 16 weeks of diet consistent with the modest fibrotic response reported by others in this model. No significant differences in fibrosis between mice given CCX872 or vehicle were observed (**figure 4.13, figure 4.14A**). To investigate whether there were measurable differences in pro-fibrotic gene transcripts RNA was isolated from liver tissue and the expression of *Col1a1* and *Acta2* were analysed by qRT-PCR. No significant expression was seen in any of the groups (**figure 4.14B, C**).
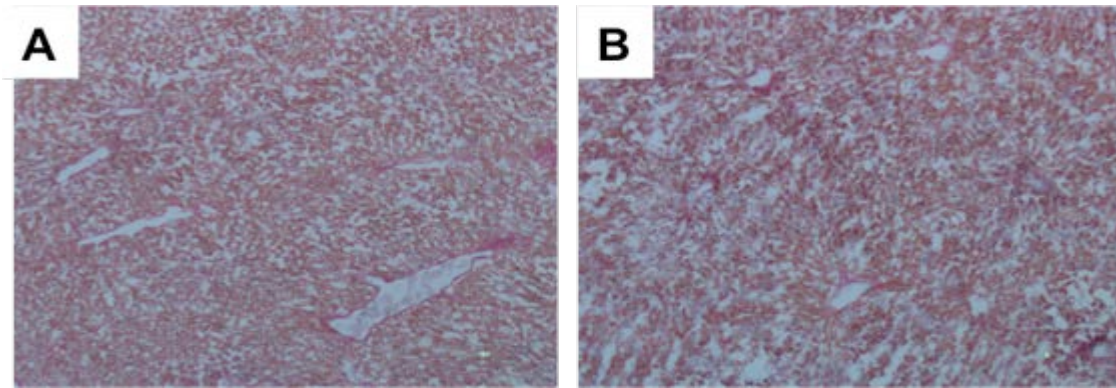
Figure 4.13: HFD caused minimal fibrosis with no significant differences between groups

*Van Gieson staining of paraffin-embedded liver sections from animals given **A** HFD and treatment with vehicle and **B** HFD and treatment with CCX872. Images taken at 10x magnification*
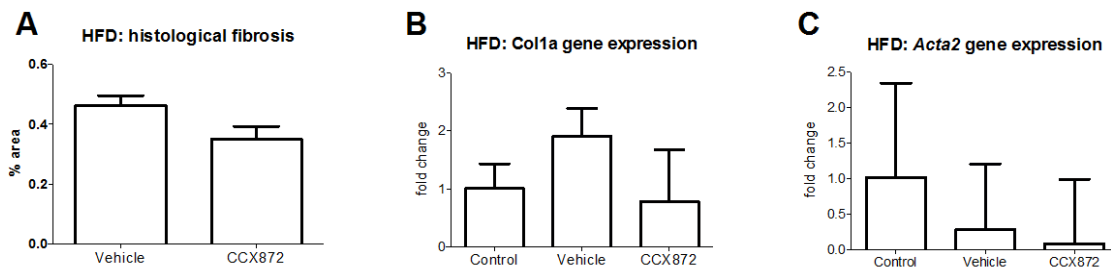
Figure 4.14: HFD causes little up-regulation of pro-fibrotic genes

*C57/Bl6 mice were given HFD diet or control diet for sixteen weeks. Mice on HFD were treated with a small molecule antagonist of CCR2, CCX872 or matched volumes of vehicle for the last 8 weeks of diet. Fibrosis caused by HFD was assessed with histology and PCR of pro-fibrotic genes. No significant differences were observed in **A** percentage collagen area **B** Col1a gene expression or **C** Acta2 gene expression, between mice given CCR2 or vehicle. Data are shown as median and IQR*

CCR2 antagonism improves glucose metabolism in mice given HFD

HFD causes insulin resistance in mice in tandem with obesity. Glucose metabolism was assessed through glucose and insulin challenges.

<u>CCR2 antagonism improved response to glucose challenge</u>

Mice were fasted overnight before being given a challenge of 2g/kg glucose by gastric lavage. Plasma glucose concentration was measured from drops of tail vein blood with a glucometer at baseline and 15, 30, 60, 90 and 120 minutes after administration of glucose.

Plasma glucose concentration over time was monitored for each mouse, and mean values for each group calculated. Groups were compared by area-under-the-curve values. At the start of treatment, response to glucose was similar between CCX872 and vehicle treated mice (**figure 4.15A, C**). However, after 8 weeks of treatment there was a significant improvement in response of CCX872 mice compared to vehicle treated mice (AUC 48545 mg/dl/min vs. 31795 mg/dl/min, student's t-test $p < 0.001$)(**figure 4.15B, C**).
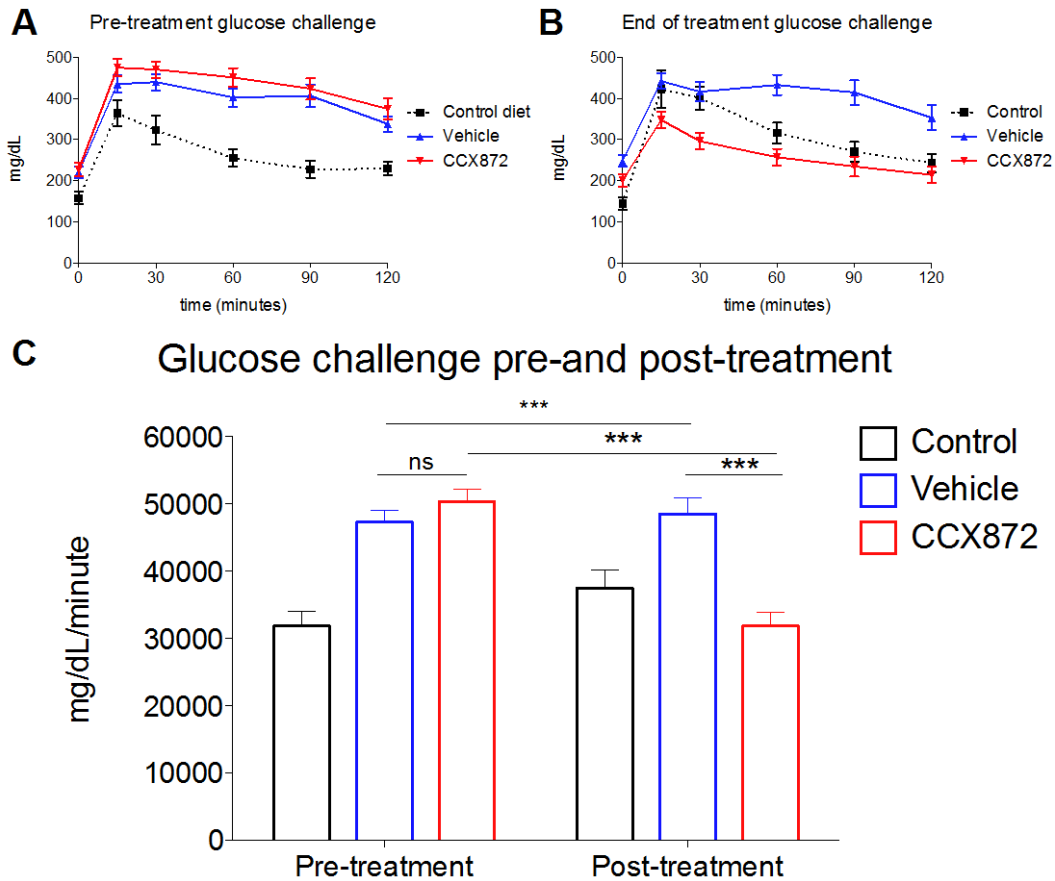
Figure 4.15: CCR2 antagonism improves glucose metabolism

C57/Bl6 mice were fed HFD or control diet for sixteen weeks. Mice on HFD were given CCX872, a small molecule CCR2 antagonist, or matched volumes of vehicle for the last eight weeks of diet. Glucose metabolism was investigated with a glucose challenge *A* plasma glucose concentration in each group of mice before treatment, *B* after treatment with CCX872 or vehicle (n=13 each), or in mice receiving control diet (n=8) and *C* area under the curve analysis of plasma glucose concentration. Data re presented as mean and SEM, ****p<0.001* by student's t-test

CCR2 antagonism improved response to insulin challenge

Insulin challenge was performed by administering a standard dose of 0.75units/g of insulin by intra-peritoneal injection to non-fasted mice. Plasma glucose concentration was measured from drops of tail vein blood with a glucometer at baseline and 15, 30, 60, 90 and 120 minutes after administration of insulin. At the start of treatment, after eight weeks of HFD, changes in plasma glucose concentration were similar in both groups of mice given HFD (**figure 4.16A, C**). After a further 8 weeks of HFD and treatment with CCX872 or vehicle, there was a significant difference between groups (AUC 21719 mg/dl/min vs. 16553 mg/dl/min, student's t-test $p<0.001$)(**figure 4.16 B,C**). Mice given a control diet showed a similar response to mice on a HFD after insulin challenge.
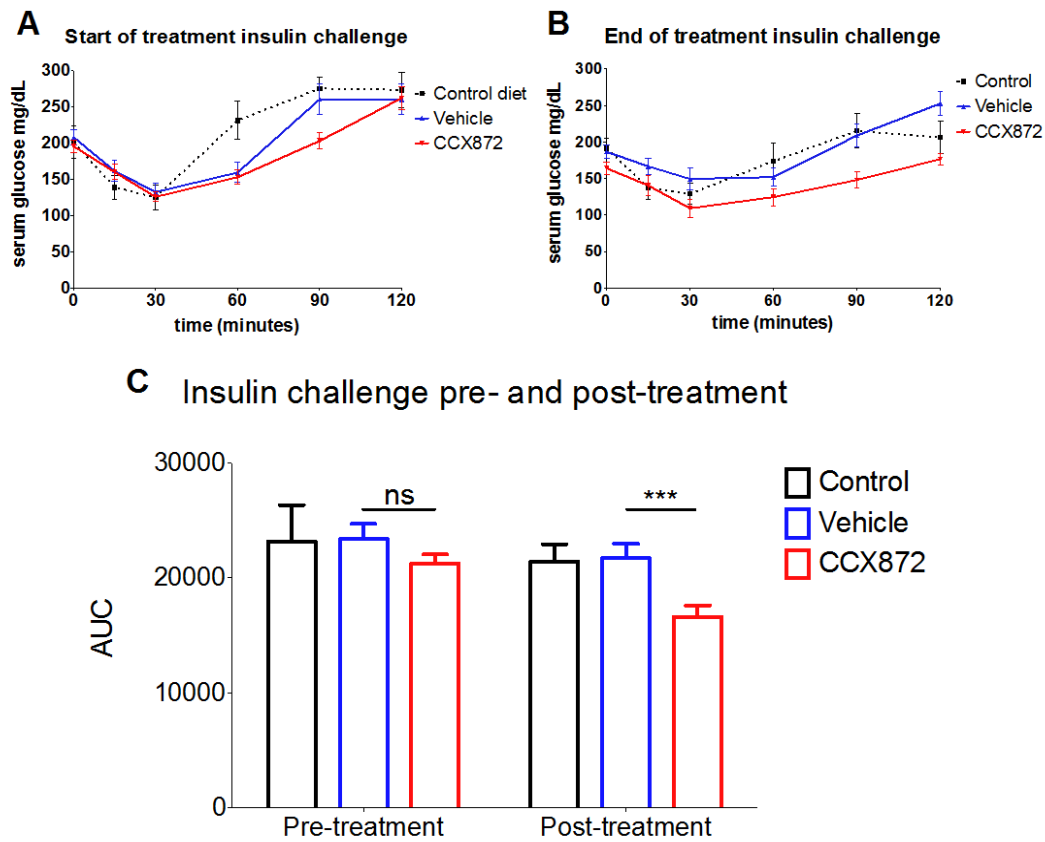
Figure 4.16: CCR2 antagonism improves insulin sensitivity

C57/Bl6 mice were given HFD diet or control diet for sixteen weeks. Mice on HFD were treated with a small molecule antagonist of CCR2, CCX872 or matched volumes of vehicle for the last 8 weeks of diet. Glucose metabolism was investigated with an insulin challenge with a standardised amount of insulin. **A** *mean and SEM plasma glucose concentration in each group of mice before treatment* **B** *after treatment with CCX872 or vehicle after and* **C** *area under the curve analysis of plasma glucose concentration before and after treatment. Data are shown as mean and SEM* ******p<0.001 by student's t-test***

Discussion

The efficacy of CCR2 antagonism was investigated in two mouse models of NAFLD. CCR2 antagonism limited hepatic accumulation of triglyceride and reduced infiltration of liver tissue by inflammatory $Ly6c^{hi}$ monocytes in steatohepatitis induced by MCD diet. In HFD induced steatohepatitis, whilst serum markers of liver injury were reduced, no reduction in overall monocyte infiltration was seen. However a subset of monocytes that have been found to mediate insulin resistance were reduced in frequency in both adipose and liver tissue. Glucose metabolism was also improved, suggesting that CCR2 antagonism improves obesity-mediated fatty liver disease through effects on both adipose and liver. The differences in the findings between the two models can be explained at least in part by the significant differences between the modes of injury. MCD diet causes retention of lipid in hepatocytes and significant weight loss, whereas HFD causes weight gain and insulin resistance. A HFD model is therefore closer to the human syndrome of obesity and NAFLD.

It is interesting that whilst a clear reduction in liver-infiltrating monocytes was not observed between groups in the HFD model, a significant difference in a subset of $CD11b^{+}CD11c^{+}F4/80^{+}$ cells was observed associated with improved steatosis, serum ALT and glycaemic control. This mirrors the findings in human liver disease of a subset of monocytes that were associated with NAFLD whilst overall monocyte infiltration did not differ between aetiologies of liver disease – discussed in the previous chapter.

In obesity-induced steatohepatitis caused by HFD, less weight gain was seen in the CCX872 treated animals. There are several explanations for this: CCX872 may reduce appetite by a direct effect or through reducing general well-being, or this is a consequence of a direct

effect on disease pathogenesis. When the difference in weight became apparent I measured food intake and assessed wellbeing, neither of which appeared to differ between groups. Thus it is likely that this is a direct consequence of CCR2 inhibition resulting in improved insulin resistance, and metabolic profile of these animals resulting in limited weight gain.

The differences in weight between treatment groups raises the possibility that the beneficial effects of CCX872 may be due to the lower weight of this group. However, AST and ALT were lower in the CCX872 group than the vehicle treated group even for mice of the same weight, as were values for glucose and insulin challenges suggesting that an effect was seen beyond that of simple weight reduction. Less straight forward to answer is the question of whether reduction in hepatic inflammation is a direct effect of CCX872, or a consequence of improved adipose tissue inflammation. Reducing adipose tissue inflammation will improve insulin resistance and flux of free fatty acids, both of which will improve liver disease. From one perspective this may not matter or reduce the translational potential of these results, but from a scientific point of view this is an important question and should be addressed in on-going studies.

Previous reports have shown that obesity in mice is associated with increased serum CCL2 concentration and greater hepatic gene expression of CCL2 (Kirovski et al., 2011). In CCR2 knockout-mice, less hepatic steatosis (Weisberg et al., 2006) and hepatic inflammation (Obstfeld et al., 2010, Miura et al., 2012) is seen in models of obesity-induced liver disease. Interestingly CCR2 knock-out mice are also protected against carbon tetrachloride-induced fibrosis (Miura et al., 2012), attributed to expression of CCR2 by hepatic stellate cells (Seki et al., 2009) although this could also be a monocyte/macrophage mediated effect. CCR2 has

been targeted with a variety of pharmaceutical agents in animal models of fatty liver disease. A CCR2 inhibitor (RS504393, Tocris Bioscience, 2mg/kg/day) administered via an implantable osmotic pump to AZIP transgenic mice (Yang *et al.*, 2009) reduced liver weight, and macrophage accumulation. Miura *et al* used a CCR2 antagonist (RS102895, Sigma, 10mg/kg/day) therapeutically (i.e. once disease was established) in a model of fatty liver induced by choline deficient diet (Miura *et al.*, 2012). Again, macrophages were reduced in number in the livers of treated animals, assessed by immunohistochemistry. ALT and fibrosis were also reduced. Pharmaceutical inhibition of CCL2, rather than its receptor also has shown beneficial effects in MCD diet (Baeck *et al.*, 2012). There is therefore a broad body of data suggesting that fatty liver disease is ameliorated through CCR2 or CCL2 antagonism.

The data presented in this chapter differ from these previous reports in a number of ways. Both models used dietary manipulation to induce steatohepatitis rather than using genetically altered animals and I used therapeutic intervention to intervene *after* establishing disease rather than preventing disease from occurring. Whilst this approach may reduce the apparent efficacy of an intervention it is more relevant to clinical practice and translation.

I used two types of diet-induced steatohepatitis in mice to model human NAFLD: methionine-choline deficient diet and high fat diet. The MCD model is widely used as a model of steatohepatitis, although it is far removed from the human condition of obesity and insulin resistance. The HFD model is superior in this respect, in that mice become obese and insulin resistant, however the lack of fibrosis in this model limited the similarity to human disease. Fructose consumption is a significant risk factor for development of NAFLD in humans (Ouyang *et al.*, 2008, Abdelmalek *et al.*, 2010). The addition of fructose to drinking

water of mice may cause greater severity of steatohepatitis in mice with fibrosis (Tetri *et al.,* 2008). This would have provided a better model to test the effects of CCR2 antagonism and been more closely related to human disease. In addition, these findings are further limited by a lack of histological correlates of liver injury. Unfortunately this was not possible as tissue had deteriorated and was unsuitable for analysis. This is an important limitation as the gold standard for assessment of human NAFLD is through histological analysis.

CCR2 antagonism as a therapeutic tool in NAFLD is already being investigated in the CENTAUR trial. This study is using Cenciviroc, a dual CCR2/CCR5 inhibitor that was initially developed for the treatment of HIV (NCT 02217475) (trials.gov, 2014). If CCR2 really does control the inflammatory consequences of obesity, the use of CCR2 antagonists could be long-term treatment similar to current therapies for diabetes. The long-term consequences of CCR2 antagonism are unknown.

CHAPTER 5: The Role of CCR9 in acute liver injury

Acute liver failure (ALF) is a rare but devastating condition typified by hepatic encephalopathy and jaundice. It is often fatal. Chronic liver disease is typified by iterative episodes of inflammation and scarring over long periods of time that leads to cirrhosis, whereas in acute liver failure there is an overwhelming inflammatory process that leads to hepatic failure with no or minimal fibrosis (Antionades *et al.*, 2008). In some cases ALF may be fulminant resulting in rapid destruction within hours or days of liver injury. Here the dominant pathway of injury is direct toxicity to the liver from drugs or toxins whereas in other cases injury is driven by an uncontrolled immune response to an autoantigen or virus resulting in liver failure over days or weeks. Recent work implicated CCR9 in a mouse model of acute liver injury (Nakamoto *et al.*, 2012). The authors used concanavalin A (conA) to induce T-cell mediated hepatitis in mice. ConA treatment leads to a massive polyclonal activation of T cells resulting in immune mediated liver damage and hepatocyte apoptosis (Tiegs *et al.*, 1992). Pro-inflammatory CCR9$^+$ macrophages – defined as CD11b$^+$CD11c$^-$ cells - were increased in number in injured liver tissue, and induced differentiation of naïve CD4$^+$ T-cells towards a Th1 phenotype thereby implicating them in the local generation of immune activation and IFNγ secretion. On the basis of these studies I investigated the role of CCR9 in human acute liver failure and the efficacy of inhibition of CCR9 in mouse models of acute liver failure.

Serum concentration of CCL25 is raised in acute liver failure

CCR9 has a single ligand, CCL25. I measured CCL25 in serum from patients with ALF (n=39), acute-on-chronic liver failure (ACLF) (n=8) chronic liver disease (CLD) (n=8) and from healthy controls (n=19) by ELISA. ALF was defined as patients with acute jaundice and hepatic encephalopathy. ACLF refers to an acute deterioration of liver function in patients with cirrhosis, either secondary to superimposed liver injury or due to extra-hepatic precipitating factors such as infection culminating in the end-organ dysfunction (Jalan *et al.*, 2012).

Serum from ALF contained significantly more CCL25 compared to serum from healthy controls (median 3.01ng/ml (IQR 1.3) vs. 0.62ng/ml (1.1), Mann-Whitney test $p<0.001$) (**figure 5.1**) and patients with chronic liver disease (median 1.17ng/ml (2.5), Mann-Whitney test $p=0.006$). There was no significant difference in serum CCL25 concentration between patients with ALF and ACLF (median 1.63ng/ml (2.57) Mann-Whitney $p=0.178$).
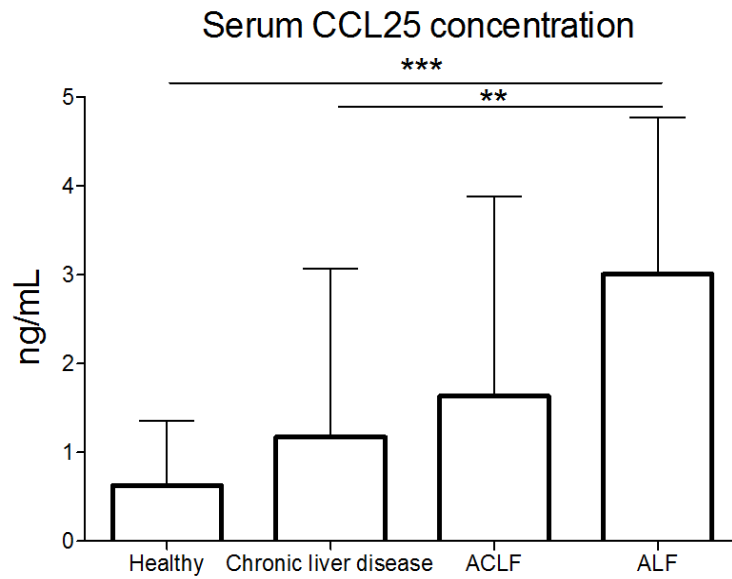
Figure 5.1: *Serum concentration of CCL25 is raised in acute liver failure*

Serum samples from healthy controls (n=19) and patients with chronic liver disease (n=8), acute-on-chronic liver failure (n=9) or acute liver failure (n=20) was analysed for CCL25 concentration by ELISA. **p<0.01 ***p<0.001 by Mann-Whitney test. Data shown as median and IQR.

Increased serum CCL25 concentration is an early event in human ALF

In order to determine whether CCL25-CCR9 pathways are activated early in the development of ALF I worked with collaborators at Kings College London and Imperial College London (Dr L Possamai, Dr G Petts, Dr C Antoniades) to analyse CCL25 in serum samples taken from twenty-seven patients with ALF at varying time points after admission. This showed that CCL25 concentration was highest within 24 hours of admission to hospital and subsequently decreased (figure 5.2), suggesting an early role for CCR9/CCL25 in ALF. There were insufficient samples available to distinguish between differing aetiologies of ALF.

CCL25 concentration by time after admission for ALF
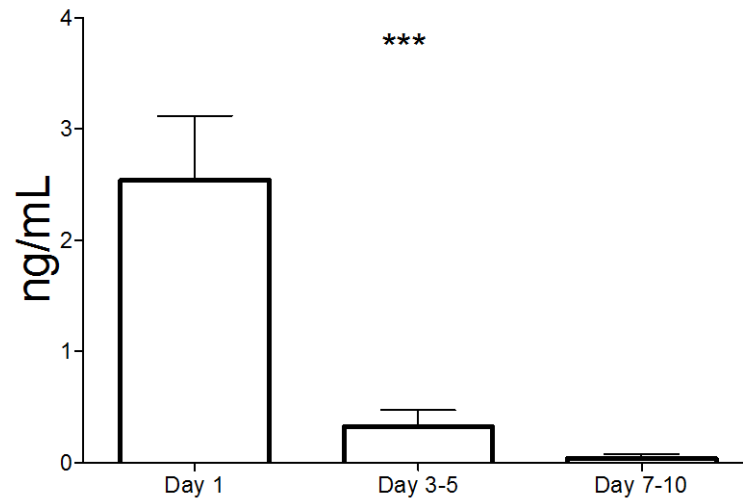
Figure 5.2 Increase in serum CCL25 concentration is an early event in human ALF

Serum from twenty-seven patients admitted to King's College Hospital, London, with acute liver failure was analysed for CCL25 concentration by ELISA. Serum samples taken within 24 hours of admission had higher CCL25 concentration compared to later time points (One-way ANOVA $p<0.001$). Data shown as mean and SEM. n=27.

Serum CCL25 does not correlate with biochemical markers of liver injury or outcome

In a small number of ALF patient samples (n=18) we were able to correlate serum concentration of CCL25 with markers of liver injury. No correlation was seen between CCL25 and serum amino transferase (AST), alanine transferase (ALT), bilirubin, creatinine or lactate concentration, or MELD score. MELD score is a composite score that is used to gauge severity of liver disease (**table 5.1, figure 5.3**). MELD is calculated by the following formula: $[0.957 \times \mathrm{Ln(creatinine)} + 0.378 \times \mathrm{Ln(bilirubin)} + 1.120 \times \mathrm{Ln(INR)}] \times 10$. Similarly, no differences in serum CCL25 concentrations were observed when considering clinical outcomes (**figure 5.4**). All of these samples were collected on admission to hospital and represent a variety of sampling times.

Variable	r^2	p
Creatinine	0.04	0.385
Bilirubin	0.13	0.140
ALT	0.14	0.167
AST	0.06	0.311
Lactate	<0.01	0.801
MELD	<0.01	0.685

Table 5.1: correlation of serum CCL25 concentration with clinical parameters in patients with ALF
(n=18) by linear regression. p value calculated by F test.
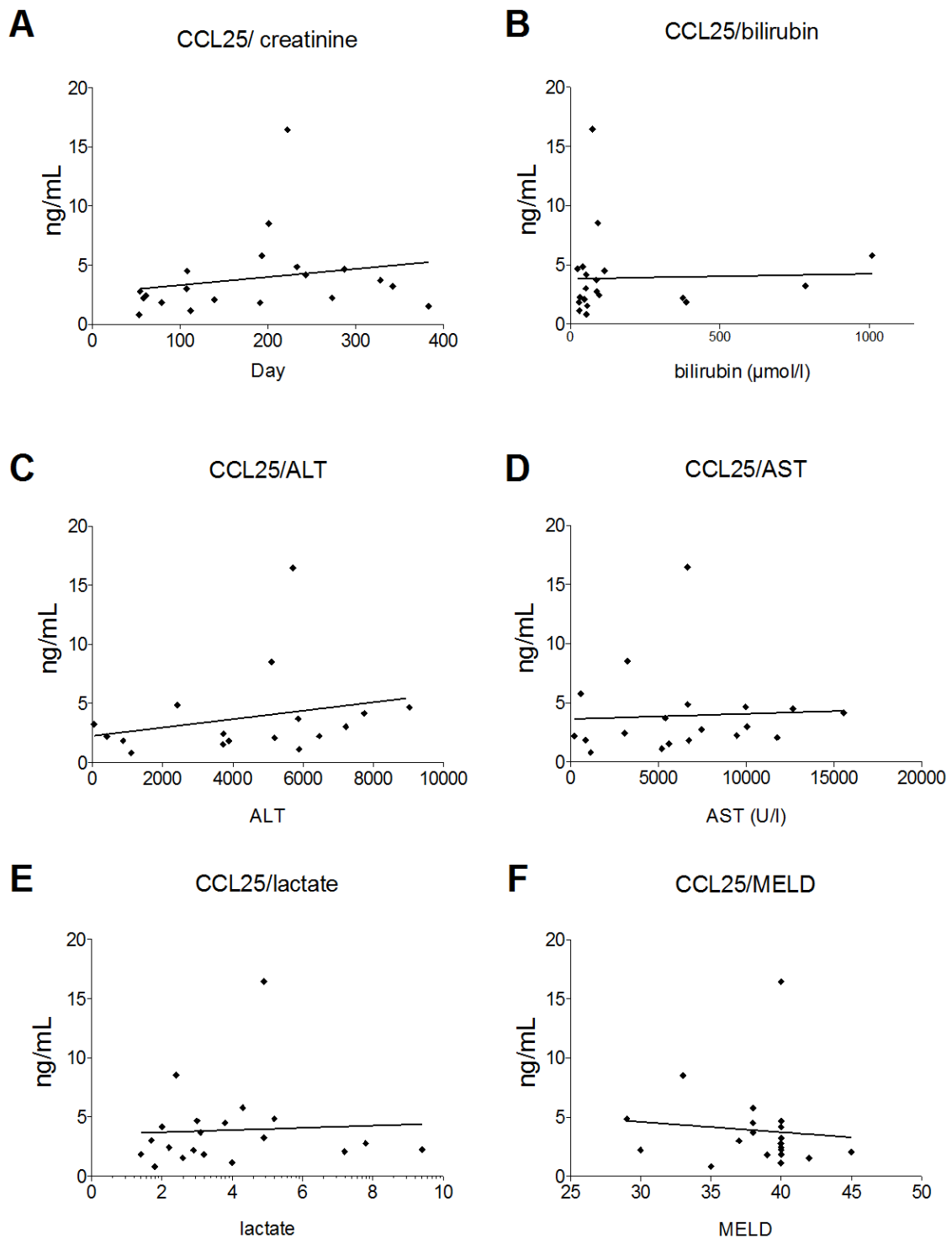
Figure 5.3: Serum CCL25 does not correlate with biochemical markers of liver injury

*Concentration of CCL25 in serum of patients with ALF (n=18) was analysed by ELISA, and correlated with selected clinical parameters: **A** creatinine **B** bilirubin **C** ALT **D** AST **E** pH **F** MELD score. No significant correlations were observed. p values were calculated by the F test. n=20 for each test.*

Serum CCL25 concentration and clinical outcome
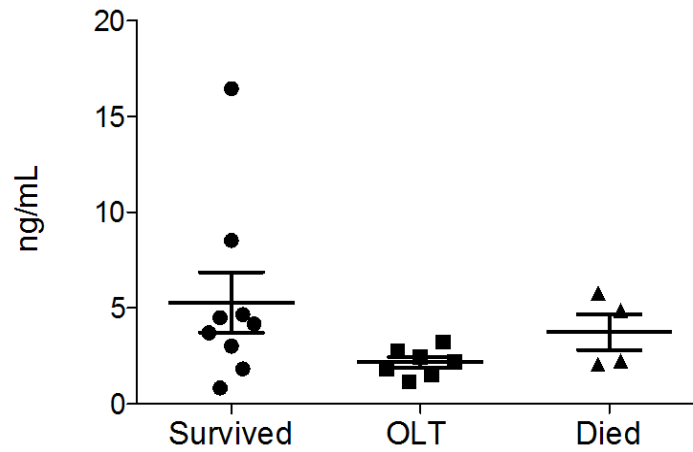
Figure 5.4: Serum CCL25 does not predict clinical outcomes

Serum CCL25 concentration was measured in serum of patients with ALF. No differences in serum CCL25 concentration were seen between patients who survived (n=9), required liver transplantation (OLT, n=7) or patients who died (n=4) (one-way ANOVA p=ns).

CCR9 is expressed by intermediate CD14^{++}CD16$^+$ intrahepatic monocytes

Monocytes were isolated from explanted liver tissue to examine CCR9 expression. These data were severely limited by the scarcity of liver tissue from patients with ALF. This flow cytometric analysis was performed with E. Triantyfillou.

Analysis of liver-infiltrating monocyte subsets by flow cytometry (gated by FS/SS criteria and on CD45$^+$ cells) showed that CCR9 was predominantly expressed by CD14^{++}CD16$^+$ monocytes, in keeping with previously published reports of CCR9 expression on blood monocytes (**figure 5.5 and 5.6**).

A

B
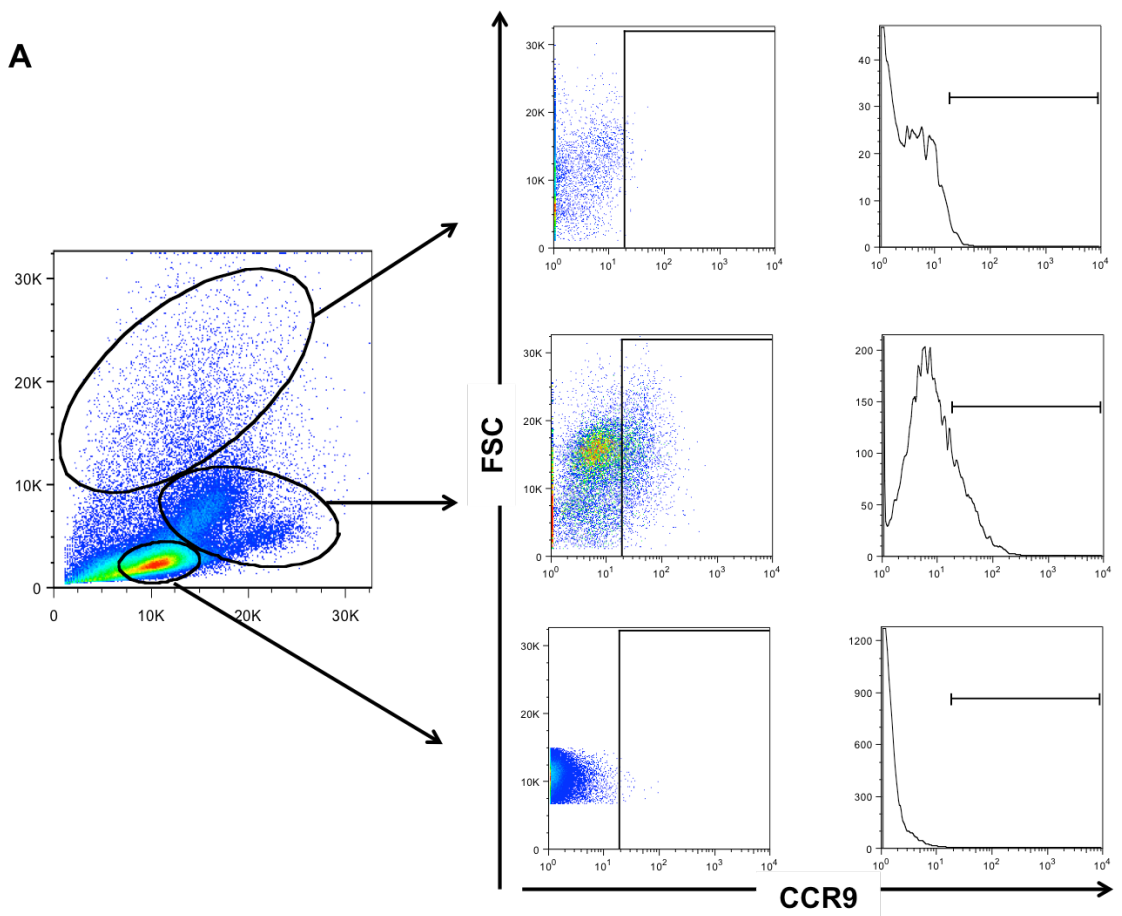
CCR9 expression by intrahepatic monocyte subsets
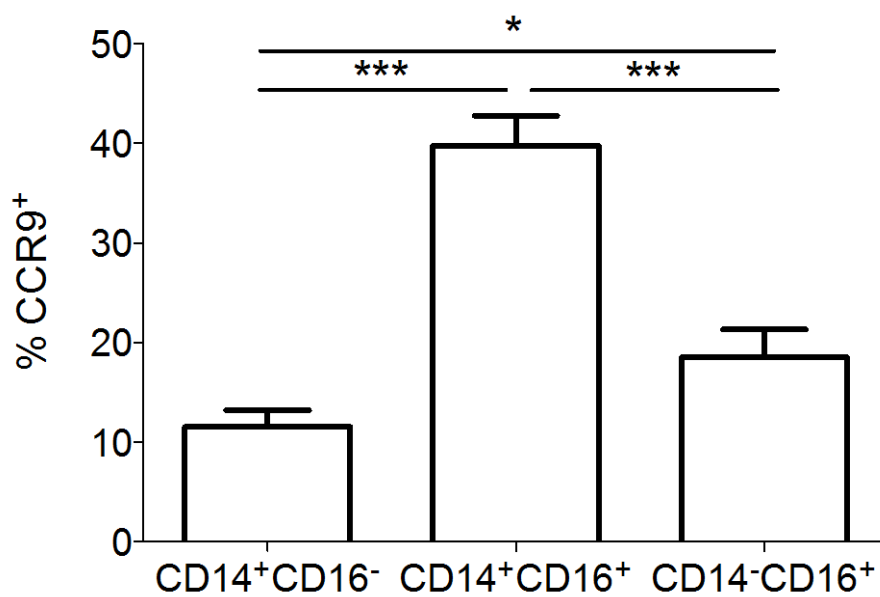
Figure 5.5: (previous page) CCR9 expression on liver infiltrating monocytes

Monocytes were isolated from explanted liver tissue from patients undergoing liver transplantation for acute liver failure and chronic liver disease. In total 21 livers specimens were analysed: 3 normal liver (resection tissue), 7 autoimmune hepatitis, 6 alcoholic liver disease and 5 acute liver failure. Percentage CCR9 expression on monocytes was analysed by flow cytometry.
A Identification of lymphoid, myeloid and granulocyte populations on the basis of forward and side scatter properties shows CCR9 expression predominantly in myeloid gate
B CCR9 expression on monocyte subsets defined by CD14 and CD16 expression. Data are shown as median and IQR. *p<0.05 ***p<0.001 by student's t-test.
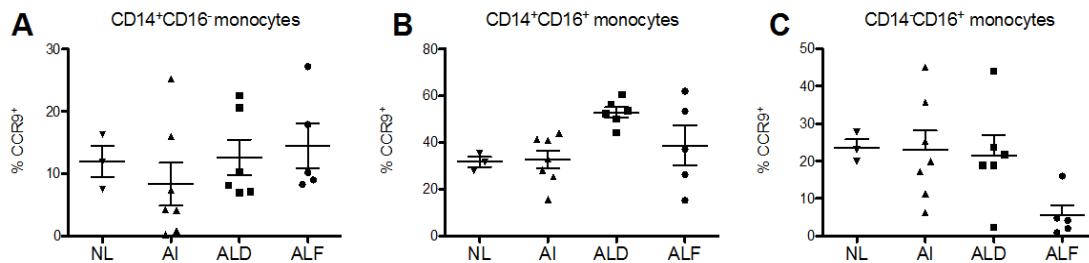
Figure 5.6: CCR9 expression by monocyte subsets in different liver diseases

Monocytes were isolated from explanted liver tissue from patients undergoing liver transplantation for acute liver failure and chronic liver disease and analysed by flow cytometry. Percentage CCR9 expression on monocyte subsets did not significantly differ between aetiologies.

Mouse models of acute liver injury

▆▆▆▆▆▆▆▆▆▆▆▆▆▆▆▆▆▆▆▆▆▆▆▆▆   ▆▆▆▆▆▆▆▆▆▆

▆▆▆▆▆▆▆▆▆▆▆▆▆. CCl_4 was diluted 1:4 in corn oil (Sigma-Aldrich, Missouri USA) and administered to mice by intra-peritoneal (IP) at a dose of 1ml/kg. CCl_4 induces a toxic acute liver failure by through generation of free radicals (Brattin *et al.*, 1985) (Recknagel *et al.*, 1989) and mediated through macrophages and T-cells (Tiegs *et al.*, 1992). Paracetamol at therapeutic doses is rapidly metabolised, predominantly through glucuronidation. A small amount of the highly toxic N-acetyl-p-benzoquinone imine (NAPQI) is generated through cytochrome P450 but is usually readily conjugated with glutathione to a nontoxic state. In overdose glucuronidation pathways are saturated and large amounts of NAPQI are generated. Glutathione stores are depleted at which point NAPQI accumulates and cause hepatic damage principally through oxidative stress (McGill *et al.*, 2012).

CCR9 is expressed on macrophages early in paracetamol-induced acute liver injury in mice

Pilot experiments with paracetamol caused wide variation in the degree of liver injury as assessed by serum AST and ALT concentration (**figure 5.7**). Fasting animals overnight, to deplete hepatic glutathione stores, produced a more consistent pattern of injury and this approach was adopted for all subsequent experiments.
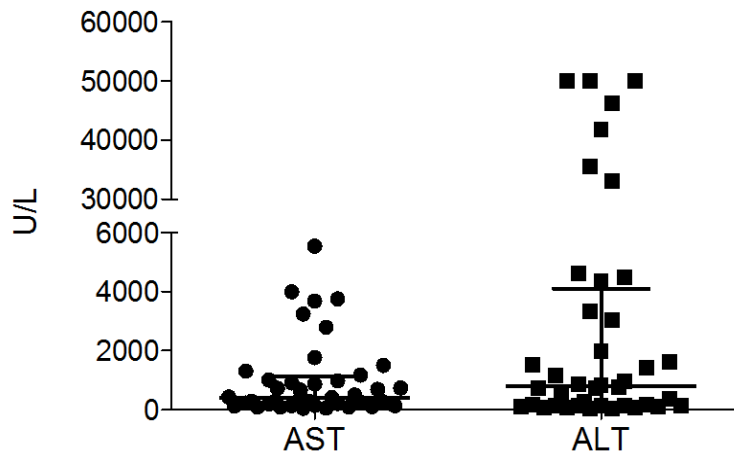
Figure 5.7: Large variations in liver injury caused by paracetamol in mice

C57/Bl6 mice were given 400mg/kg of paracetamol by intra-peritoneal injections to establish the magnitude of liver injury caused be paracetamol. After 24 hours liver injury was assessed by measuring serum AST and ALT concentration. Large variations in serum AST and ALT were observed (n=40). Each dot represents a single animal. Aggregate data from three experiments shown.

Thirty C57/Bl6 male mice aged 6 weeks were administered ▮▮▮▮▮▮▮▮ paracetamol at 400mg/kg following an overnight fast, delivered by intra-peritoneal injection. Five mice were ▮▮▮▮ by CO_2 inhalation at each of six time points: 0, 6, 12 24, 48 and 72 hours after administration of paracetamol. Serum was analysed for ALT concentration as a marker of hepatic injury, and liver-infiltrating cell subsets were analysed by flow cytometry.

Mice lost weight, with maximum weight loss observed 24 hours after administration of paracetamol (**figure 5.8A**). Serum ALT showed considerable variation between animals, but was maximally elevated at 12 and 24 hours after paracetamol and quickly returned to normal (**figure 5.8B**). These results are consistent with previous reports (Nakamoto *et al.*, 2012) and are comparable to the clinical syndrome of acute paracetamol poisoning.

Analysis of infiltrating myeloid cells in liver tissue showed increases in $CD11b^+CD11c^-$ macrophages and $CD11b^+F4/80^{dim}Ly6c^{hi}$ monocytes. $CD11b^+CD11c^-$ macrophages peaked at 12-24h post-paracetamol, and then fell but had not returned to baseline by 72 hours injury. Pro-inflammatory $CD11b^+F4/80^{dim}Ly6c^{hi}$ monocytes were elevated by 6 hours and numbers were maintained until 72 hours. This was paralleled by a decrease in $CD11b^+F4/80^{dim}Ly6c^{lo}$ monocytes (**figure 5.9A, B, C**). The frequency of infiltrating $CD11b^+CD11c^-$ macrophages correlated closely with serum markers of liver injury (**figure 5.8B**).

CCR9 expression by CD11b+CD11c- monocytes peaks shortly after liver injury

In addition the prevalence of CCR9 expressing $CD11b^+CD11c^-$ macrophages correlated with clinical markers of injury, with an early peak around 6-24 hours after administration of paracetamol (**figure 5.10**).
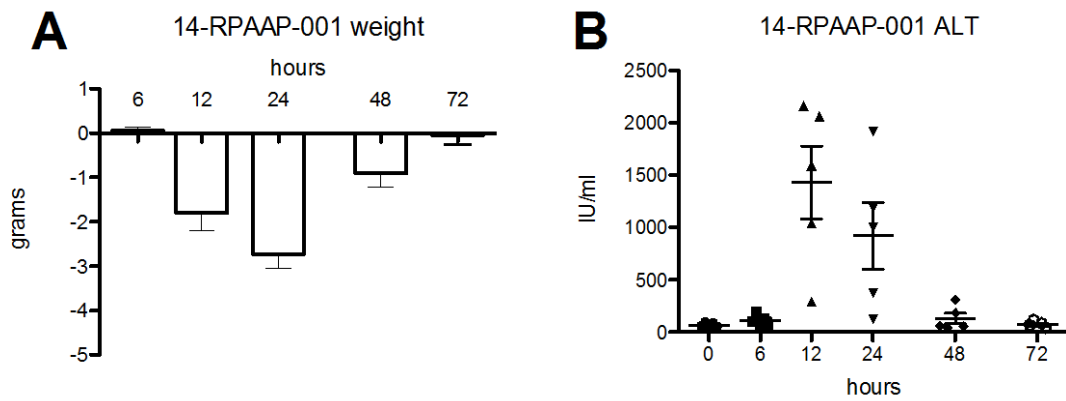
Figure 5.8: Administration of 400mg/kg of paracetamol causes weight loss and liver injury

Mice were ▆▆▆▆ at fixed time points after being given 400mg/kg of paracetamol **A** weight loss and **B** serum ALT concentration after paracetamol-induced liver injury. Data are shown as mean and SEM.
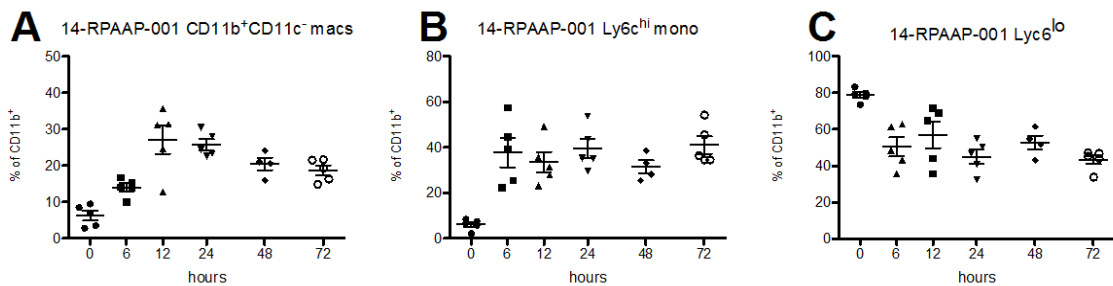
Figure 5.9: Paracetamol causes influx of inflammatory macrophages and monocytes to liver tissue

FACS analysis of liver-infiltrating monocyte subsets after paracetamol induced liver injury **A** CD11b⁺CD11c⁻ macrophages **B** CD11b⁺Ly6c^{hi} monocytes **C** CD11b⁺Ly6c^{lo} monocytes. Gated on liver CD45⁺CD11b⁺ cells. Data shown as mean and SEM.

CD11b⁺CD11c⁻ macrophage CCR9 expression
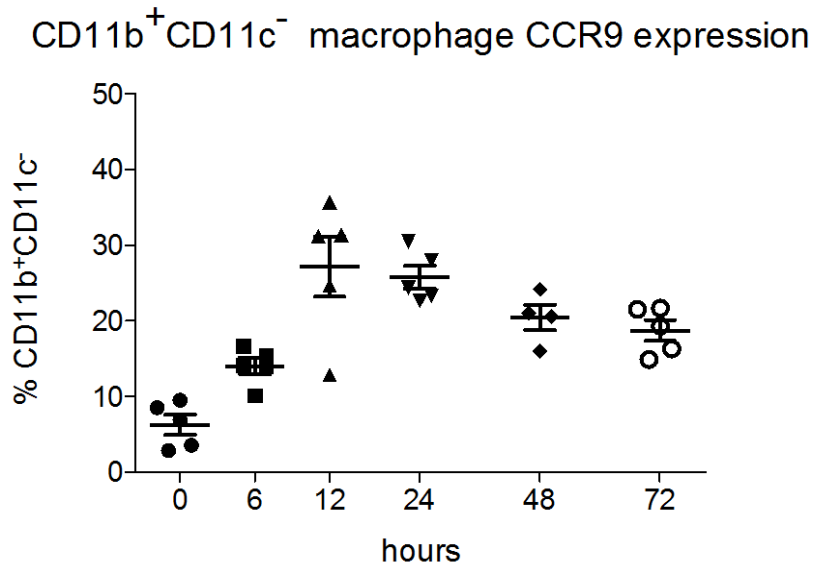
Figure 5.10: CCR9 expression by CD11b+CD11c- monocytes peaks shortly after paracetamol-induced liver injury

CCR9 expression on CD11b⁺CD11c⁻ macrophages after paracetamol induced liver injury. Gated on liver CD45⁺CD11b⁺ population. Data shown as mean and SEM.

CCR9 is expressed on macrophages early in carbon tetrachloride induced acute liver injury

Administration of CCl_4 was also evaluated as a model of acute liver injury. Thirty male C57/Bl6 mice aged 6 weeks were given 1ml/kg of CCl_4 by intra-peritoneal injection. Mice lost weight with maximum weight loss seen at 12 hours after CCl_4 administration (**figure 5.11A**). Peak ALT was seen at 24 hours after injury with rapid resolution to baseline levels at 72 hours (**figure 5.11B**). ALT took longer to peak than in paracetamol-induced liver injury (around 12 hours) but the average peak ALT concentration was much higher.

Analysis of liver-infiltrating monocytes subsets showed early infiltration of $CD11b^+Ly6c^{hi}$ monocytes within 6 hours of CCl_4 administration (**figure 5.12B**). $CD11b^+CD11c^-$ macrophage infiltration of liver tissue paralleled serum ALT concentration with peak infiltrate seen at 24 hours after CCl_4 administration (**figure 5.11A**).

CCR9 expression on CD11b+CD11c- macrophages was seen to increase after CCl4 administration with peak expression at 12 hours after injury which slowly returned to baseline by 72 hours post administration (**figure 5.13**).

This pattern of infiltrating monocyte/macrophages was comparable to that seen in paracetamol-induced liver injury but with the interesting distinction that paracetamol induced a much more profound and persisting $Ly6c^{hi}$ infiltrate and was associated with a much higher proportion of $CCR9^+$ macrophages in the hepatic infiltrate.
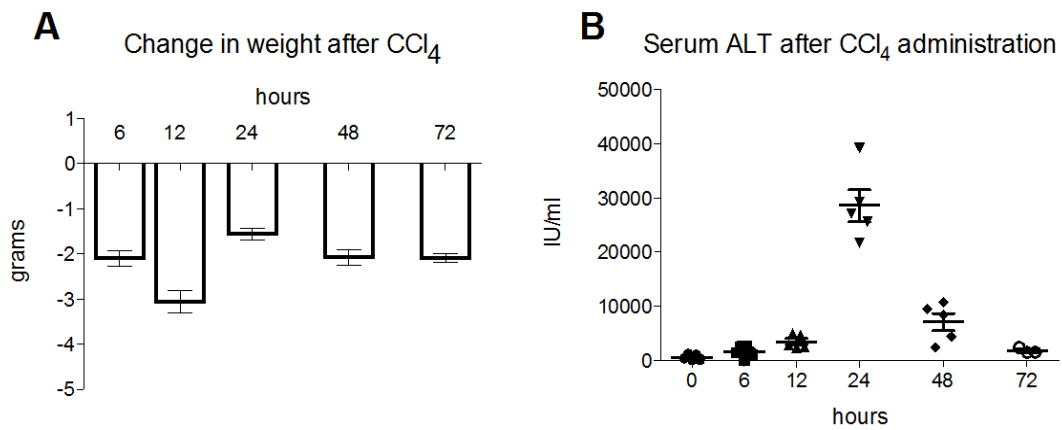
Figure 5.11: Administration of 1mL/kg of CCl₄ causes weight loss and liver injury

C57/Bl6 mice were administered 1mg/kg of CCl₄ and ▓▓▓▓▓ at different time points following injury. **A** weight loss and **B** serum ALT concentration were measured after CCl₄. Data are shown as mean and SEM, n=30.
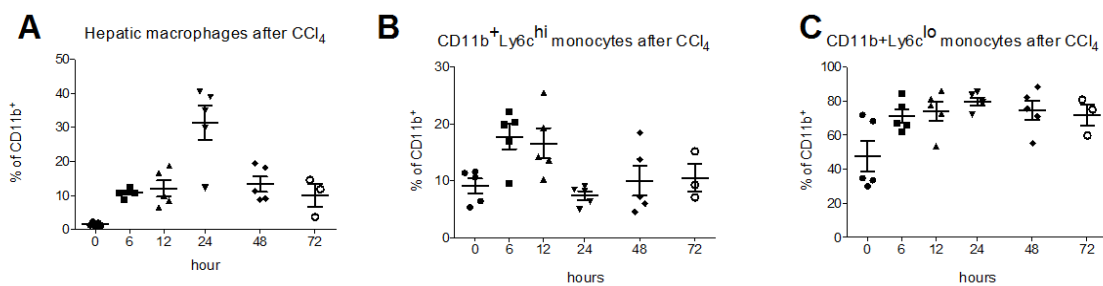
Figure 5.12: CCl₄ causes influx of inflammatory macrophages and monocytes to liver tissue

FACS analysis of liver-infiltrating monocyte subsets after CCl₄ mediated liver injury, gated on liver CD45⁺cells **A** CD11b⁺CD11c⁻ macrophages **B** CD11b+Ly6cʰⁱ monocytes **C** CD11b+Ly6cˡᵒ monocytes. Data are shown as mean and SEM.
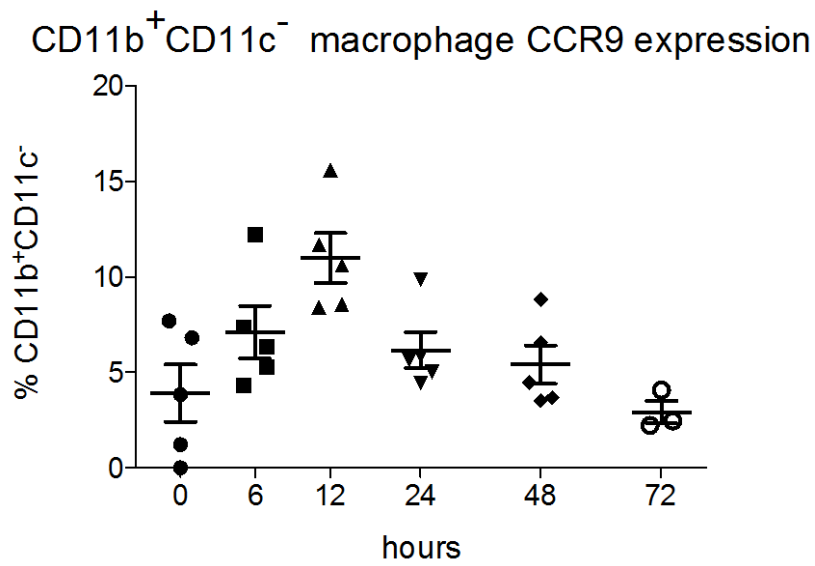
Figure 5.13: CCR9 expression by CD11b+CD11c- monocytes peaks shortly after CCl₄-induced liver injury

C57/Bl6 mice were administered 1mg/ml of CCl₄ and ▨▨▨▨ at specified time point afterwards. CCR9 expression on liver-infiltrating CD11b⁺CD11c⁻ macrophages after CCl₄ induced liver injury. Data shown as mean and SEM, n=3-5 per time point as two mice died before the 72 hour time point.

Comparison of paracetamol and CCL4 induced liver failure models

Paracetamol-induced liver injury induced a greater population of CCR9 expressing liver-infiltrating macrophages when compared with CCl_4-induced injury (compare **figures 5.10** and **5.13**). As paracetamol toxicity is the commonest cause of human acute liver failure this model has direct relevance to the human clinical syndrome. I therefore used paracetamol-induced liver injury as a model to investigate the effect of CCR9 antagonism in acute liver injury.

Inhibition of CCR9 in paracetamol-induced liver injury in mice

Male C57/Bl6 mice aged 6 weeks and fasted overnight, were administered a small molecule inhibitor of CCR9 (30mg/kg of CCX507,   ) by subcutaneous injection 1 hour prior to administration of paracetamol. Previous pharmacokinetic experiments had shown that this dose of CCX507 caused over 90% of receptor coverage for over 24 hours (data not shown). A group of litter-mate control animals were given matched volumes of vehicle (1% hydroxypropyl methylcellulose, HPMC), without drug. Mice were   24, 48, or 72 hours after administration of paracetamol, by CO_2 inhalation. Blood samples were taken by cardiac puncture. A 24-hour initial time point was used despite peak liver injury being seen at 12 hours as a pragmatic measure - this allowed sufficient time for administration of inhibitor, paracetamol and analysis.

CCR9 antagonism reduced serum AST and ALT concentration over the course of the experiment (**figure 5.14**): two-way ANOVA p=0.0034 and p=0.0079 respectively.
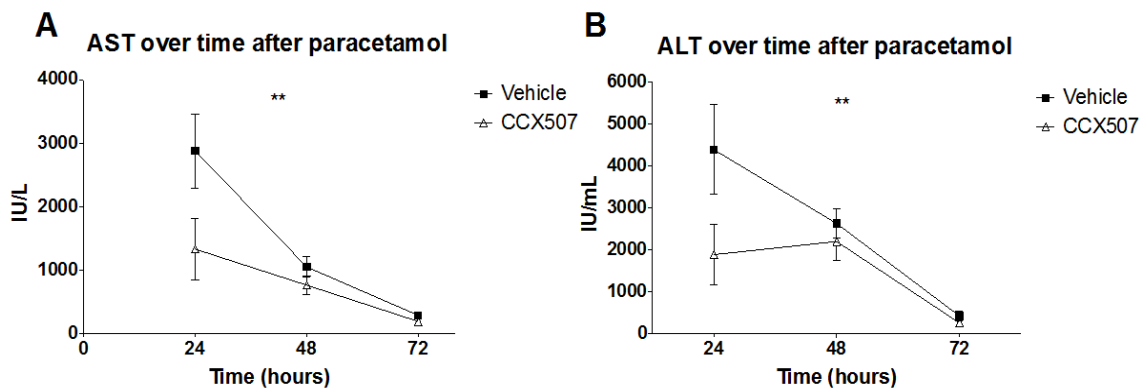
Figure 5.14: Inhibition of CCR9 in paracetamol-induced liver injury in mice

C57/Bl6 mice were given a small molecule inhibitor of CCR9, or comparable volume of vehicle, prior to administration of 400mg/kg of paracetamol. Serum AST and ALT concentration was measured at various time points after administration of paracetamol. **Two-way ANOVA p<0.01. Data are shown as mean and SEM, 5 mice per time-point

CCR9 antagonism with CCX507 reduces tissue CD11b$^+$CD11c$^-$ macrophages

Monocyte infiltration of liver tissue was analysed by flow cytometry 24 hours after administration of paracetamol in ten mice – the peak of injury and inflammation (see figures 10.8, 10.9 and 10.10). In view of previous reports implicating CCR9 expressing CD11b$^+$CD11c$^-$ macrophages in the development of acute injury, the accumulation of these cells post-paracetamol administration was assessed by flow cytometry. One mice died in the CCX507 group. Other mice treated with CCX507 had fewer liver-infiltrating CD11b$^+$CD11c$^-$ macrophages as a proportion of CD45$^+$CD11b$^+$ cells when compared to vehicle treated controls (median 13.2% (IQR 10.25) vs. 19.3 (8.63), Mann-Whitney test p=0.0034)(**figure 5.15**).

CD11b⁺CD11c⁻ macrophages
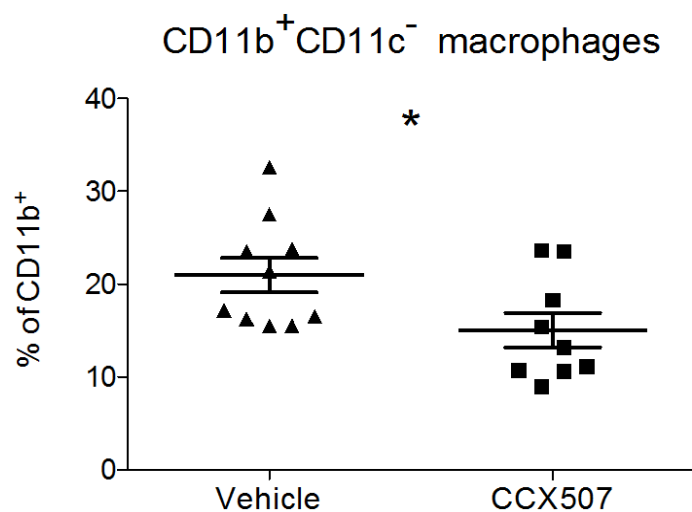
Figure 5.15: CCR9 antagonism reduces infiltration of liver tissue by macrophages

C57/Bl6 mice were given 400mg/kg of paracetamol and ▮▮▮▮ after 24 hours. Liver-infiltrating immune cells were analysed by flow cytometry, gated on CD45⁺ cells. CD11b⁺CD11c⁻ macrophages were reduced in mice given CCR9 antagonist CCX507 prior to paracetamol administration. *p<0.05 by student's t-test. Data are shown as median and IQR, *p<0.05 by Mann-Whitney test.

Prophylactic CCR9 antagonism does not improve survival after Paracetamol-induced liver injury

Little mortality was seen when using 400mg/kg of paracetamol. A higher dose of paracetamol - 750mg/kg - was used to establish if inhibition of CCR9 could confer a survival benefit. Ninety C57/Bl6 mice aged 6 weeks were given 750mg/kg of paracetamol after an overnight fast, with CCX507 (30mg/kg) or matched volumes of vehicle given 1 hour before paracetamol. Over the course of three experiments, an overall trend towards greater survival was seen in the mice given CCX507, but this was not statistically significant (log-rank p=0.075) (**figure 5.16**). The median time to death in the two groups was significantly different (median time to death, 40 hours (IQR 32) vs. 46 (24), Mann-Whitney test p=0.028) (**figure 5.17**).

Survival after high dose paracetamol
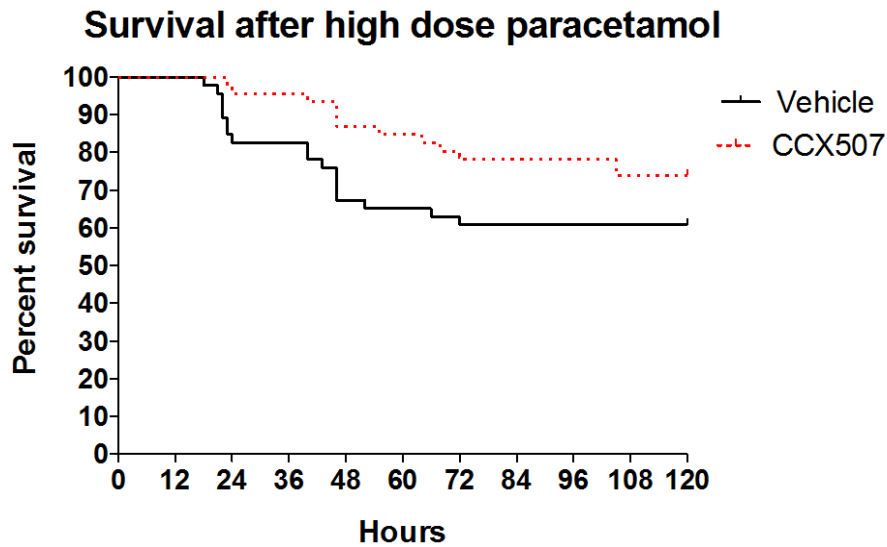
Figure 5.16: Prophylactic CCR9 antagonism does not improve survival after Paracetamol-induced liver injury

C57/Bl6 mice were given high dose paracetamol after administration of CCR9 antagonist CCX507 or vehicle. n=45 in each group, p=ns by log-rank test.

Median time to death after high dose AAP
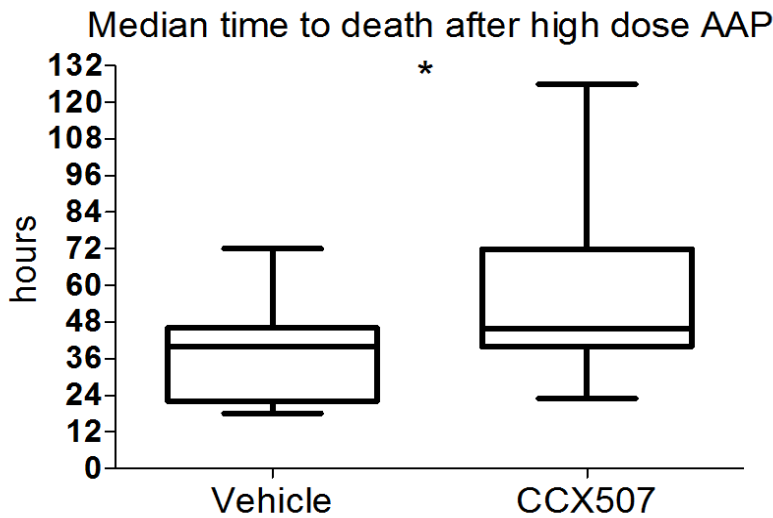
Figure 5.17: Prophylactic CCR9 antagonism improves median survival after Paracetamol-induced liver injury

C57/Bl6 mice were given high dose paracetamol after administration of CCR9 antagonist CCX507 or vehicle. Data are shown as median and IQR with whiskers showing minimum and maximum values. n=45 for each group, *p<0.05 by Mann-Whitney test.

Discussion

The CCR9/CCL25 axis is up regulated in human acute liver failure, where increased serum levels of CCL25 were observed. Data from human and mouse studies show that an increase in levels of CCL25 in serum is an early feature of ALF. In patients admitted to hospital with ALF, levels of CCL25 were greater early after admission and declined subsequently. In mice there was a marked increase in CCR9$^+$ macrophages within 12 hours of acute liver injury induced by either paracetamol or CCl_4, which corresponded to peak levels of liver injury as assessed by serum ALT concentration. CCR9$^+$ monocytes were observed in the explanted liver tissue of a patient undergoing liver transplantation for acute liver failure.

To study the role of CCR9 *in vivo* I used murine models of liver failure induced by carbon tetrachloride or paracetamol. Paracetamol was used in experiment with a CCR9 antagonist as a model that most closely reflects human disease. Prophylactic antagonism of CCR9 in mice improved early liver injury as assessed by serum AST and ALT concentration and significantly reduced infiltration of liver tissue by CD11b$^+$CD11c$^-$ macrophages. In high dose paracetamol toxicity, CCR9 antagonism did not improve survival, although a trend towards improved mortality was seen.

CCR9 was expressed on CD14^{++}CD16$^+$ monocytes in liver tissue from a patient with ALF. The CD14^{++}CD16$^+$ intermediate subset of monocytes is enriched in normal and diseased liver (Liaskou *et al.*, 2013)and secretes pro-inflammatory and pro-fibrotic cytokines and chemokines. In the context of acute liver injury, CCR9-mediated recruitment of monocytes may contribute to early inflammatory changes in the liver. This is supported by the observation that serum CCL25 concentration is highest in the early phase of hospital

admissions, and mouse data showing early increase in circulating pro-inflammatory CCR9^{+} cells. This increase in serum CCL25 also suggests that monocytes are recruited from blood as CCR9+ cells rather than expressing CCR9 after transmigration into liver. Liver transplant is performed relatively late after the onset of liver injury, and thus findings in explanted liver tissue may not reflect an early, pro-inflammatory phenomenon.

CCR9 is expressed on other cells other than monocytes/macrophages which are the focus of this chapter. As discussed in the introduction, CCR9 expression defines a population of gut-homing T lymphocytes (Svensson *et al.*, 2002, Johansson-Lindbom *et al.*, 2003) as well a T-lymphocytes observed in PSC (Eksteen *et al.*, 2004). B-cell expression of CCR9 is also seen in the context of the gastro-intestinal tract (Mora *et al.*, 2006). In terms of monocyte/macrophage CCR9 expression, pro-inflammatory myeloid cells expressing CCR9 have been reported in inflammatory bowel disease (Linton *et al.*, 2012) and rheumatoid arthritis (Schmutz *et al.*, 2010) in humans. Thus, the immunology of CCR9 antagonism has potentially more consequence than pure myeloid recruitment. However, in analysis of human liver specimens from patients with ALF, we saw the greatest CCR9 expression in cells of the myeloid gate (**figure 5.6A**) and confirmed that prophylactic CCR9 antagonism in mouse models of ALD reduced macrophage accumulation suggesting that this subset of leukocytes are mobilised at least in part by CCR9 in acute liver injury. In contrast plasmacytoid dendritic cells that were recruited via CCL25 were shown to be hepato-protective (Reid D *et al.*, 2013) in a sub-acute model of biliary injury.

In my data, an improvement in AST and ALT was observed at 24 hours after injury induced by paracetamol, as well as reduced accumulation of hepatic macrophages. That these changes occurred so early raises the possibility of other explanations other than immunological. Hepatocytes express some chemokine receptors with roles in regeneration – see chapter 7 – but no evidence for hepatocyte expression of CCR9 has been found (Autschbach *et al.*, 2005). Inhibition of CCR9 signalling has been investigated in other models: in murine peritoneal sepsis models, CCR9 is found on macrophages where it appears to control recruitment of macrophages to the peritoneum of mice subjected to caecal ligation in to control systemic sepsis during early phases of peritoneal infection (Mizukami *et al.*, 2012). Similar to my data, CCR9 knock-out mice were more vulnerable to microbial sepsis than wild-type black 6 mice and this was evident in terms of the clinical condition of mice as soon as 24 hours after the onset of caecal ligation. CCR9 antagonism may therefore have a very prompt effect on liver injury.

Thus, CCL25/CCR9 appears to be activated in a variety of disease states and models where the function of immune cells that express CCR9 differs. The function of CCR9^{+} cells may depend n the environment in which they are found and could conceivably change within an individual over the course of a disease. Functional experiments may illuminate this further.

CHAPTER 6: Role of CXCR6 in murine models of acute and chronic liver injury

Work from our laboratory showed the CXCR6/CXCL16 receptor/ligand pairing playing a role in the recruitment of lymphocytes to biliary epithelium (Heydtmann *et al.*, 2005). However contrasting results are evident in the published literature: Geissman et al. showed that CXCR6 knock out mice display reduced liver injury in a T-cell mediated model of acute liver damage induced by Concanavalin-A (Geissmann *et al.*, 2005), an effect attributed to a reduction in liver-resident NKT cells. In contrast Wehr et al reported that CXCR6 appears harmful in liver injury (Wehr *et al.*, 2013).

This led me to investigate the role of CXCR6 in liver injury *in vivo*, using a strain of CXCR6$^{GFP/GFP}$ mice ▓▓▓▓▓▓▓▓▓▓▓. These mice express green fluorescent protein instead of CXCR6 and are functional CXCR6 knockouts. The animals were backcrossed onto a C57/Black 6 (C57/Bl6) background, and C57/Bl6 mice were used as controls in all experiments.

CXCR6$^{GFP/GFP}$ mice were indistinguishable from wild type mice before induction of liver injury in terms circulating liver enzymes (ALT) and liver histology. CXCR6$^{GFP/GFP}$ mice and control mice were subjected to an acute liver injury by administration of carbon tetrachloride (CCl$_4$), or a chronic liver injury by administration of 5 weeks of hepatotoxic methionine-choline deficient (MCD) diet. The nature of injury differs between these two experiments: CCl$_4$ causes an acute toxic injury to liver tissue mediated through oxidative

stress. MCD diet prevents the export of lipids from hepatocytes causing marked steatosis and liver injury over weeks.

Knock out of CXCR6 in acute liver injury

Six male mice (three wild type, three CXCR6$^{GFP/GFP}$ mice) aged 6 weeks were administered a single dose of 1mg/kg of CCl$_4$ suspended in corn oil, or corn oil alone by intra-peritoneal injection. After 24 hours, mice were ▮▮▮▮▮▮ nd blood and liver samples were taken.

CXCR6$^{GFP/GFP}$ mice and serum markers of liver injury

Serum concentrations of AST and bilirubin were measured to assess liver injury. CXCR6$^{GFP/GFP}$ mice had lower levels of AST although this was not statistically significant (median concentration 101.0 IU/mL (IQR 142) vs. 250 IU/mL (379), Mann-Whitney test p=0.200). Bilirubin concentration was the same between groups (median 4.0 μmol/L (IQR 6.0) vs. 4.0 (1.00), student's t-test p=0.427) (**figure 6.1**).
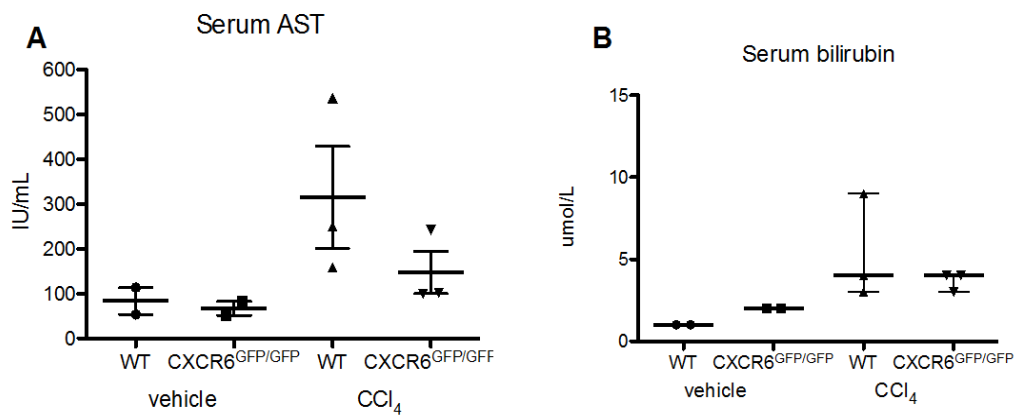
Figure 6.1: *Serum markers of liver injury after administration of carbon tetrachloride*

*Acute liver injury was induced in C57/Bl6 mice and CXCR6^{GFP/GFP} mice by administration of CCl4. When compared to WT C57Bl/6 animals CXCR6^{GFP/GFP} mice had lower serum concentrations of **A** AST but **B** bilirubin did not differ, 24h post administration of CCl4 although these differences did not reach significance. Data are shown with a point representing each animal, with lines at median and IQR.*

Infiltration of liver tissue by leukocytes

Sections of liver tissue were stained with haematoxylin and eosin, and imaged at 10x magnification with an Axioskop 40 microscope. Analysis of sections was performed by counting the number of infiltrating cells in ten $100\mu m^2$ areas over each section. In keeping with the data regarding liver injury, the CXCR6$^{GFP/GFP}$ tended to have fewer infiltrating cells in liver tissue but this was not statistically significant (median 7.1 cells per $100\mu m^2$ (IQR 2.5) vs. 10.1 (IQR 4.4), Mann-Whitney test p=0.20) (**figure 6.2**)(**figure 6.3**).
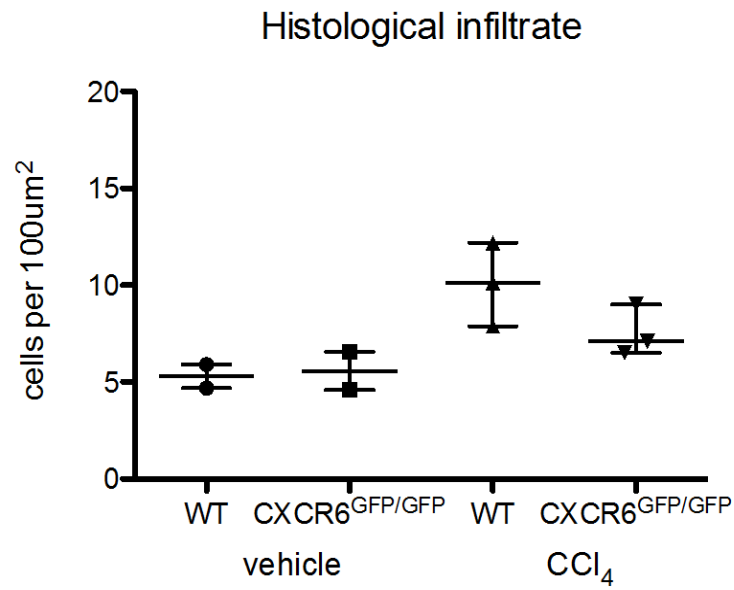
Figure 6.2: Histological assessment of leukocyte infiltration after administration of carbon tetrachloride

Acute liver injury was induced in C57/Bl6 mice and CXCR6^GFP/GFP mice by administration of CCl₄. When compared to WT C57Bl/6 animals CXCR6^GFP/GFP mice had fewer infiltrating cells assessed by histology, although these differences did not reach significance. Data are shown with a point representing each animal, with lines at median and IQR.
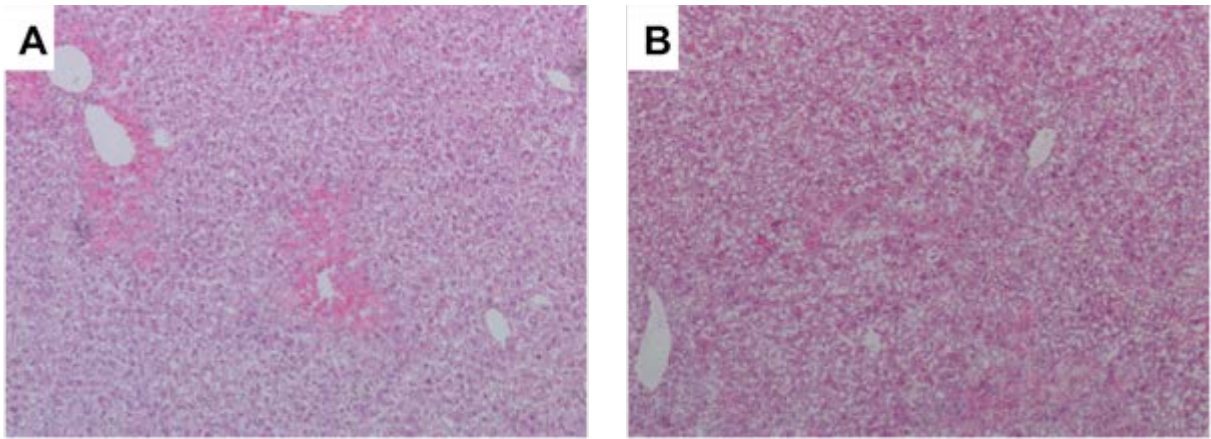
Figure 6.3: histological appearance of liver injury after acute CCl₄ injury

Wild type and CXCR6GFP/GFP mice were given 1ml/kg of CCl4 and ▓▓▓▓▓ *24 hours later.*

Sections of tissue stained with haematoxylin and eosin from A wild type and B CXCR6GFP/GFP mice.

Knock-out of CXCR6 in chronic liver injury

Response to MCD diet in the absence of CXCR6

Five male CXCR6^{GFP/GFP} and five male C57/Bl6 mice aged six weeks were administered a MCD diet for 6 weeks to induce a chronic model of hepatic injury. Reduced lipid export from hepatocytes causes liver injury. Animals on an MCD diet typically develop steatohepatitis and a very mild fibrotic response over the course of the diet. At the end █ blood and liver samples were taken for analysis.

MCD diet causes similar weight loss in CXCR6^{GFP/GFP} and control mice

It has been shown that the MCD diet induces significant weight loss (typically up to 40% over 5-6 weeks) and therefore the weight of each animal was monitored closely throughout the duration of the experiment. Control mice were heavier at baseline and throughout the experimental period, but proportional weight loss did not differ between groups (**figure 6.4 A, B**).

MCD diet causes similar hepatic steatosis in CXCR6^{GFP/GFP} and wild type mice

MCD diet causes hepatic steatosis through inhibition of lipid export from hepatocytes. To assess steatosis, frozen sections of liver tissue were incubated with Oil-red-O which stains neutral triglycerides and lipids. Steatosis was quantified by proportion of the area of the section that stained positive for the dye as assessed by ImageJ analysis. No difference in steatosis was observed between CXCR6^{GFP/GFP} mice and control mice (mean percentage area 26.8% (SEM 0.45) vs. 26.8 (0.82), student's t-test p=0.992) (**figure 6.5**, **figure 6.6**).
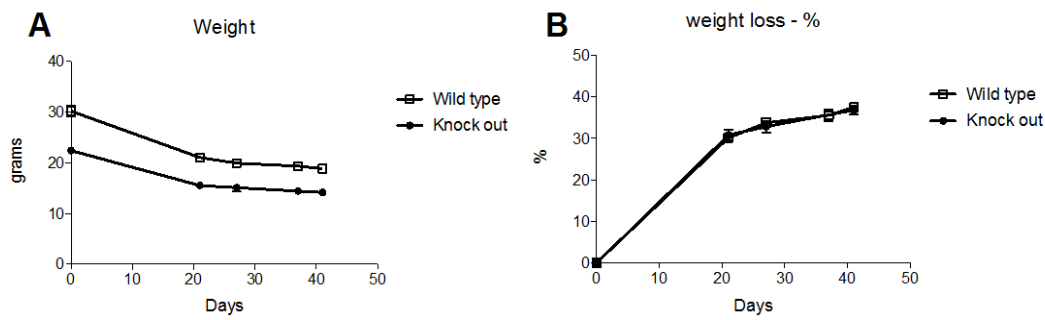
Figure 6.4: MCD diet causes similar weight loss in CXCR6GFP/GFP and control mice

C57/Bl6 (n=5) and CXCR6$^{GFP/GFP}$ (n=5) male mice were given MCD diet for 5 weeks. **A** Absolute weight was higher in wild type mice, but **B** proportional weight loss did not differ between groups. Data shown as mean and SEM.
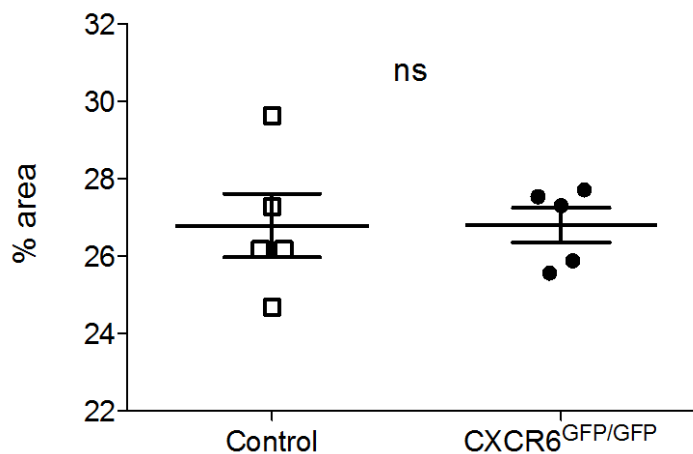
Figure 6.5: MCD diet causes similar hepatic steatosis in CXCR6GFP/GFP and wild type mice

C57/Bl6 (n=5) and CXCR6$^{GFP/GFP}$ (n=5) mice were given MCD diet for 5 weeks. Oil-red O staining of liver sections was performed, and hepatic steatosis quantified by measuring percentage area of staining over 5 fields at 10x magnification for each animal. Each data point represents one animal, lines represent mean and SEM, p=ns by student's t-test.

Serum markers of liver injury are higher in CXCR6^{GFP/GFP} mice on MCD diet

Blood samples taken by cardiac puncture at the time of ███████ were analysed for AST activity and bilirubin concentration. Serum AST concentration was significantly higher in CXCR6^{GFP/GFP} mice than in wild type (mean 689 IU/ml (SEM 144) vs. 233 (45.5), students t-test p=0.03) (**figure 6.7**). Bilirubin concentration also differed between groups but this was not statistically significant (mean 26 μmol/L (IQR 12.5) vs 9.3 (0.63), student's t-test 0.229).

Infiltration of NKT cells is reduced in CXCR6^{GFP/GFP} mice

Infiltrating lymphocytes were isolated from liver tissue and analysed by flow cytometry. No significant differences were observed between wild type mice and CXCR6GFP/GFP mice with regard to CD3+ T lymphocytes or CD3-Nk1.1+ NK cells as frequency of all lymphoid cells (**table 6.1, figure 6.6 A, B**). However the frequency of CD3+Nk1.1+ NKT cells as a proportion of all lymphoid cells was markedly reduced in CXCR6GFP/GFP mice (**table 6.1, figure 6.8 C**) as might be expected given the role of CXCR6 in the recruitment of this subset (see introduction). Distribution of leukocytes was similar in wild type and CXCR6GFP/GFP mice (**figure 6.8**).
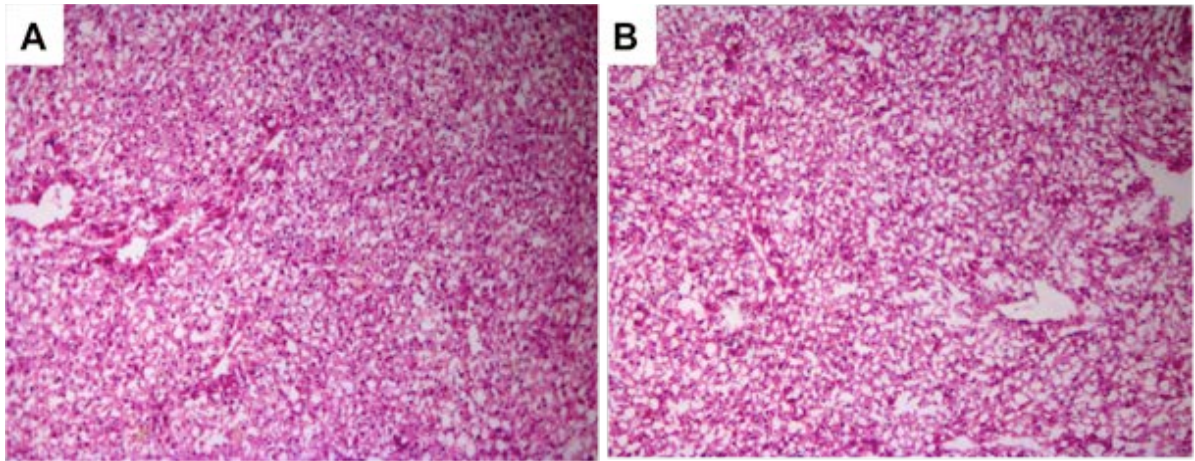
Figure 6.6: histological appearance of liver injury after MCD diet

Wild type and CXCR6GFP/GFP mice were given MCD diet for 5 weeks. Sections of liver tissue from A wild type mice and B CXCR6GFP/GFP mice were stained with haematoxylin and eosin. Images at 10x magnification. Steatosis was similar between the two groups in terms of quantity and distribution.
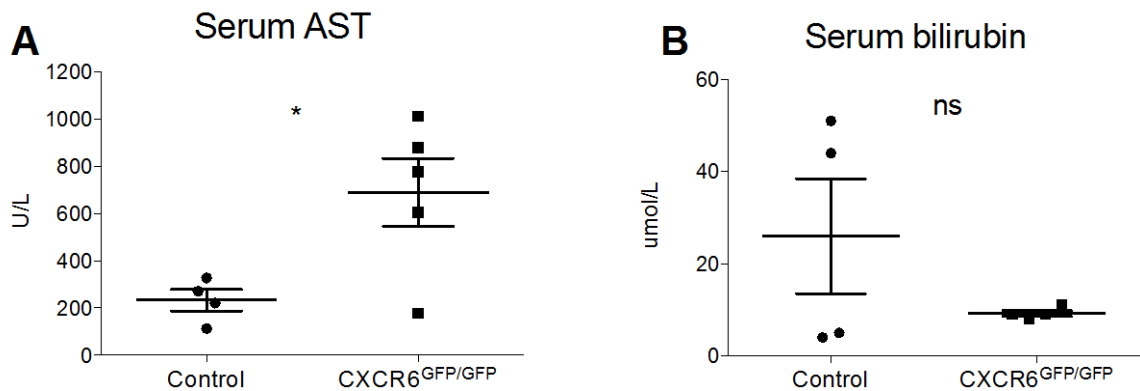
Figure 6.7: Serum markers of liver injury in CXCR6GFP/GFP mice on MCD diet

C57/Bl6 and CXCR6GFP/GFP mice were given MCD diet for 5 weeks. A Serum AST concentration was higher in CXCR6GFP/GFP mice B no difference was seen in bilirubin concentration. * student's t-test p<0.05

	Control mice		CXCR6$^{GFP/GFP}$ mice		p
	Frequency of lymphoid gate (median)	IQR	Frequency of lymphoid gate (median)	IQR	
CD3$^+$ T lymphocytes	17.9	6.82	12.36	15.34	0.421
CD3$^+$Nk1.1$^+$ NKT cells	7.63	4.31	1.86	1.74	0.008
CD3$^-$Nk1.1$^+$ NK cells	15.5	4.80	23.2	21.1	0.151

Table 6.1: C57/Bl6 (n=5) and CXCR6GFP/GFP (n=5) mice were given MCD diet for 5 weeks.

Infiltrating lymphocytes isolated from liver tissue were analysed by flow cytometry. Lymphocyte subsets were gated on CD45+cells and then categorised by CD3 and Nk1.1 expression as CD3 lymphocytes, NKT cells or NK cells. Analysed with Mann-Whitney test.
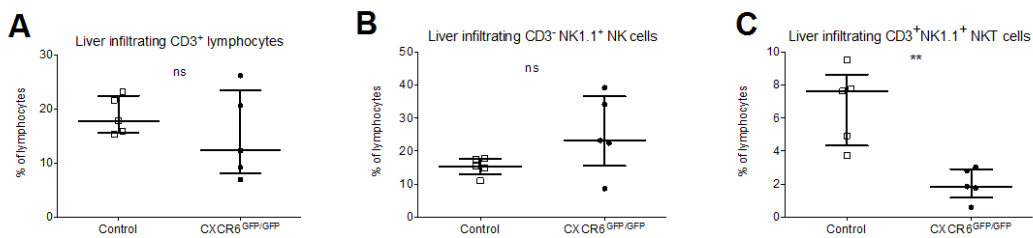
Figure 6.8: Infiltration of NKT cells is reduced in CXCR6GFP/GFP mice

*C57/Bl6 (n=5) and CXCR6GFP/GFP (n=5) mice were given MCD diet for 5 weeks. Infiltrating lymphocytes were isolated from liver tissue and analysed by flow cytometry. No differences were observed in frequency of infiltrating A T lymphocytes or B NK cells. C Fewer NKT cells were seen as proportion of all lymphoid cells. Each data point represents a single animal, lines at median and IQR **p<0.01, ns=p>0.05 by Mann Whitney test*

Pro-fibrotic genes are up-regulated in CXCR6$^{GFP/GFP}$ mice following 5 weeks of MCD diet

Fibrosis is a common feature of chronic liver injury. The MCD diet model of liver injury results in increased fibrogenesis although this is mild compared with human fatty liver disease.

Frozen sections of liver tissue were processed with Van Gieson staining to detect total collagen. The extent of fibrosis was then quantified using Image-J software to measure the collagen proportionate area of the section that was stained. No significant differences in area of staining were observed although there was a trend for more fibrosis in CXCR6$^{GFP/GFP}$ mice (mean percentage area 1.83% (SEM 0.05) vs. 1.99 (0.05), Mann-Whitney test p=0.151) (**figure 6.7**)(**figure 6.10**).

Due to the mild nature of fibrosis routinely observed in the MCD diet model of liver injury early changes in fibrogenesis might be better reflected in gene expression of pro-fibrotic genes rather than by assessing mature matrix by van Gieson staining. To this end, the expression of *Col1a1* (collagen 1a1) and *Acta2* (α-smooth muscle actin) were analysed by qRT-PCR. Expression of both genes was significantly increased in the liver tissue taken from CXCR6$^{GFP/GFP}$ mice, suggesting that the absence of CXCR6 promotes fibrogenesis (**figure 6.11 A** and **B**).
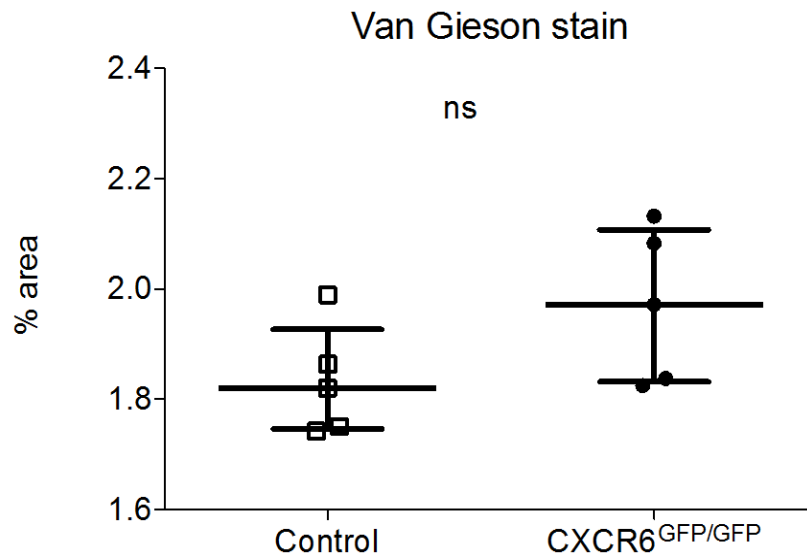
Figure 6.9: No differences in histological appearances of fibrosis between wildtype and CXCR6GFP/GFP mice after MCD diet

C57/Bl6 and CXCR6GFP/GFP mice were fed an MCD diet for 5 weeks. Fibrosis induced by diet was assessed by Van Gieson staining of liver sections. Five mice in each group. Data are shown as median and IQR
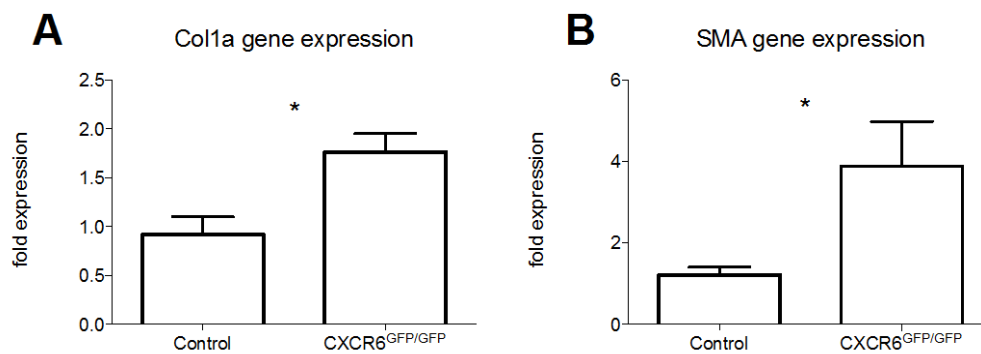
Figure 6.10 Pro-fibrotic genes are up-regulated in CXCR6$^{GFP/GFP}$ mice following 5 weeks of MCD diet

*C57/Bl6 and CXCR6GFP/GFP mice were fed an MCD diet for 5 weeks. Fibrosis induced by diet was assessed by Van Gieson staining of liver sections, A Col1a1 gene expression and D Acta2 gene expression Five mice in each group. Data are shown as mean and SEM. *p<0.05 by student's t-test.*

Conclusion

Acute and chronic models of liver injury in mice showed contrasting effects of CXCR6. In acute injury induced by CCl_4, a pattern towards reduced injury in CXCR6$^{GFP/GFP}$ mice was seen although numbers of mice was too small to allow for statistical significance. In contrast, in a chronic or sub-acute injury caused by MCD diet, mice without functional CXCR6 demonstrated worse liver injury – higher serum AST concentration and more fibrosis - despite reduced infiltration of NKT cells.

██. Acute liver injury in this strain of mice has been reported by other investigators. In particular, Wehr et al. who administered a slightly lower dose of CCl4 than I did (0.6mL/kg compared to 1.0mL/kg) (Wehr *et al.*, 2013). This group reported attenuated liver injury in CXCR6GFP/GFP mice, measured by ALT. Interestingly this difference was significant at 6 and 72 hours after iniation of injury, but did not appear to be at 24 hours after injury, which was the time point that I used. This group were also able to analyse the infiltrate in CCl_4 injury where significantly fewer NKT cells and monocytes were seen. In a T-cell mediated hepatitis induced by injection of concanavalin-A, CXCR6$^{GFP/GFP}$ mice were protected with lower serum AST concentration and less pronounced necrotic changes on histology.

Other models of acute liver injury have demonstrated the harmful role of CXCR6/CXCL16: Xu and colleagues gave primed mice with Bacille Calmette-Geurin (BCG) injection and then administered LPS to induce liver injury (Xu *et al.*, 2005). Anti-CXCL16 antibodies reduced ALT concentration and protected against death. Sato et al. used a model of graft versus host disease (GvHD) with wild-type or CXCR6$^{-/-}$ lymphocytes, where reduced CD8$^+$ lymphocyte

recruitment was observed although direct measures of liver injury are not reported. My data regarding CCl_4 are therefore consistent with other reports of the role of CXCR6 in acute liver injury.

Liver injury induced by MCD diet is a much more chronic process than the injury caused by CCl_4. I saw no effect on steatosis caused by MCD diet, which would be expected as this is mediated by dietary deficiency. However I saw a statistically significant *increase* in serum AST, despite a decrease in infiltrating NKT cells. The only other data reported on this type of injury in the context of CXCR6 knock out mice is from Wehr (Wehr *et al.*, 2013, Wehr *et al.*, 2014). These investigators saw a similar decrease in infiltrating NKT cells, but reduced histological necrosis and fibrosis. Interestingly serum AST or ALT is not reported. The only differences between my experiment and this group seems to be the length of diet – I gave mice 5 weeks of MCD, whereas Wehr and colleagues report 4 and 8 week outcomes. It is hard to see how this might make a difference to the findings as similar results were seen at each time point.

A possible explanation for this observation is that NKT cells, noted to be markedly reduced in CXCR6$^{GFP/GFP}$ mice by the Wehr group and myself, have been shown to be able to drive the migration and activate T regulatory (Treg) cells (Santodomingo-Garzon and Swain, 2011). An absence of Treg activation by NKT cells could lead to the more severe liver injury that I observed. Unfortunately neither I nor the Wehr paper show data regarding Treg numbers of function. An alternative explaination is suggested by the data previously discussed from Gao et al. (Gao *et al.*, 2012) showing CXCR6 expression by hepatocytes. CXCR6 may play a protective role, where knock-out would be detrimental.

The divergent results between acute and sub-acute models of liver injury, and between my data and published work, and the important differences between the distribution of CXCR6 on lymphoid cells between humans and mice lead to examination of CXCR6 in human liver disease, described in the next two chapters.

CHAPTER 7: Expression and function of CXCR6 on hepatocytes

Most of the focus on chemokine receptors as targets in liver disease has been on their expression and function of leukocytes and how this may regulate the balance between inflammatory and regulatory pathways in inflammatory diseases. However chemokine receptors are also expressed on non haematopoetic cell types including stromal and epithelial cells and a full understanding of the effects of inhibiting chemokine signalling needs to take into account possible effects on these cell types.

Hepatocytes express the chemokine receptors CXCR1 (Clarke *et al.*, 2011) and CXCR2 (Hogaboam *et al.*, 1999, Bone-Larson *et al.*, 2001, Kuboki *et al.*, 2008). The expression of these receptors has been suggested to be protective against liver injury. Antagonism of CXCR1/2 exacerbated ischaemic/reperfusion injury while CXCR1$^-$/- mice showed reduced hepatocyte proliferation (Clarke *et al.*, 2011). Administration of recombinant CXCL10 (a CXCR2 ligand) protected mice against paracetamol-induced acute liver injury through induction of CXCR2 (Bone-Larson *et al.*, 2001) although these results are contradicted by a later study using ischaemia/reperfusion injury as a model of acute liver injury, where CXCR2-/- mice and CXCR2 antagonists were protective (Kuboki *et al.*, 2008). The authors found evidence of opposing concentration-dependent effects of the CXCR2 ligand CXCL2: low concentrations were hepato-protective whereas higher concentrations were hepatotoxic.

CXCR6 is expressed by specific subsets of effector lymphocytes and is has been implicated in the development of inflammation and injury in several liver diseases making it a potential target for therapeutic intervention. In addition, CXCR6 is expressed by hepatoma cell lines *in vitro* and has been described *in vivo* on tumour cell in tissue in HCC (Gao *et al.*, 2012). In this report, CXCR6 expression in HCC specimens was associated with vascular invasion of tumours, and also HCC progression suggesting it plays a functional role. Outside of the liver, CXCR6 and its ligand CXCL16 are expressed in a variety of tumours where expression has been associated with a more aggressive phenotype (Porta, 2012). For example CXCR6 expression has been shown in glial precursor cells in the central nervous system where it guides migration and invasion (Ludwig *et al.*, 2005, Hattermann *et al.*, 2008). Interestingly CXCR6 signalling has shown a protective function in the gut where it can facilitate epithelial restitution in gut tissue (Furuya *et al.*, 2011).

To further elucidate the role of this chemokine receptor:ligand pairing in the development of chronic liver disease I investigated the expression of CXCR6 on parenchymal liver cells, and used hepatoma cell lines in functional assays to explore the effects of CXCR6 signalling.

CXCR6 expression on parenchymal liver cells

CXCR6 is expressed by immune cells and hepatocytes in injured liver

Immunohistochemistry was performed on formalin fixed paraffin-embedded liver sections to identify cells that expressed CXCR6. Initial experiments were unsuccessful with non-specific staining seen despite trying a variety of different antibody concentrations and protocols.

However, a low-temperature antigen-retrieval step proved to be successful and allowed us to study CXCR6 expression. CXCR6 was detected on infiltrating immune cells, as expected, but also on hepatocytes, particularly at the edge of regenerating nodules adjacent to fibrous septa (**figure 7.1**).

To confirm these findings and better define cellular localisation, I used simultaneous staining of different cell lineages using antibodies conjugated to fluorochromes imaged by confocal microscopy. Hepatocytes were identified through staining sections with an antibody against CK18 and this confirmed CXCR6 expression on hepatocytes (**figure 7.2**).
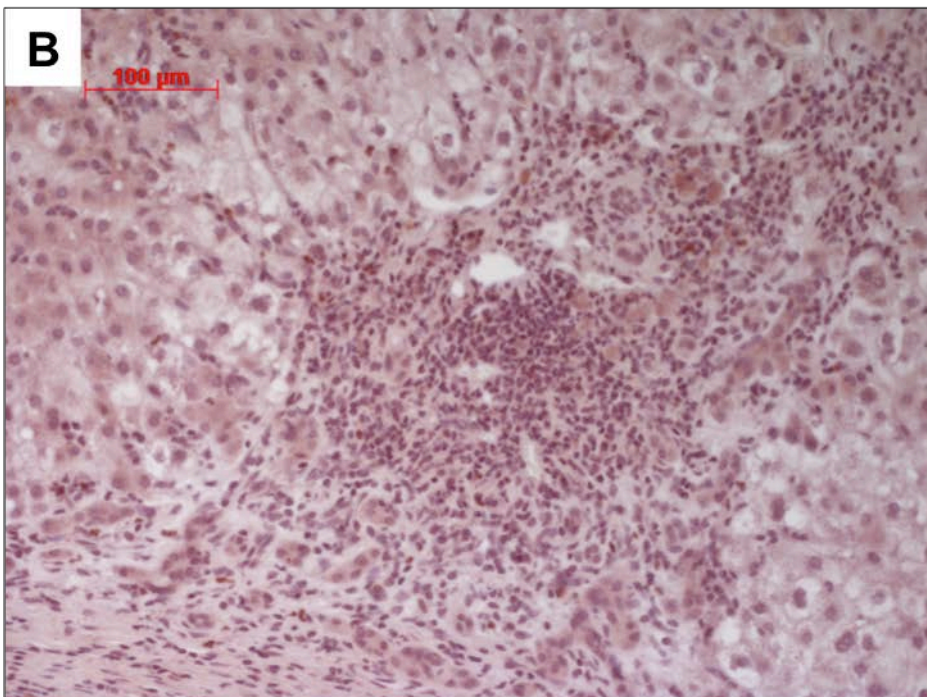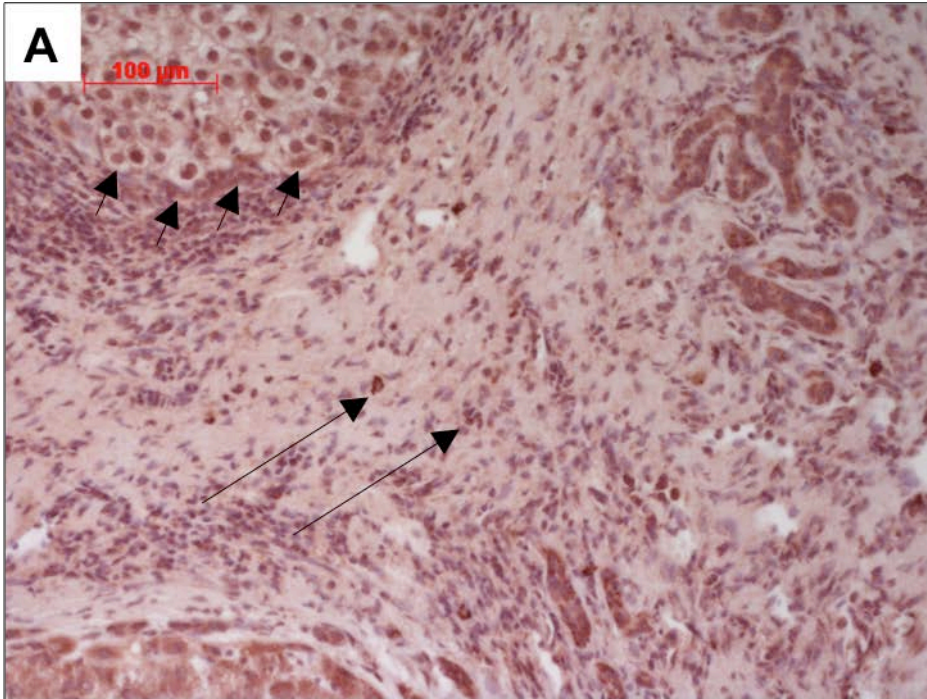
Figure 7.1: CXCR6 is expressed by leukocytes and hepatocytes in injured liver

*Paraffin embedded sections of explanted liver tissue was stained for CXCR6. Sections are shown at 40x magnification **A** CXCR6 was expressed on infiltrating immune cells (long arrows) and also on hepatocytes, particularly at the edge of regenerative nodules (short arrows). **B** staining with isotype matched antibody.*
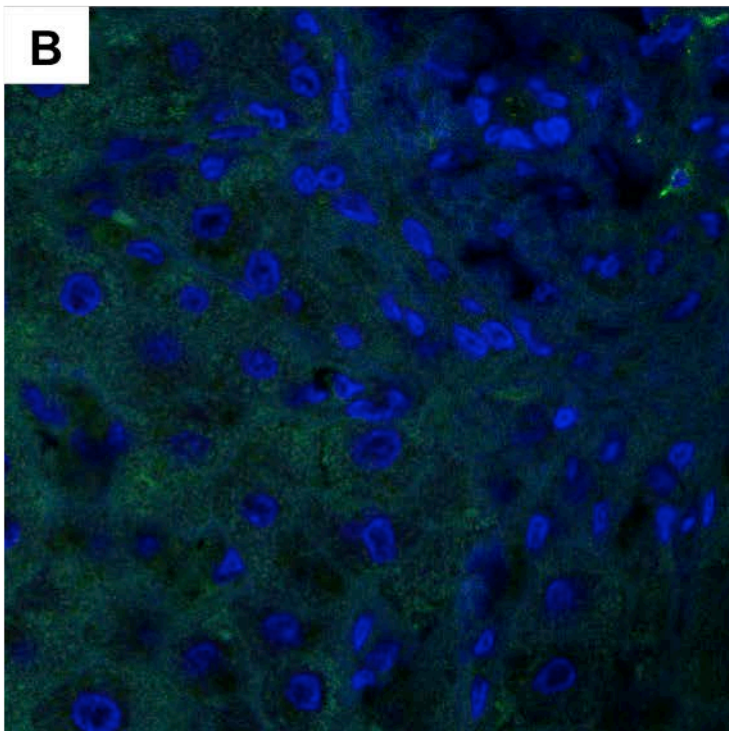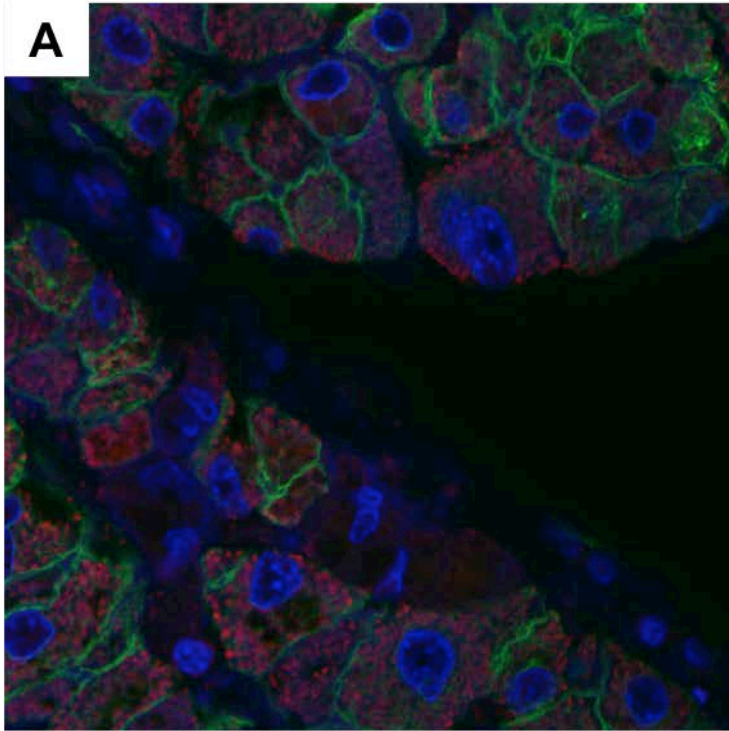
Figure 7.2: CXCR6 is expressed by hepatocytes

Paraffin-embedded sections of liver tissue were stained with antibodies conjugated to fluorochromes and imaged with confocal microscopy at 63x magnification. In this image CK18 is shown in green, DAPI in blue and CXCR6 shown in red. CXCR6 is expressed by hepatocytes, marked by membrane

CK18 expression, and to a lesser extent by infiltrating immune cells in the fibrous septum. Image B shows staining with DAPI, CK18 and an isotype matched control antibody in place of CXCR6

CXCR6 gene expression in cirrhotic liver

RNA was isolated from whole liver tissue from patients with cirrhosis removed at the time of transplantation, and non-involved liver tissue distal to resected liver tumours tissue from resections performed to remove malignancy, distal to the cancerous lesion) was used. *CXCR6* gene expression was analysed by qRT-PCR relative to β-*ACTIN* as a control gene. Cirrhotic liver showed increased gene expression of *CXCR6* compared to non-cirrhotic liver tissue (**figure 7.3**), although this was not statistically significant (median fold expression in cirrhotic tissue 2.09 (IQR 5.70) vs. 0.44 (1.22), Mann Whitney test p=0.095).

Whole liver CXCR6 gene expression
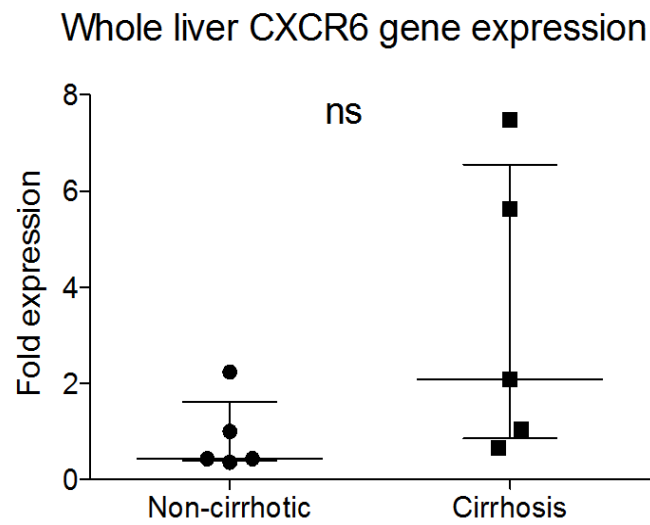
Figure 7.3 CXCR6 gene expression is not up-regulated in cirrhotic liver

 RNA was isolated from cirrhotic (n=5) and non-cirrhotic (n=5) liver tissue. Gene expression of CXCR6 was analysed by qRT-PCR with reference to β-ACTIN as a housekeeping gene. Each data point represents a single isolate of liver tissue, normalized to average CXCR6 expression in normal liver tissue. Lines represent median and IQR. ns=p>0.05 by Mann Whitney test

Gene expression of CXCR6 is increased in hepatocellular carcinoma

The finding of CXCR6 expression on hepatocytes was consistent with previous reports of CXCR6 expression in HCC (Gao *et al.*, 2012). In view of this, *CXCR6* gene expression in HCC was investigated.

RNA was isolated from samples of tissue taken from both HCC and distal, non-cancerous tissue in the same liver. *CXCR6* gene expression was analysed with qRT-PCR, using *β-actin* as a housekeeping gene and found to be significantly up regulated in HCC compared to distal tissue (mean fold expression in HCC 6.09 (SEM 8.56), paired t-test p=0.031)(**figure 7.4**). The increase in gene expression was not consistent in all samples. Expression appeared to segregate into at least two discrete populations and therefore the histological grade of tumour tissue was examined with regard to *CXCR6* expression. There was a trend for the differentiation grade of the tumour to associate with *CXCR6* expression although this was not significant (one-way ANOVA p=0.306)(**figure 7.5A**). However, when considering the background liver tissue, greater expression of *CXCR6* was seen in tumours arising in cirrhotic liver tissue than those arising in non-cirrhotic tissue (mean fold *CXCR6* gene expression from distal tissue 8.12 (SEM 3.12) in cirrhotic tissue vs. 0.916 (0.195) in non-cirrhotic tissue, student's t-test p=0.046) (**figure 7.5B**).

Distal/tumour CXCR6 gene expression
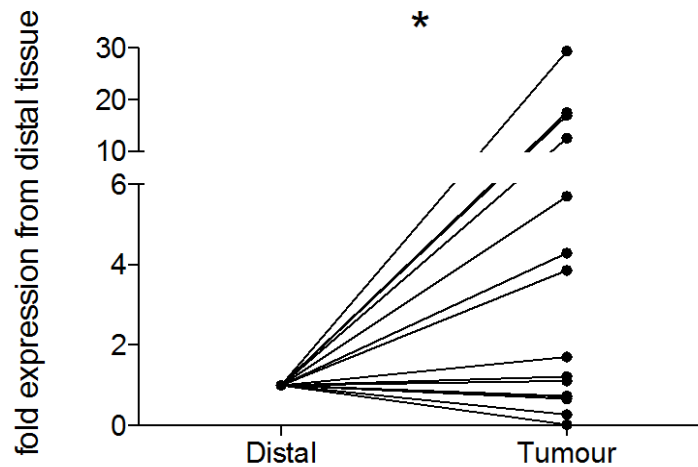
Figure 7.4: Gene expression of CXCR6 is increased in hepatocellular carcinoma

RNA was isolated from cancerous lesions or distal non-cancerous liver tissue and CXCR6 gene expression analysed by qRT-PCR. CXCR6 gene expression was higher in cancerous tissue. n=16, *p<0.05 by paired t-test. Each pair of data points represents tumour or distal tissue from one liver, where CXCR6 expression is normalized to expression in distal tissue.
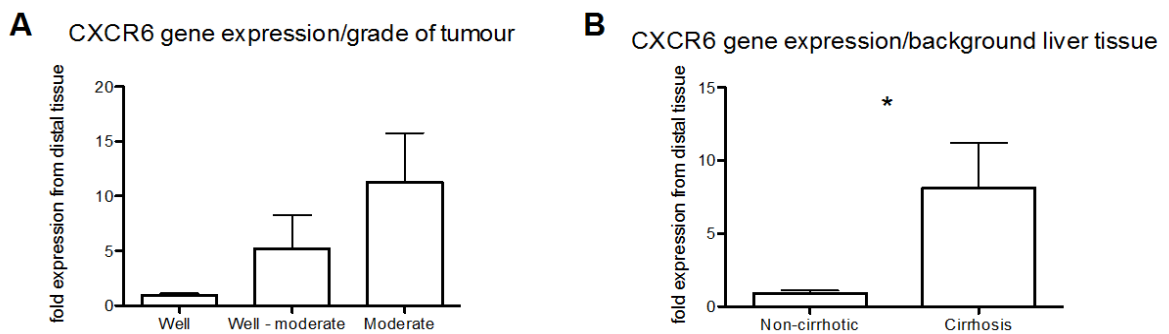
Figure 7.5: CXCR6 gene expression is associated with phenotype of background liver

RNA was isolated from cancerous and distal non-cancerous liver tissue. Gene expression of CXCR6 was analysed by qRT-PCR and changes in expression categorised by **A** grade of tumour differentiation categorised as well (n=2), well-moderate (n=5) or moderate (n=6) (one way ANOVA p=0.306) and **B** background liver disease categorised as non-cirrhotic (n=3) or cirrhotic (n=13) *p<0.05 by student's t-test.

CXCR6 is expressed by HCC tumour tissue

Paraffin-embedded paired sections of tumour tissue and non-involved liver tissue from patients with HCC were stained for CXCR6 expression. Immunohistochemistry showed diffuse staining for CXCR6 throughout liver parenchyma as described above, but particularly at the margins of regenerative nodules in liver resected for HCC (**figure 7.6 and 7.7**).

In very few cases, it was possible to perform both qRT-PCR and immunohistochemistry. In these few samples, higher gene expression was associated with stronger staining. Comparison between gene expression data and immunohistochemistry was not possible in most cases due to limitations of tissue available – many samples were stored as frozen or in formalin, but not both.
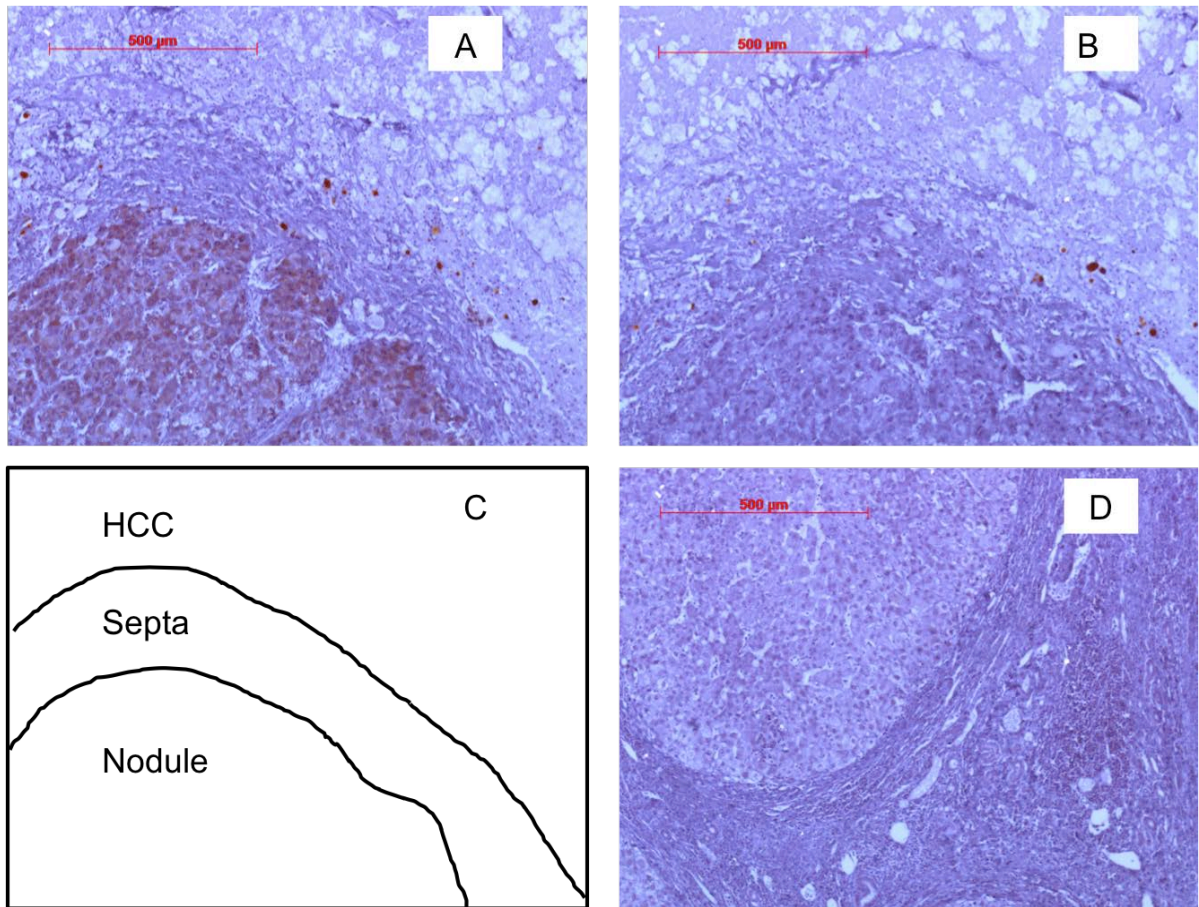
Figure 7.6: CXCR6 is expressed by hepatocellular carcinoma

Paraffin-embedded sections of tumour tissue and distal, non-involved liver form the same patient were stained for CXCR6. Images at 10x magnification are shown

A margin of HCC showing strong CXCR6 expression in neighbouring regenerative nodule (red) B staining of same area with isotype matched control antibody C cartoon of image A to demonstrate relevant areas of image D staining of distal liver tissue from the same patient without evidence of CXCR6 expression
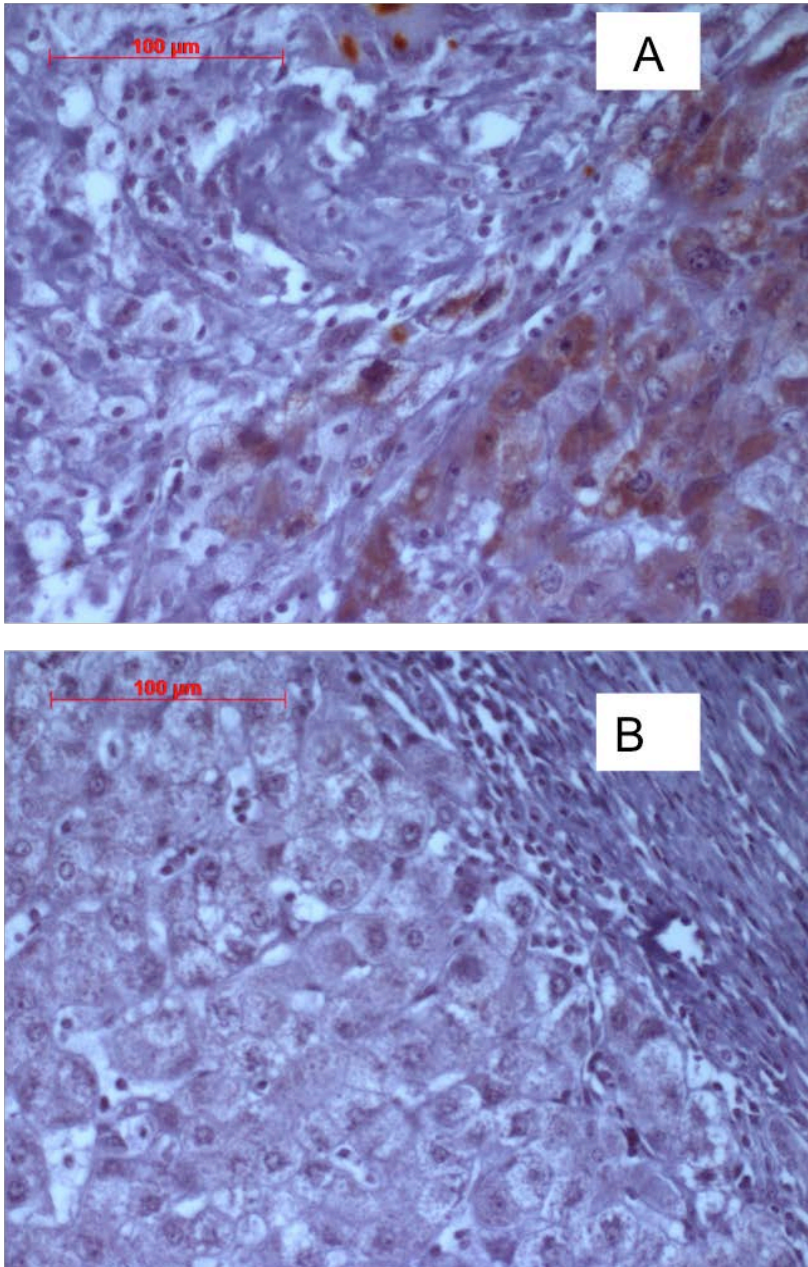
Figure 7.7: CXCR6 is expressed by hepatocellular carcinoma

Paraffin-embedded sections of tumour tissue and distal, non-involved liver form the same patient were stained for CXCR6. Images at 40x magnification are shown

A CXCR6 staining from margin of HCC showing strong CXCR6 expression in neighbouring regenerative nodule B CXCR6 staining of distal uninvolved liver from the same patient, without overt CXCR6 expression

Expression of CXCR6 in hepatoma cell lines

Having confirmed increased gene and protein expression of CXCR6 in HCC, I investigated whether hepatocyte associated CXCR6 retained function. For these experiments, the hepatoma cell lines Huh-7 and HepG2 were used. The HuH-7 cell line was established from a well-differentiated hepatocellular carcinoma in a 57-year-old Japanese man in the early 1980s (Nakabayashi *et al.*, 1982). In contrast, the HepG2 cell line was established from biopsies of a hepatocellular blastoma in a fifteen-year-old Caucasian boy in the 1970s (Aden *et al.*, 1979). These cell lines are useful surrogates for primary hepatocytes, or of cells from HCC for *in vitro* studies as they are amenable to culture.

Expression of CXCR6 transcripts in hepatoma cell lines

HepG2 and HuH-7 hepatoma cells were serum starved for 24 hours and then incubated with TNF-α and IFN-γ (both at 10ng/ml), or varying concentrations of the CXCR6 ligand CXCL16 for 24 hours. CXCR6 gene expression was then analysed by qRT-PCR. Both HepG2 and HuH-7 cells expressed CXCR6 (**figure 7.8**), the levels of which were increased significantly upon the addition of 10ng/ml of CXCL16 for 24 hours (HuH cells, fold CXCR6 gene expression 12.84 compared to no treatment, $p < 0.001$ by student's test, HepG2 cells, mean fold CXCR6 gene expression 7.06 compared to no treatment, $p = 0.015$ by student's t-test) (**figure 7.8**). Conversely, the addition of a lower concentration of CXCL16 (2.5ng/ml) or a combination of the pro-inflammatory cytokines TNF-α and IFN-γ had no effect.
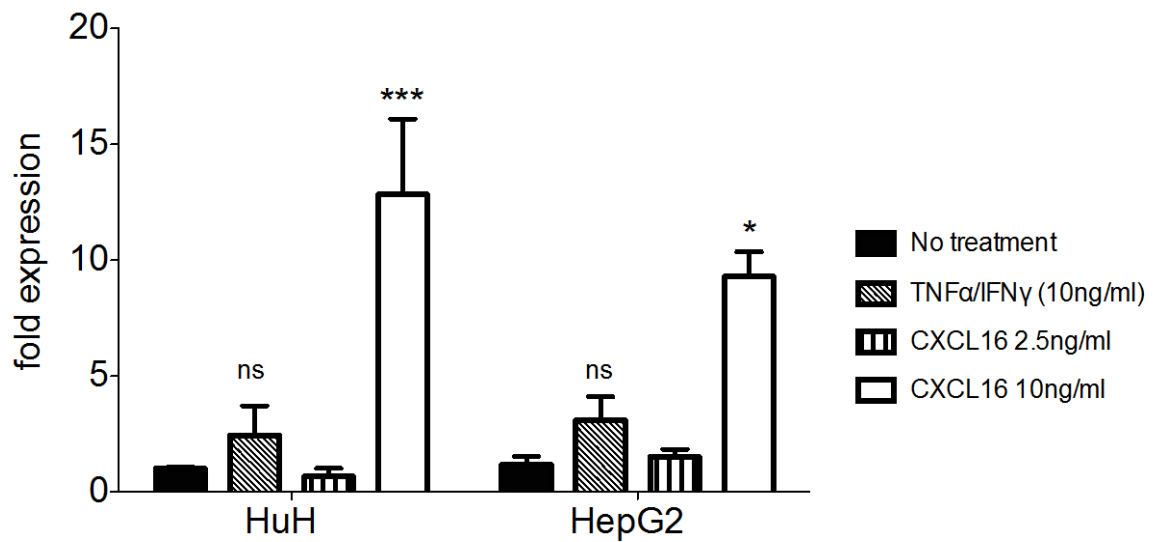
Figure 7.8: Hepatoma cell lines show CXCR6 gene expression

Hepatoma cell lines were incubated in media treated with TNFa and IFNg or CXCL16. CXCR6 gene expression was analysed by qRT-PCR. n=5 for each replicate. Expression was measured relative to B-ACTIN, and normalized to the no treatment control. Data are shown as mean and SEM, ns:p<0.05, *p<0.05, ***p<0.001 by student's t-test.

Function of CXCR6 on hepatoma cell lines

Given the presence of CXCR6 in HCC, I studied the effect of CXCR6 on the proliferation of hepatoma cell lines as a measure of the functionality of CXCR6. The proliferation of hepatoma cells was analysed by analysis staining of DNA with Hoescht dye and by analysis of dividing cells with flow cytometry.

CXCR6 increases proliferation of hepatoma cells

Analysis of proliferation by DNA staining with Hoescht dye

HuH-7 and HepG2 hepatoma cell lines were seeded into wells of a 24 well plate. Cells were serum starved for 24 hours and then incubated with varying concentrations of recombinant CXCL16 (rCXCL16) for 72 hours. At baseline and 24-hour intervals, cells were fixed and stained with Hoescht dye (reflecting DNA content), and the fluoresence of the dye was measured to determine the extent of cell proliferation. HuH-7 and HepG2 hepatoma cell lines demonstrated a dose-dependent increase in cellular proliferation when incubated with recombinant CXCL16 (one-way analysis of variance $p=0.008$ and $p=0.024$ respectively) (**figure 7.9**). Proliferation was comparable between HepG2 and HuH-7 cells with greatest proliferation induced with 10ng/mL of rCXCL16, although data were more robust as evidence of proliferation in HuH-7 cells. One-way analysis of variance (ANOVA) tests were used to compare the effect of all concentrations of CXCL16 on proliferation.

A Hoescht assay: proliferation of HuH-7

B Hoescht assay: proliferation of HepG2
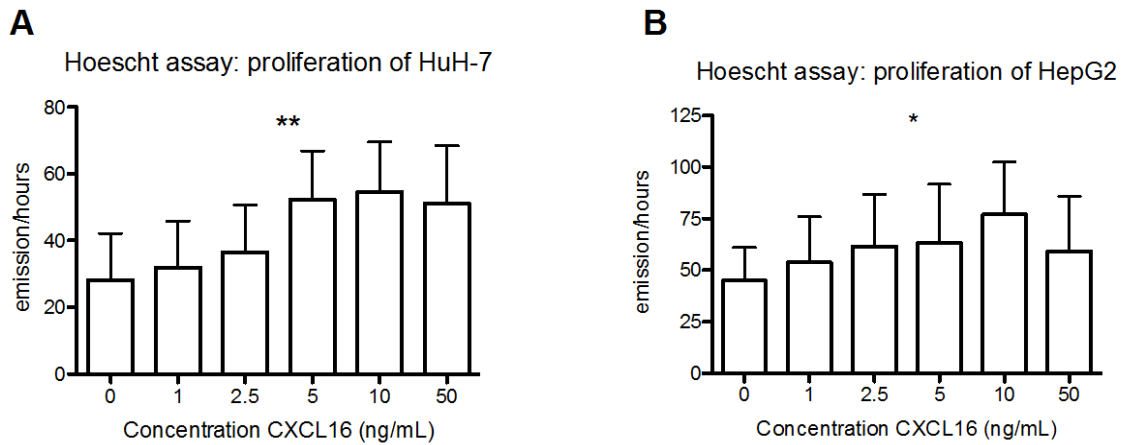
Figure 7.9: Incubation with CXCL16 increases proliferation of hepatoma cell lines

*Hepatoma cell lines were incubated with varying concentrations of CXCL16 and cellular proliferation was assessed by DNA staining with Hoescht dye, Results are presented as area-under-the-curve for fluorescence over time. CXCL16 increased proliferation of **A** HuH and **B** HepG2 cell lines $* p<0.05$ $**p<0.01$ by one-way analysis of variance, n=5 for each concentration.*

<u>Analysis of proliferation by flow cytometry</u>

HuH-7 cells were stained with Celltrace-CFSE and incubated with standard media or varying concentrations of recombinant CXCL16. CFSE is taken up by cells and remains intra-cellular through mitosis. Cell division creates daughter cells with half the CFSE content of the parent cell. In this way generations of dividing cells are distinguishable by flow cytometry (FC). HuH-7 cells were used given the data described above showing slightly greater CXCR6 expression and more robust proliferation in response to rCXCL16. The extent of cellular proliferation was assessed at 5 days (example plot shown in **figure 7.10**). Greater proliferation was seen with CXCL16 compared to standard media, with a dose-dependent response. Consistent with the Hoescht dye technique maximal proliferation was observed with 10ng/mL of rCXCL16.
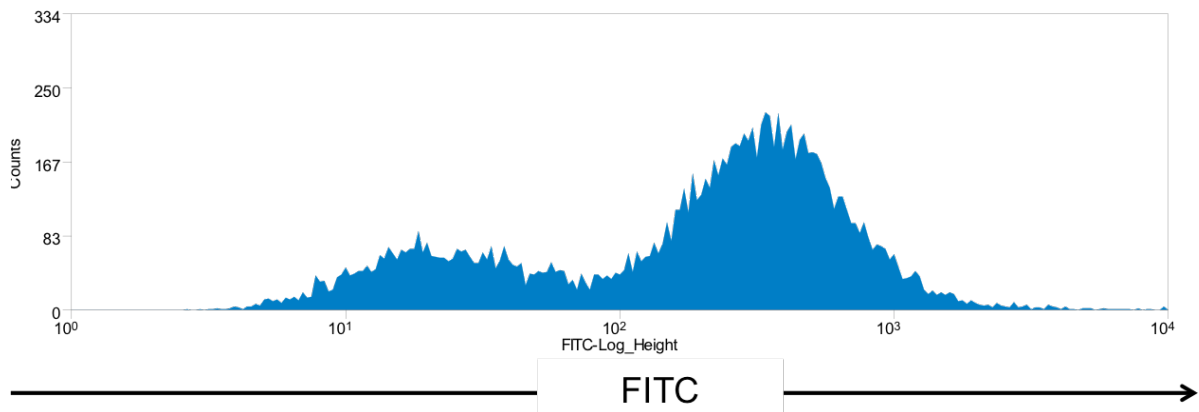
Figure 7.10: Analysis of proliferation by flow cytometry

HuH-7 cells were stained with CFSE dye. Cellular proliferation was assessed by flow cytometry to identify dividing cells, marked by a reduction in CFSE signal. Division of cells was quantified by noting reduction in CFSE signal by FACS.

Peak proliferation 2.2.14
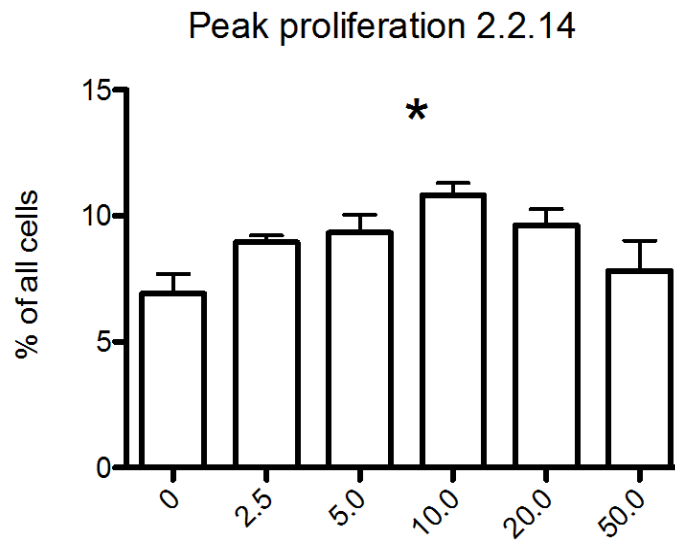
Figure 7.11: CXCL16 increases proliferation of hepatoma cells, assessed by numbers of dividing cells by flow cytometry

*HuH-7 cells were stained with CFSE dye. Cells were then incubated with varying concentrations of CXLC16 for 5 days. Peak proliferation of HuH cells was observed following incubation with 10ng/ml recombinant CXCL16. Aggregate data from four experiments each run in triplicate. Data shown as mean and SEM, *p<0.05 by 1-way ANOVA*

Function of CXCR6 in primary human hepatocytes

CXCR6 signalling downregulates pro-apoptotic gene expression in hepatocytes

To analyse how CXCL16/CXCR6 signalling might mediate its effects in hepatocytes, primary hepatocytes obtained from Bioreclaimation Inc. were incubated in the presence or absence of recombinant human CXCL16 (10ng/ml) for 24 hours. This dose was used based on results from experiments with hepatoma cells as described previously. The characteristics of hepatocyte donors are shown in **table 7.1**. A high-throughput PCR assay (SAbiosciences) allowed for simulataneous comparison of gene expression of multiple pathways between untreated and treated hepatocytes. Data were analysed with online tools provided by Qiagen (http://www.qiagen.com/gb/).

	Donor 1	**Donor 2**
Age (years)	28	39
Comorbidity	Paraplegia	Hypertension
Cause of death	Haemorrhagic stroke	Anoxia secondary to cardiac arrest
Weight (kg)	98.8	90.0
Height (m)	1.78	1.60
BMI (kg/m^2)	31.2	35.2

Table 7.1: characteristics of donors of primary hepatocytes used for PCR array

Incubation of primary hepatocytes with rCXCL16 did not alter the gene expression of the majority of genes evaluated by the assay that were associated with a wide range of signalling pathways (**figure 7.12A**). Four genes (*WNT3A*, *HEY1*, *HES5*, *HEYL*) showed small increases in expression. Importantly, it should be noted that *CXCR6* was not included in the panel of genes examined. The most striking feature was the down regulation of a genes, the majority of which being regulators of apoptosis or the cell cycle (**figure 7.12B, table 7.2**). A full list

of differentially expressed genes upon addition of rCXCL16 is shown in **appendix 1**. This is consistent with observations showing increased proliferation of hepatoma cell lines when incubated with rCXCL16.
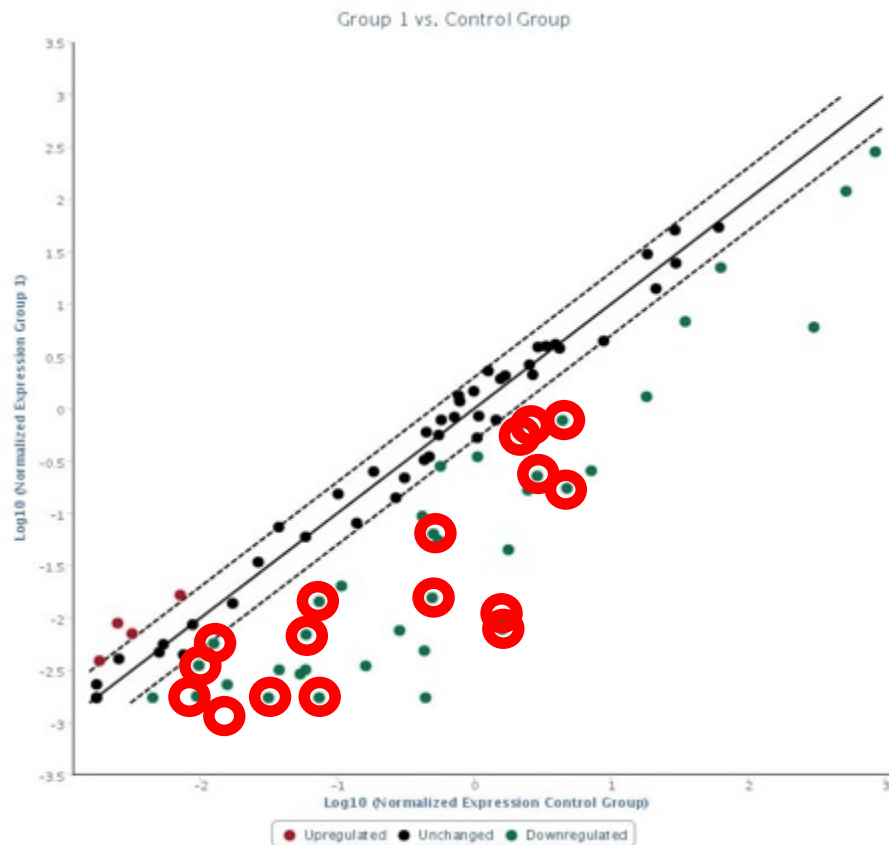
Figure 7.12: CXCR6 signalling down regulates pro-apoptotic gene expression in hepatocytes

Cell signalling pathways were analysed by qRT-PCR from pooled samples of primary human hepatocytes. Relative expression of genes between primary hepatocytes incubated with standard media (x-axis) or 10ng/ml of CXCL16 (y-axis). Data are shown as a cluster analysis showing up regulated genes in red and down regulated genes in green. The solid line represents no change between groups, dashed lines represent two-fold change in expression between groups. Red circles identify pro-apoptotic genes that are down regulated in primary hepatocytes after incubation with 10ng/ml of recombinant CXCL16.

Up regulated				Down regulated			
Gene symbol	Protein	Function	Fold change	Gene symbol	Protein	Function	Fold change
WNT3A	wingless-type MMTV integration site family, member 3A	These proteins have been implicated in oncogenesis and in several developmental processes	5	CPT2	carnitine palmitoyltransf erase 2	Nuclear protein which oxidizes long-chain fatty acids in the mitochondria	-254
HEY1	hes-related family bHLH transcription factor with YRPW motif 1	basic helix-loop-helix (bHLH)-type transcriptional repressors.	5	BAX	BCL2-associated X protein	forms a heterodimer with BCL2, and functions as an apoptotic activator	-205
HES5	Hes family bHLH transcription factor 5	Regulates cell differentiation	4	BCL2L1	BCL2-like 1	regulates mitochondrial membrane channel opening thus controls production of inducers of apoptosis	-167
HEYL	hes-related family bHLH transcription factor with YRPW motif-like	an effector of Notch signalling and a regulator of cell fate decisions.	2.23	GCLC	glutamate-cysteine ligase, catalytic subunit	Glutamate-cysteine ligase. First rate-limiting enzyme of glutathione synthesis.	-89

Table 7.2 Primary human hepatocytes were incubated in the absence or presence of 10ng/ml recombinant CXCL16. Gene expression covering to a range of signalling pathways were analysed by a qRT-PCR array.

*This table shows transcripts that exhibited the greatest regulation following incubation with CXC16 (treated vs. untreated). A complete list of differentially expressed genes upon the addition of recombinant CXCL16 is shown in **appendix 1**.*

Discussion

These data show that CXCR6 expression is not confined to immune cells, and is expressed by hepatocytes. Expression is increased in cirrhotic liver tissue compared to normal tissue. A subset of human hepatocellular carcinoma over express CXCR6, where expression is linked to particular biological phenotypes for example grade of differentiation. This finding is consistent with previous data published by Gao et al (Gao *et al.*, 2012). The data presented in this chapter suggest a role for CXCR6/CXCL16 signalling on proliferation of hepatocytes mediated via several pathways that regulate the balance between apoptosis and proliferation. A proliferative effect of this axis may be hepato-protective in liver injury – this is discussed again in the chapter dealing with mouse models of liver injury in CXCR6 knock out mice.

Hepatoma immortalized cell lines were used for many of these experiments. Although these cell lines are very different from primary human hepatocytes they remain useful tools for research given the difficulty of isolation and culture of primary hepatocytes. Hepatoma cell lines express CXCR6 and activation with CXCL16 increased proliferation. The same concentration of 10ng/mL of CXCL16 both increased proliferation and had a marked effect on expression of CXCR6 on hepatoma cells. This is consistent with an autocrine feedback loop in which CXCL16/CXCR6 signalling can amplify the CXCR6 response by increasing receptor expression.

The PCR array data from primary hepatocytes supports the preceding data by demonstrating down-regulation of several pathways that govern cell function and pro-apoptotic pathways. These data should be confirmed by further analysis with single-target PCR or western blotting.

CHAPTER 8: Expression and function of CXCR6 on Lymphocytes in Liver Disease

The CXC chemokine receptor CXCR6 is expressed on multiple immune cells. CXCR6^{+} cells are enriched in diseased liver where CXCR6 is highly expressed on T cells, natural killer T (NKT) cells and natural killer (NK) cells (Boisvert *et al.*, 2003). CXCR6 expression is associated with markers of an effector phenotype (Northfield *et al.*, 2008, Billerbeck *et al.*, 2010). Importantly there are differences between humans and mice in the distribution of CXCR6 on intrahepatic lymphoid cells: in mice greatest expression of CXCR6 is seen on NKT (Campbell *et al.*, 2001, Wehr *et al.*, 2013) whereas in humans greatest expression is seen on NK cells (Boisvert *et al.*, 2003, Heydtmann *et al.*, 2005). Mouse data may therefore not accurately reflect the role of CXCR6 in the pathogenesis of human disease.

Work with human tissue from our group has shown that CXCL16, the only identified ligand for CXCR6, is widely expressed in human liver, where adhesion of lymphocytes to biliary epithelial cells is mediated in part by CXCL16 (Heydtmann *et al.*, 2005). This work concentrated on lymphocytes from hepatitis C infected liver tissue and despite showing greatest expression on CD56^{+} cells, did not differentiate between NKT and NK cells and used unfractionated leukocyte populations to investigate the role of CXCR6/CXCL16 in adhesion. I investigated CXCR6 expression by lymphoid cells in a range of human liver disease and focussed on the functional role of CXCR6 expression by NK cells.

Expression of CXCL16 in liver disease

CXCL16 gene expression is increased in diseased liver

CXCR6 has a single ligand, CXCL16. *CXCL16* gene expression was analysed by qRT-PCR of total RNA isolated from whole liver tissue taken from a variety of chronic liver disease (15 in total: NASH, n=8, ALD, n=3, PBC, n=3, PSC, n=1), acute liver disease (n=3) and normal liver tissue (n=3). *β-ACTIN* was used as a housekeeping gene. Gene expression of *CXCL16* was increased in both chronic and acute liver disease relative to that of normal liver (**figure 8.1A**). The highest expression was observed in liver tissue from individuals with acute liver failure and in the context of chronic liver disease, liver tissue from PBC affected liver showed the highest expression (**figure 8.1B**).
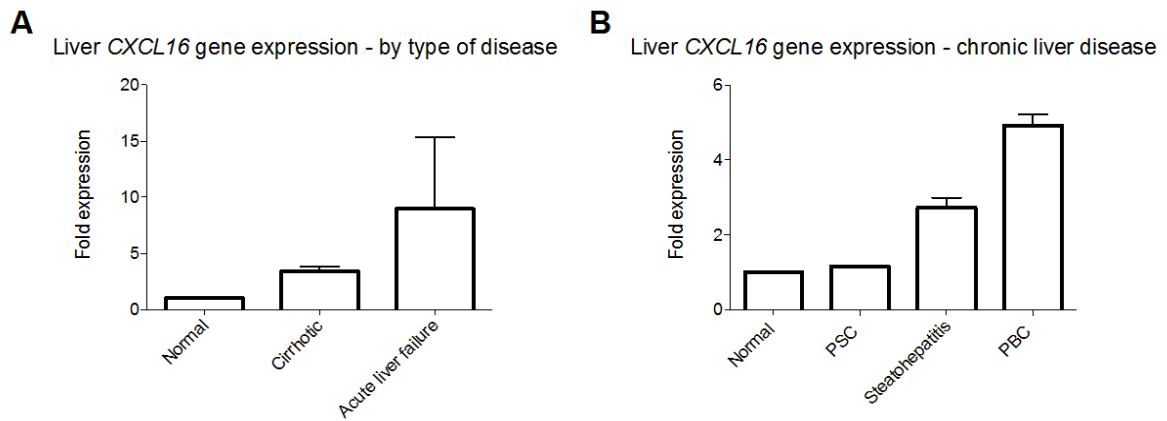
Figure 8.1: CXCL16 gene expression is increased in diseased liver

Total RNA was isolated from whole liver tissue and gene expression of CXCL16 measured by qRT-PCR with β-ACTIN as a housekeeping gene. RNA as isolated from normal liver (n=3), acute live failure (n=3) and chronic liver disease: (15 in total: NASH, n=8, ALD, n=3, PBC, n=3, PSC, n=1) **A** Gene expression of CXCL16 was increased in chronic and acute liver disease, **B** where highest expression was seen in liver tissue from PBC. Data were normalised to relative CXCL16 expression in normal liver tissue, and are shown as mean and SEM.

CXCL16 is expressed by endothelial cells, hepatocytes and biliary epithelial cells

Hepatic endothelial cells (HSEC) and biliary epithelial cells (BEC) were isolated from explanted livers and cultured. The hepatoma cell line Huh7, originally isolated from an adult patient with HCC (Nakabayashi *et al.*, 1982) was used to investigate hepatocyte function.

Analysis of total RNA extracted from isolated cells or hepatoma cell lines showed *CXCL16* gene expression in all cell types, consistent with previous reports (Heydtmann *et al.*, 2005)(**figure 8.2**). Furthermore the addition of lipopolysaccharide (LPS, 10ng/ml), TNF-α alone (10ng/ml) or TNF-α and IFN-γ (10ng/ml) to media increased CXCL16 gene expression in all cell types at 24 hours, with the greatest response seen in BEC (**figure 8.2**). Cells were serum starved prior to the addition of cytokines to media to ensure a pure effect of cytokine stimulation.
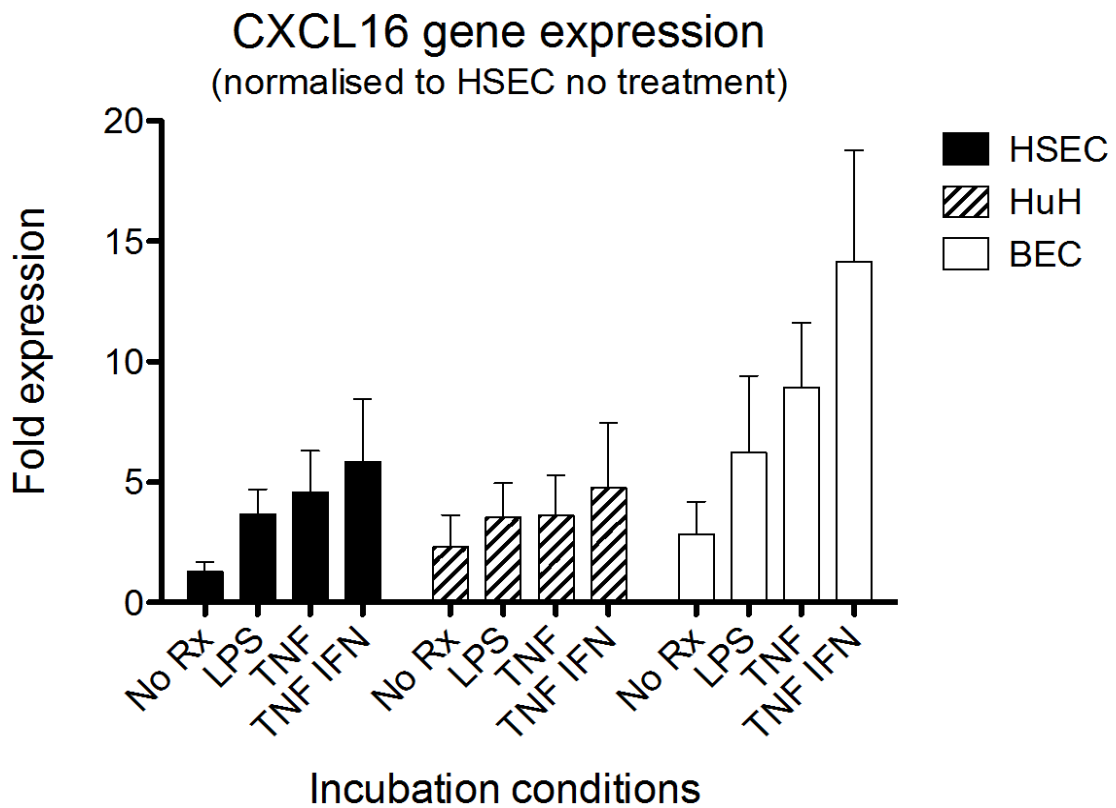
Figure 8.2: CXCL16 is expressed by endothelial cells, hepatocytes and biliary epithelial cells

Isolated endothelial or epithelial cells and hepatoma cell line cells were cultured under a variety of conditions. Total RNA was isolated and gene expression of CXCL16 was measured by rt-PCR. CXCL16 was expressed by all cell types. The addition of LPS/inflammatory cytokines promoted gene expression, particularly in the case of BEC. Three isolates were used for each cytokine condition. Data are shown as mean and SEM.

CXCL16 is localized to biliary ductules in injured liver

Given the increased expression of CXCL16 in PBC and its association with biliary epithelial cells I examined the expression of CXLC16 in liver by immunohistochemistry. This process was difficult to optimise with initial work using frozen sections showing non-specific staining despite careful titration of the antibody. Use of paraffin-embedded sections with multiple steps to block non-specific staining (sequential incubation steps with hydrogen peroxide, casein and horse serum) showed good results (detailed in chapter 2) and this technique was used to investigate CXCL16 expression in tissue.

Immunohistochemistry showed that, consistent with the qRT-PCR data, CXCL16 was strongly expressed on biliary epithelium and also throughout the parenchyma of diseased liver tissue, with little or no expression in non-cirrhotic liver (**figures 8.3** and **8.4**). Some staining was seen on infiltrating immune cells within fibrous septa but this was weak compared to staining on liver tissue.
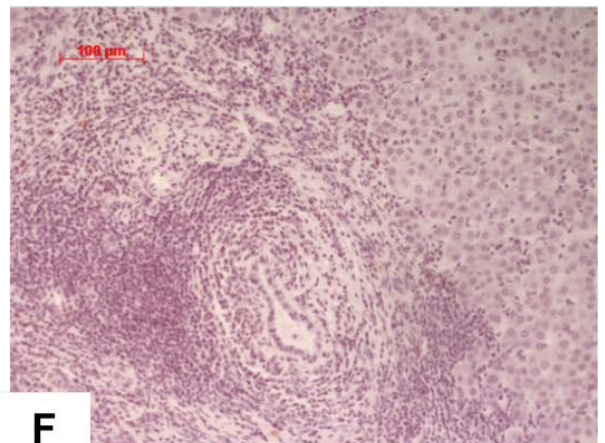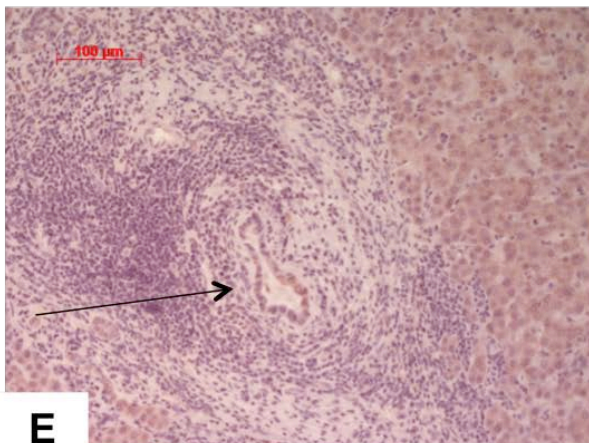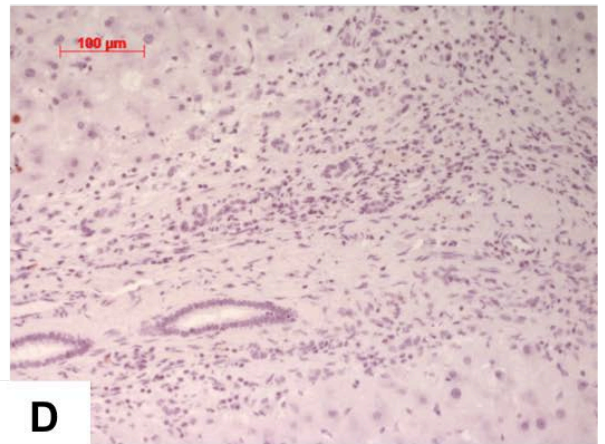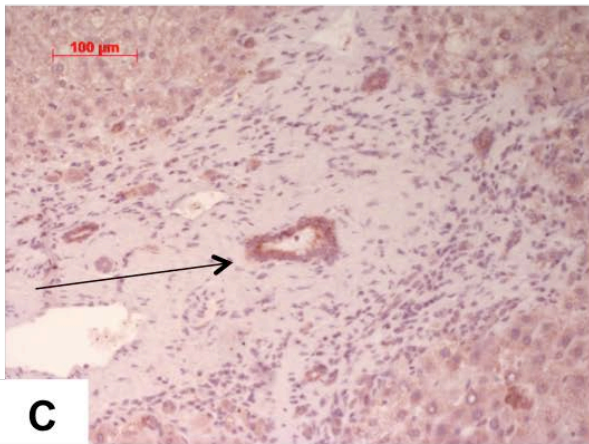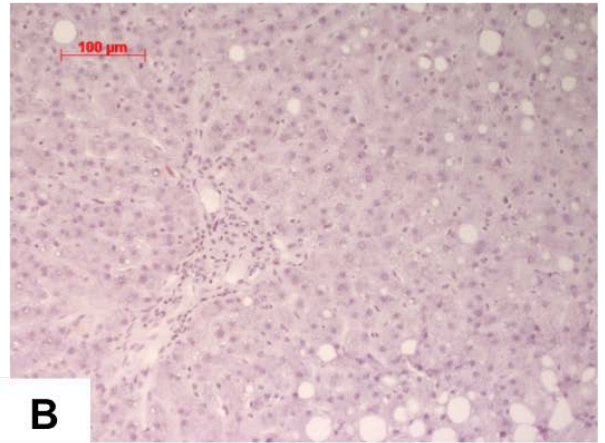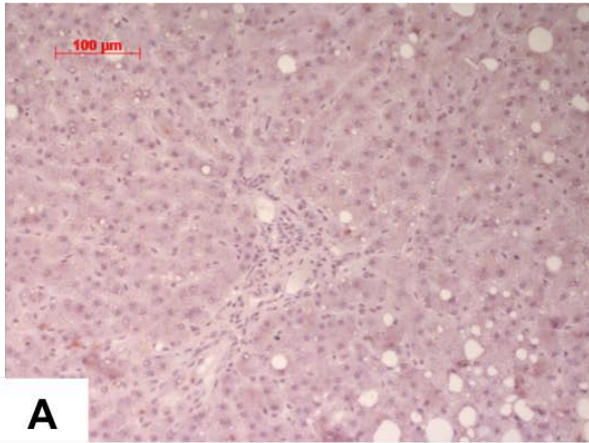
Figure 8.3 (previous page) CXCL16 is localized to biliary ductules in injured liver

Paraffin-embedded sections of liver tissue were stained for CXCL16 or with an isotype matched control antibody. Photographs were taken at 20x magnification. The chromogen stains CXCL16 red-brown against a blue background counter-stain. Corresonding ontrol sections, stained with a non-specific isotype-matched antibody are shown in the left hand column. **A, B** normal liver, **C, D** alcoholic liver disease **E, F** primary biliary cirrhosis
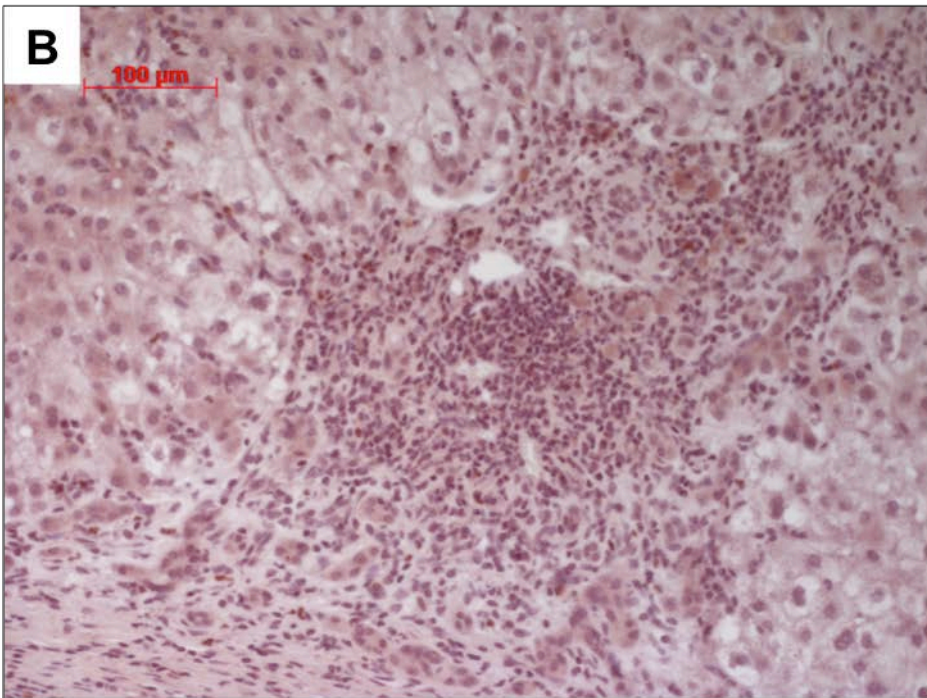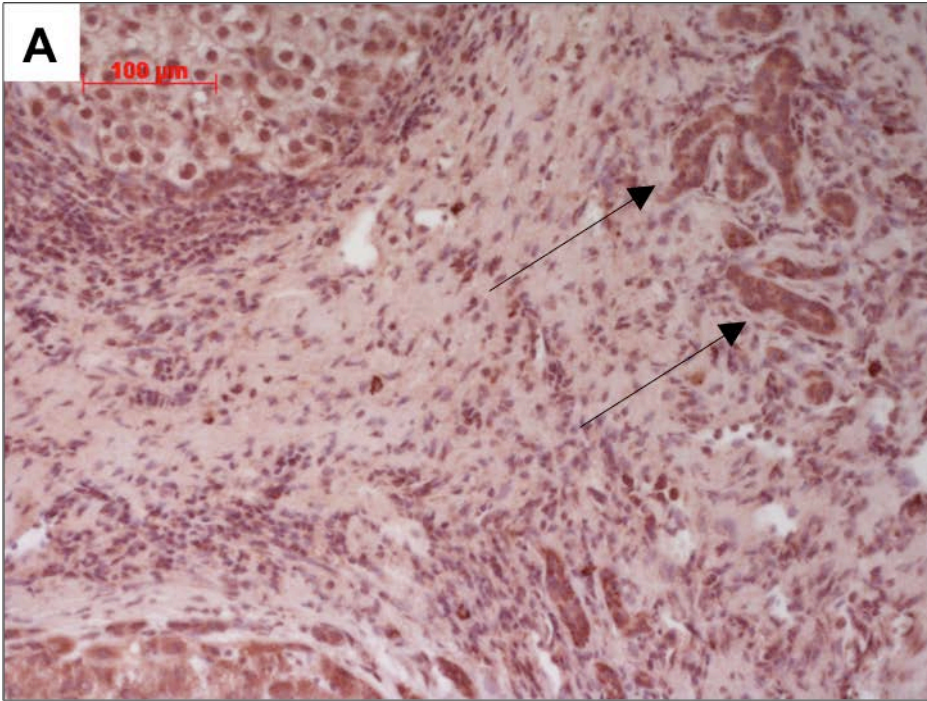
Figure 8.4 (previous page) liver tissue stained for CXCL16 at 40x magnification.

A Sections from PBC liver showing CXCL16 expressed on bile ductules (long arrows) and B matched area from section of same liver stained with isotype matched control antibody

Serum CXCL16 concentration is increased in chronic liver disease but decreased in Primary Biliary Cirrhosis

The concentration of soluble CXCL16 in serum samples from patients with chronic liver disease (CLD) (n=41: 9 NASH, 8 ALD, 3 HCV and 21 PBC) and healthy volunteers (n=10) was measured by ELISA. No statistically significant increase in circulating CXCL16 concentration was observed between healthy volunteers and patients with CLD (mean CXCL16 concentration 2.78ng/ml (SEM 0.212) vs. 2.95 (0.289), student's t-test $p=0.756$)(**figure 8.5A**).

When PBC was considered separately to other causes of CLD, patients with PBC had significantly lower CXCL16 levels than healthy controls (2.07ng/ml (0.112), student's t-test $p<0.001$)(**figure 8.5B**).
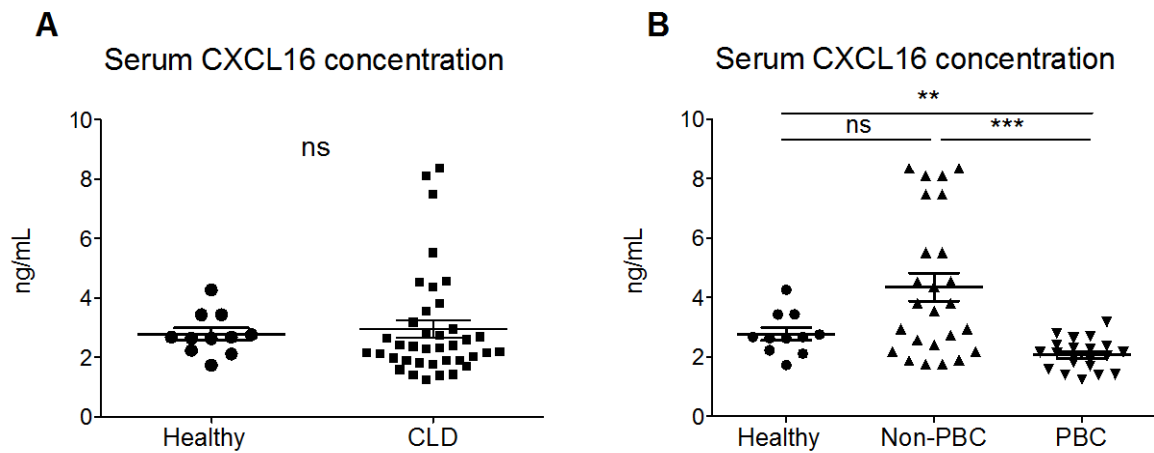
Figure 8.5: Serum CXCL16 concentration is increased in chronic liver disease but decreased in Primary Biliary Cirrhosis

*Serum samples from healthy controls (n=11), and patients with chronic liver disease (n=46) were analysed for CXCL16 concentration by ELISA. **A** There was no significant difference in the concentration of CXCL16 between healthy donors and patients with chronic liver disease. **B** The concentration of CXCL16 in PBC (n=21) was significantly lower than that of healthy controls and individuals with non-PBC related chronic liver disease (n=25). Data are shown as mean and SEM.*

Expression of CXCR6 on lymphoid cells in liver disease

CXCR6⁺ cells are present in diseased liver tissue

Having demonstrated that the expression of CXCL16 was differentially expressed in chronic liver disease I then investigated the expression of its cognate receptor, CXCR6, on liver infiltrating lymphocyte populations. Immunohistochemistry for CXCR6 on paraffin embedded tissue sections identified CXCR6⁺ cells expressed by infiltrating immune cells around portal tract in non-cirrhotic liver, and around fibrous septa and in the parenchyma in injured liver tissue (**figure 8.6**).
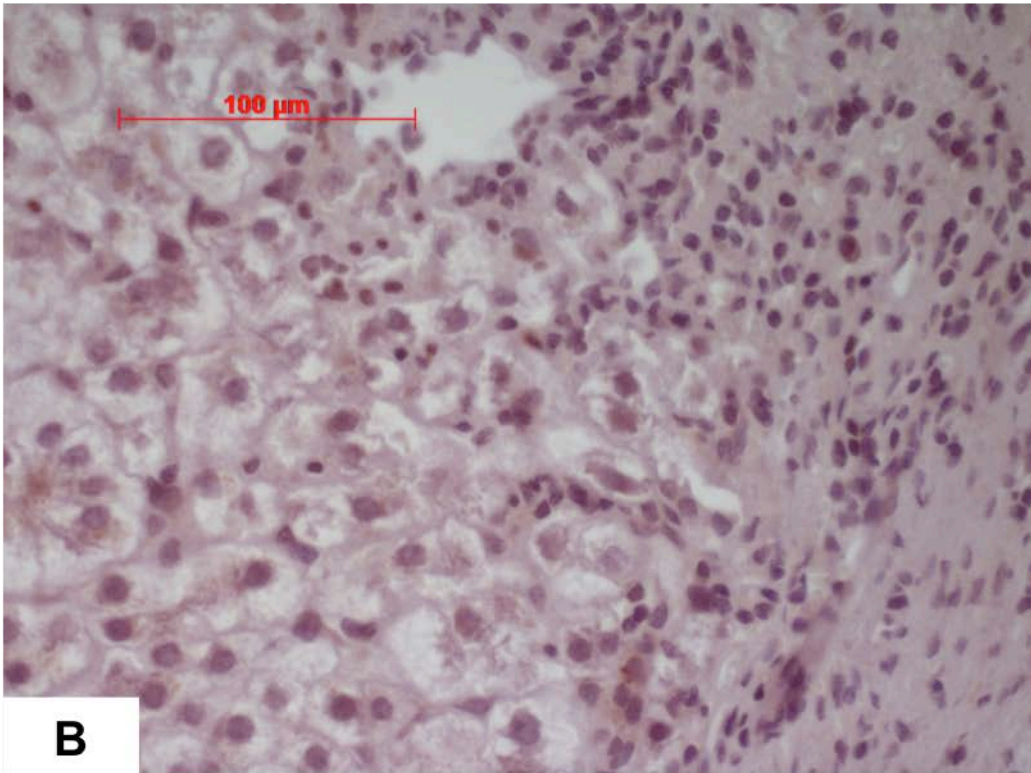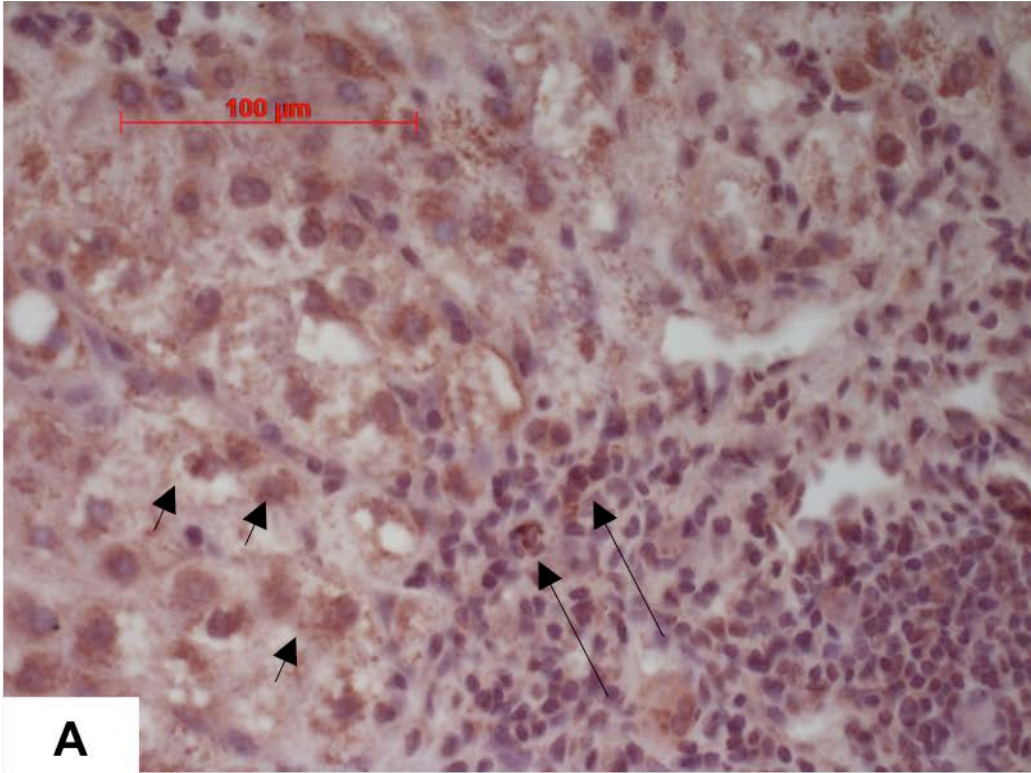
Figure 8.6: CXCR6+ cells are present in diseased liver tissue

*Paraffin embedded sections of tissue from explanted PBC liver stained for CXCR6. Images shown at 40x magnification. **A** . Multiple cells expressing CXCR6 (in red) in inflammatory foci (long arrows) as well as hepatocyte expression (short arrows) **B** matched area from section from same liver stained with isotype matched control antibody*

Flow cytometric analysis of CXCR6 on inflammatory cells

To further characterise the nature of the intrahepatic CXCR6+ cell population lymphocytes were isolated from liver tissue and peripheral blood, and flow cytometry (FC) was used to characterise and identify CXCR6-expressing subpopulations.

CXCR6 expression on lymphoid cells differs between blood and liver compartments

Expression of CXCR6 on lymphocytes in liver and blood compartments was assessed by FC. Lymphocytes were identified by forward and side scatter characteristics, and doublets excluded by pulse width. CXCR6 expression was analysed on this whole population (**figure 8.7A, 8.7B**). After gating on CXCR6$^+$ cells, lymphocyte subpopulations were identified by CD3 and CD56 immunoreactivity to distinguish T cell, NKT cell and NK cell populations (**figure 8.7C, 8.7D**).

In blood, the majority of CXCR6$^+$ cells were CD3$^+$CD56$^-$ T cells, whereas in liver most CXCR6$^+$ cells were CD3$^-$CD56$^+$ NK cells (**figures 8.8A, 8.8B**).
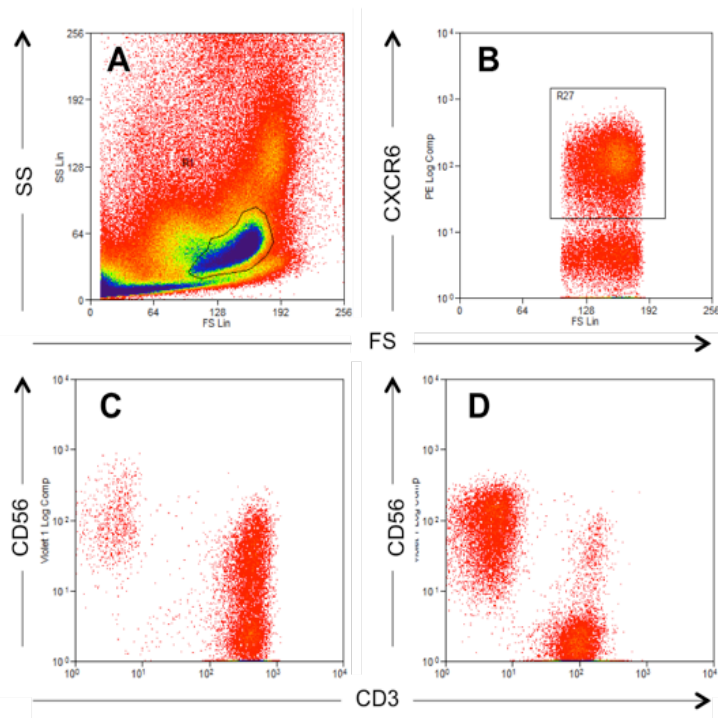
Figure 8.7: Gating strategy to identify CXCR6⁺ lymphoid cells in liver tissue

A gating on lymphocytes on the basis of forward and side scatter B CXCR6⁺ cells. T cells, NKT cells and NK cells were identified by CD3 and CD56 immunoreactivity. Representative plot from C peripheral blood and D liver-infiltrating lymphocytes.
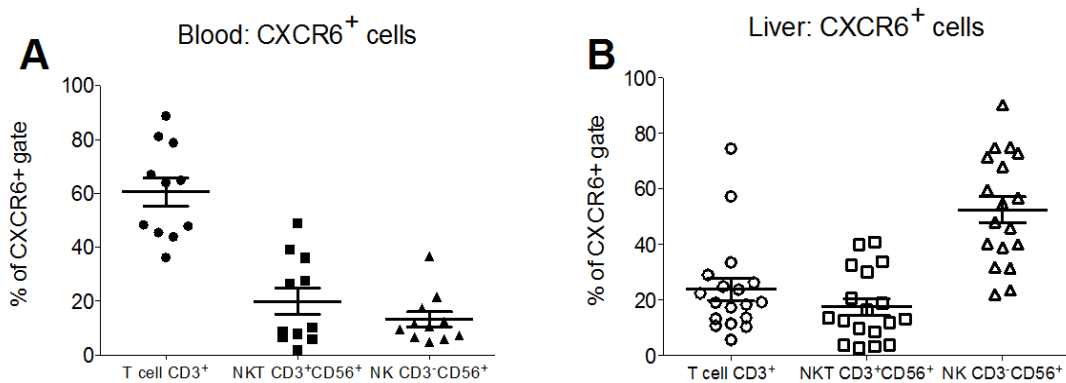
Figure 8.8: CXCR6 expression on lymphoid cells differs between blood and liver compartments

Figures A and B show distribution of CXCR6⁺ expression in blood (n=11) and liver tissue (n=20) respectively, where each data point represents an isolate from single individual, lines at mean and SEM.

185

Natural Killer T cells show highest percentage expression of CXCR6

In both blood and liver the percentage of cells expressing CXCR6 was highest on CD3$^+$CD56$^+$ NKT cells (**figure 8.9A**), although the surface expression of the receptor (as measured by median fluorescence intensity, MFI) was similar across all lymphocyte subsets (**figure 8.9B**) suggesting similar levels of expression on individual cells. Liver-infiltrating lymphocytes demonstrated markedly increased expression of CXCR6 compared to peripheral blood, both in terms of both percentage positive cells (Two-way ANOVA p<0.001) and MFI (Two-way ANOVA p<0.001).

Expression of CXCR6 on T lymphocytes and NK cell subsets

Analysis of T lymphocytes showed a greater expression of CXCR6 on CD8$^+$ when compared to CD4$^+$ T cells in both the blood and the liver (**figure 8.10A**). Within NK cells, CXCR6 expression was enriched in the CD56^{hi} NK cell population in comparison to the CD56^{lo} subset. This was particularly marked for intrahepatic NK cells (**figure 8.10B**).
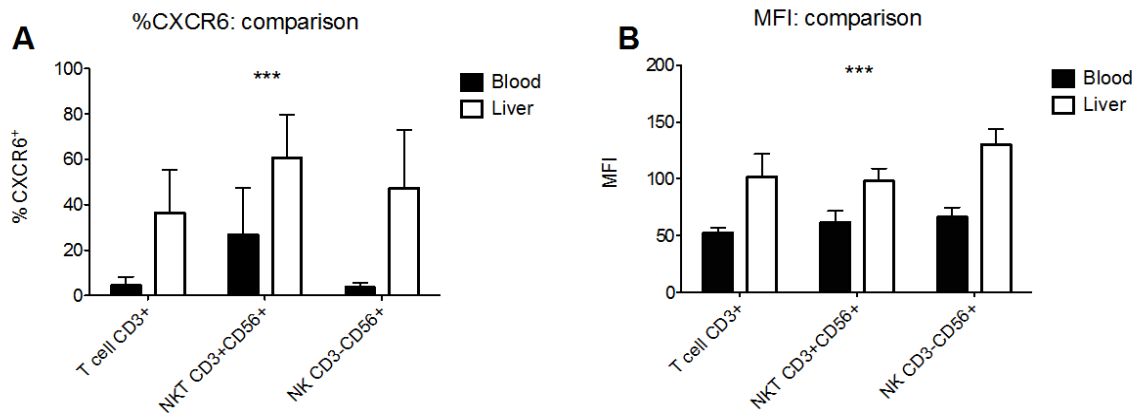
Figure 8.9: Expression of CXCR6 is higher on liver-infiltrating lymphocytes

Lymphoid cells were isolated from blood (n=11) or liver (n=20). CXCR6 expression was analysed by FC. CXCR6 expression was higher on liver-infiltrating cells in terms of **A** percentage CXCR6 positivity and **B** MFI. Data are shown as mean and SEM, *** 2way ANOVA p<0.001.
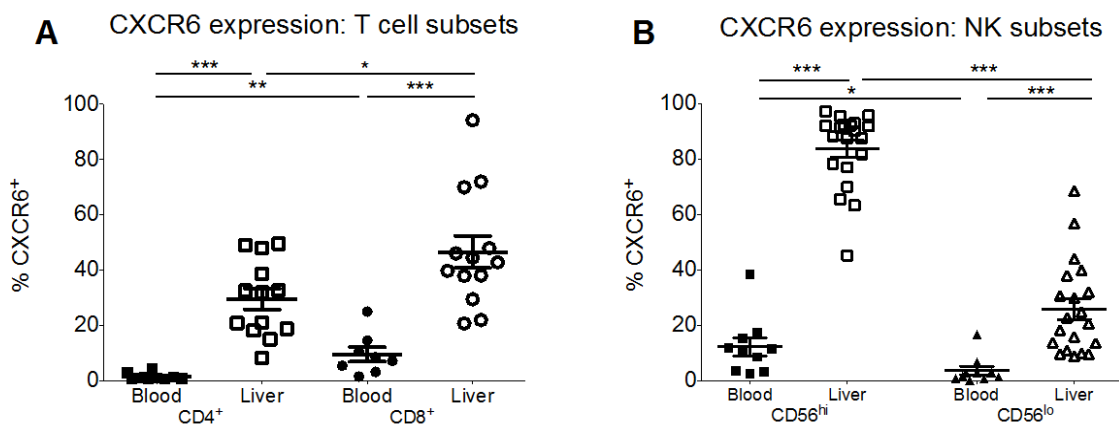
Figure 8.10: Lymphocytes were isolated from blood and liver and analysed by FC. T lymphocyte subsets were identified by labelling of CD4 and CD8.

A CXCR6 expression was significantly higher on liver-infiltrating T lymphocytes, particularly in the CD8+ population. **B** CXCR6 expression (percentage) by NK cells was higher for all liver-infiltrating subsets and was particularly elevated on CD56hi cells. Each individual point represents a single isolation, lines at mean and SEM. *p<0.05, **p<0.01, ***p<0.001 by student's t-test

CXCR6⁺ expression is increased on NK cells in injured liver

Having established that CXCR6 expression was enriched on liver-infiltrating lymphoid cells and NK cells in particular, I investigated a possible association of CXCR6 expression with liver disease. Liver tissue slices were harvested from livers from individuals with chronic liver disease and from distal, uninvolved tissue from hepatic resections of malignant lesions. Lymphoid cells were subsequently isolated and analysed by FC, and CXCR6 expression was then compared between cells taken from normal and cirrhotic tissue.

CXCR6 expression on lymphoid cells varied between normal and cirrhotic liver tissue (**figure 8.11**). Fewer T lymphocytes from cirrhotic patients expressed CXCR6 compared to cells isolated from normal liver (median percentage expression 36.4% (IQR 13.1) vs. 49.7% (13.7), Mann-Whitney test p=0.040); a similar pattern was observed for NKT cells (median 53.1% (IQR 32.7) vs. 80.0% (14.0), Mann-Whitney test p=0.014). In contrast, NK cells tended to shower greater percentage CXCR6 expression in diseased liver although this was not statistically significant (55.4% (46.9) vs. 33.0 (26.5), Mann-Whitney p=0.211).

NK CXCR6 expression is highest in Primary Biliary Cirrhosis

As expression of CXCR6 decreased on other major lymphoid subsets but tended to increase on NK cells, I analysed differences in NK cell CXCR6 expression between differing aetiologies of liver disease. NK cell expression of CXCR6 was highest in PBC (one-way ANOVA p=0.035) but was not elevated in any other disease studied (**figure 8.12**).

NK CXCR6 expression in normal and cirrhotic liver
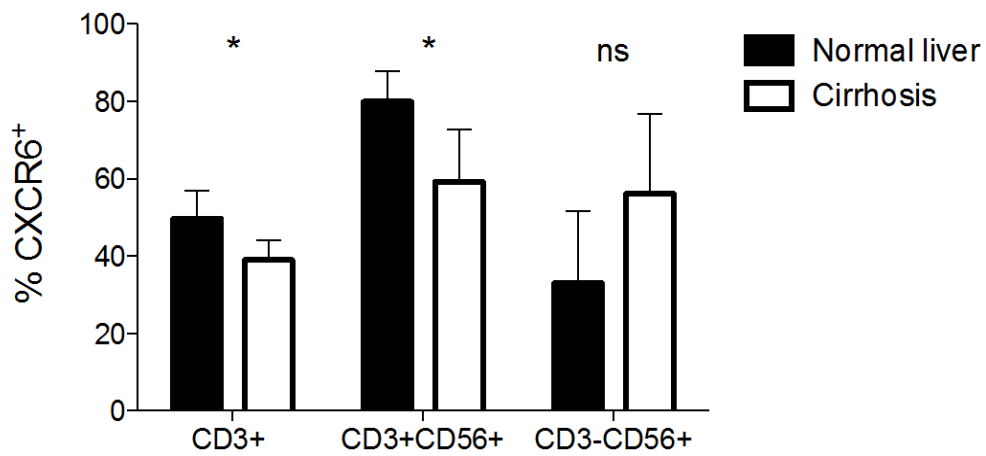
Figure 8.11: CXCR6+ expression on liver lymphocytes in cirrhotic and normal liver

Lymphocytes were isolated from liver and analysed by FC. CXCR6 expression on lymphocyte subsets in normal (n=4) and cirrhotic (n=16) liver. Data are shown as median and IQR. *p<0.05, ns: p>0.05 by Mann Whitney test
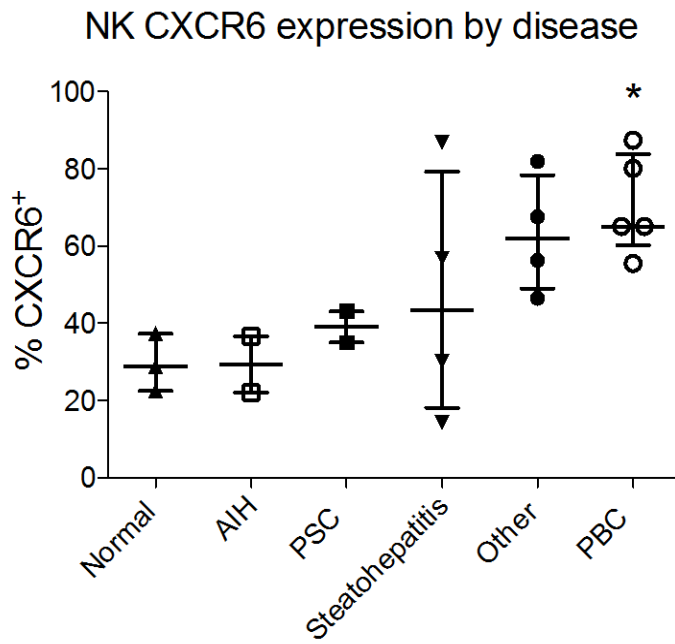
Figure 8.12: NK CXCR6 expression is highest in Primary Biliary Cirrhosis

Lymphocytes were isolated from normal (n=4) and diseased liver n=16 (AIH, 2, PSC 2, steatohepatitis 5, PBC 4 and other causes 4 (2 polycystic, 1 acute liver failure, 1 chronic rejection)) and analysed by FC. Most frequent CXCR6 expression by NK cells was observed in PBC liver, which was the only category to differ significantly from normal liver tissue. Each data point represents a single sample, lines at median and IQR *p<0.05 by one-way ANOVA.

Immunophenotype of CXCR6^{+} Natural Killer cells

CXCR6 expression on intra-hepatic NK cells is associated with markers of effector function

To examine the phenotype and possible function of CXCR6^{+} NK cells, further FC analysis was performed on cells isolated from liver tissue. In addition to being associated with CD56^{hi} expression (see above, **figure 8.10**), the expression of Nkp30 and CD16 were examined. CD16 expression is inverse to CD56 expression on NK cells (Vivier *et al.*, 2008). The natural cytotoxicity receptors NKp30, NKp44, NKp46 induce strong NK cell activation when engaged by ligand (Biassoni *et al.*, 2001).

Expression of CXCR6 on NK cells was associated with NKp30, (**figure 8.13B**), and inversely associated with CD16 (**figure 8.13C**). These data indicate that CXCR6 expression on NK cells is associated with a tissue-infiltrating effector phenotype (Pende *et al.*, 1999, Poli *et al.*, 2009)
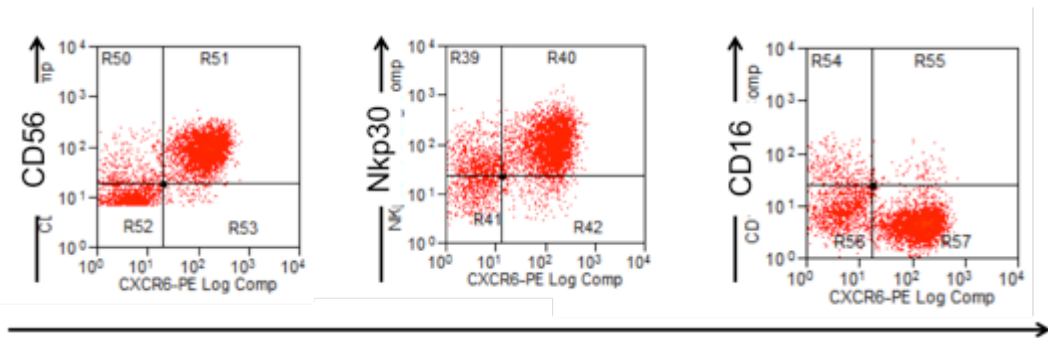
Figure 8.13: Lymphocytes were isolated from liver and analysed by FC.

*CXCR6 expression on NK cells correlated with **A** CD56^{hi} **B** NKp30 expression and **C** low expression of CD16*

In order to investigate the function of CXCR6+ NK cells, flow-assisted cell sorting (FACS) was used to isolate this population with a view to determine both the cytokine secretion profile of these cells and their ability to kill parenchymal and non-parenchymal liver cells. Initially PBMC isolated from peripheral blood that had been monocyte depleted by incubating in a plastic T75 flask for 1 hour, were stained for CD3, CD56 and CXCR6 and subsequently flow-sorted. The yield of CXCR6+ NK cells was very low, resulting in too few cells for analysis. To improve the yield and allow for useful number of cells to be collected, lymphocytes were isolated from liver, and following depletion of monocytes by plastic adherence, NK cells were isolated by bead isolation (Miltenyi, Germany) with about 90% purity. This enriched NK cell population was then sorted. However when isolating intrahepatic NK populations this technique involved a long delay between explant of the liver and eventual cell sorting. The cell yields were always low and of insufficient number and viability for functional studies.

Function of CXCR6 on NK cells

The role of CXCR6 in the recruitment of lymphoid cells to the liver was investigated using a dynamic flow assay. Whole lymphoid populations or purified NK cells were used. In some cases, bead isolation of CD3$^-$CD56$^+$ NK cells from peripheral blood was used as described above in order to investigate the function of CXCR6 on NK cells, (**figure 8.12**). NK cells isolated with this method were used for experiments to investigate the role of CXCR6 in the transendothelial migration of NK cells across hepatic endothelium.

CXCR6 mediates recruitment of Natural Killer Cells across hepatic sinusoidal endothelium

The flow assay system developed in the Adams group based on assays originally established by Nash and colleagues in Birmingham allows modelling of the conditions of the hepatic sinusoid to examine leukocyte trafficking under physiological levels of shear stress (Lalor *et al.*, 1997). Primary human HSEC were cultured until confluent in chambers of a microslide. Once confluent HSEC were stimulated with TNFα and IFNγ (both 10ng/ml) for 24 hours. The HSEC were then washed with PBS and maintained in flow media (endothelial SFM containing 10% BSA). Lymphocytes were incubated in RPMI/10%BSA with a small molecule inhibitor of CXCR6 (C0335224,   ) dissolved in DMSO to a final concentration of 10uM, or DMSO alone for twenty minutes. Cells were then washed and suspended in RPMI at a known density and flowed at physiological levels of shear stress across HSEC with direct visualization allowing for analysis of the adhesion cascade. From these data it is possible to evaluate the extent to which the inflammatory cells both adhere to and migrate across the hepatic endothelial cell monolayer.

In preliminary experiments a mixed population of lymphocytes isolated from peripheral blood were studied. Antagonism of CXCR6 did not significantly reduce recruitment of lymphocytes across HSEC (two-way ANOVA p=0.992)(**figure 8.14A**). A similar effect was observed for liver-infiltrating lymphoid cells (two-way ANOVA p=0.859) (**figure 8.14B**).

Given that earlier results demonstrated an increase in CXCR6 expression solely on NK cells in chronic liver disease, the effect of CXCR6 antagonism on recruitment of isolated NK cells was investigated. A marked reduction in transmigration was observed (Two-way ANOVA p=0.0073) (**figure 8.15**).

A Peripheral blood lymphocytes

B Liver infiltrating lymphocytes
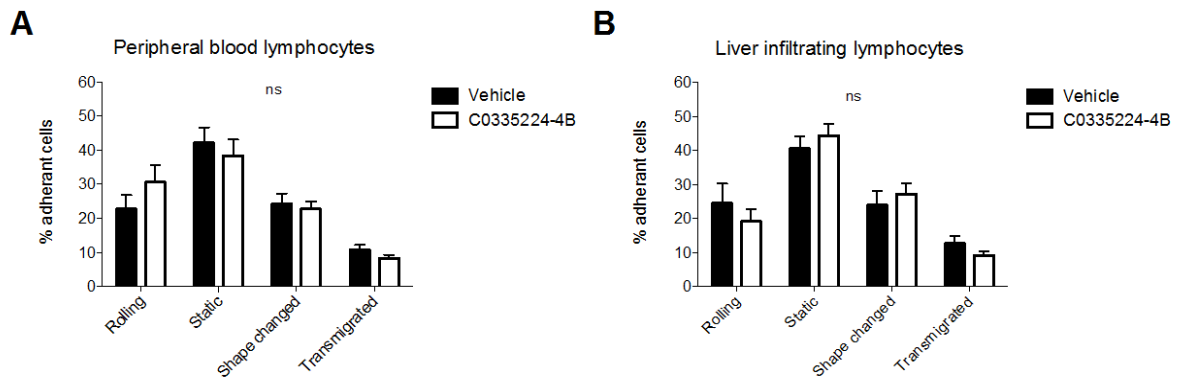
Figure 8.14: CXCR6 is not required for recruitment of leukocytes across hepatic sinusoidal endothelium

Lymphocytes were isolated from blood or liver and incubated with a small molecule inhibitor of CXCR6 or DMSO before being flowed over confluent HSEC. No significant changes in leukocyte trafficking were observed following antagonism of CXCR6 with C0335224. Lymphocytes isolated from A peripheral blood or B liver tissue. ns: p>0.05 by two-way ANOVA. Data expressed as mean and SEM, three isolates of leukocytes examined for each condition.

Peripheral blood NK cells
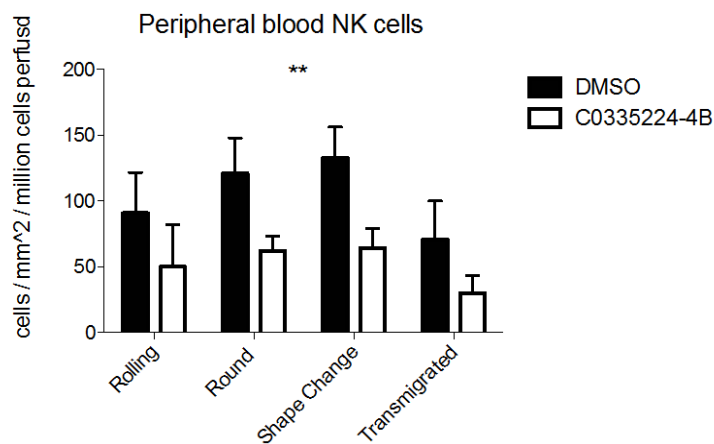
Figure 8.15: CXCR6 mediates recruitment of Natural Killer Cells across hepatic sinusoidal endothelium

NK cells were isolated by negative selection from peripheral blood and incubated with a small molecule inhibitor of CXCR6 or DMSO. Cells were flowed over confluent HSEC and the extent of leukocyte trafficking was assessed. A significant reduction in the transmigration NK cells was observed **p<0.01 by two-way ANOVA. Data expressed as mean and SEM, three isolates of leukocytes examined for each condition.

195

CXCR6 signalling does not affect NK cell survival

In light of other experiments showing that CXCR6 can mediate proliferative signals in hepatocytes (see chapter 9), the function of CXCR6 in promoting survival of lymphoid cells was investigated.

Liver-infiltrating lymphocytes were isolated and incubated in low-serum media for 24 hours to promote apoptosis and cell death. Recombinant CXCL16 was included in low-serum media at varying concentrations to evaluate the effect of CXCR6 signalling. Flow cytometry was used to identify lymphoid subsets and markers of apoptosis and cell death. Cells were categorized as alive (7AAD negative, Annexin V negative), apoptotic (7AAD negative, Annexin V postive) or dead (7AAD positive) (**figure 8.16**). No significant effect of CXCL16 on the proportion of surviving, apoptotic or dead cells was observed (One-way ANOVA >0.05 for all categories (**figure 8.17**).
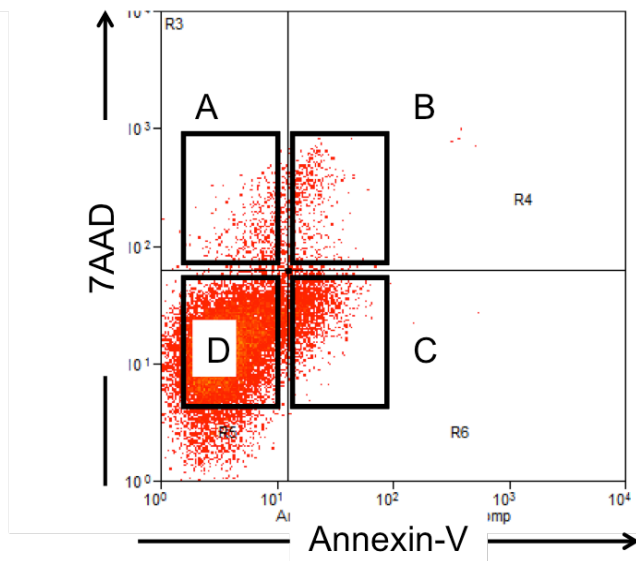
Figure 8.16 Identification of dead and apoptotic cells by flow cytometry

Flow cytometry was used to identify lymphoid subsets and markers of apoptosis and cell death. Cells were categorized as alive (7AAD negative, Annexin V negative), apoptotic (7AAD negative, Annexin V positive) or dead (7AAD positive).

A Liver infiltrating CD3⁻CD56⁺ cells: dead cells
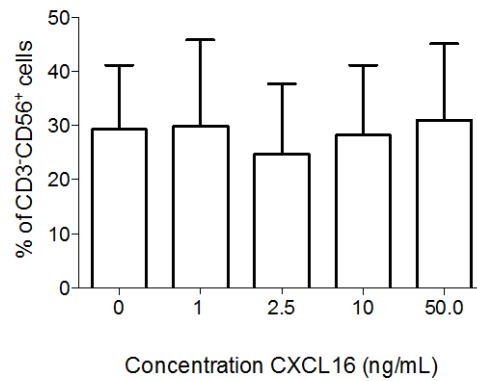
B Liver infiltrating CD3⁻CD56⁺ cells: apoptotic cells
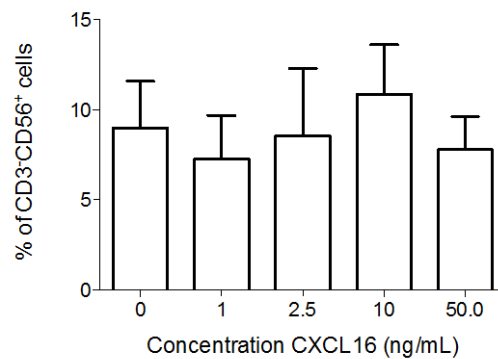
C Liver infiltrating CD3⁻CD56⁺ cells: live cells
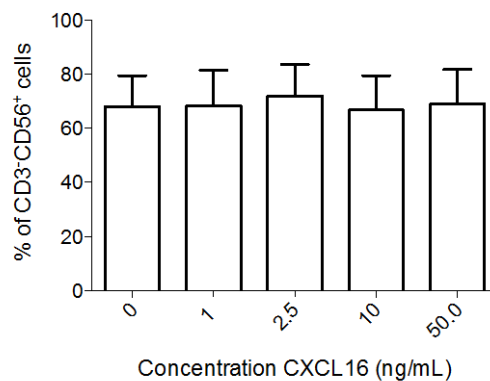
Figure 8.17: CXCR6 signalling does not affect NK cell survival

*Lymphoid cells were isolated from liver tissue and incubated in low-serum media for 24 hours to induced apoptosis and cell death. Recombinant CXCL16 was added at varying doses to evaluate the effect of CXCR6 signalling on cell survival on NK cells. No effect was seen on **A** cell death **B** apoptosis or **C** cell survival. Three isolates tested in triplicate for each condition, data are presented as mean and SEM.*

CXCR6 signalling does not affect NK cell proliferation

To investigate the effect of CXCR6 signalling on NK cell proliferation, lymphoid cells were isolated from liver tissue and stained with Celltrace (a dye similar to CFSE). Cells were then incubated with varying concentrations of recombinant CXLC16 for 5 days. No effect of CXCL16 on cell proliferation was observed (one-way ANOVA p=0.990)(**figure 8.18**).

Proliferation of liver infiltrating CD3⁻CD56⁺ cells
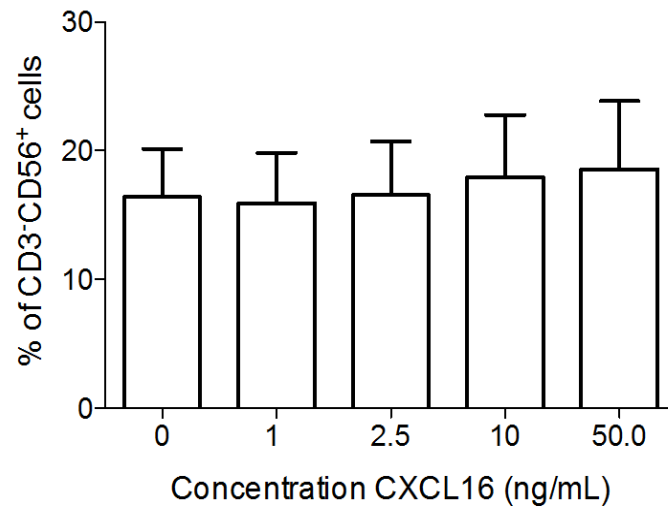
Figure 8.18: CXCR6 signalling does not affect NK cell proliferation

Lymphoid cells were isolated from liver tissue and incubated with recombinant CXCL16 for 5 days. Proliferation was assessed by staining cells with CFSE to allow for identification of dividing cells. No effect of CXCL16 on proliferation of NK cells was observed. Three isolates prepared for each condition, data presented as mean and SEM

Conclusion

The work presented in this chapter describes the hepatic expression of CXCL16 and distribution and function of CXCR6 on liver-infiltrating cells. In keeping with previous work from our laboratory and others, multiple cell types within the liver expressed CXCL16. However, biliary epithelium appeared to be the main source of CXCL16 as shown both by rt-PCR and immunohistochemistry. Interestingly, PCR of whole liver tissue showed greatest gene expression in PBC, a disease characterised by biliary inflammation although serum concentration of soluble CXCL16 was lowest in PBC.

CXCR6 expression is predominantly a feature of CD8$^+$ T lymphocytes in blood. In contrast to peripheral blood, NK cells are the major type of CXCR6$^+$ cell in liver tissue where expression is associated with an effector phenotype. Moreover, CXCR6 expression by T lymphocytes and NKT cells was decreased in cirrhosis, whereas expression tended to increase on NK cells.

The main role of chemokines and chemokine receptors is to regulate the trafficking and positioning of immune cells. Antagonism of CXCR6 significantly reduced the transendothelial migration of isolated NK cells, whereas no significant effect was seen in unselected lymphocyte populations. It should be borne in mind that I have not investigated the effect of the small molecule antagonist on endothelium; it is possible that there is an effect on HSEC that alters transmigration that may confound the results. Similarly a toxic effect on NK cells that reduces migration cannot be ruled out from these data although incubation with or

without the antagonist did not appear to reduce or increase apoptosis, necrosis or proliferation of NK cells.

Within the limits of these caveats, this suggests that CXCR6 has a major role in the hepatic recruitment of NK cells whilst it may be dispensable for the recruitment of other cells types. No role was seen for CXCL16/CXCR6 interaction with regard to survival or proliferation of NK cells – in contrast to previously published mouse data showing decreased survival of NKT cells in CXCR6 deficient mice (Geissmann *et al.*, 2005). These differences may be due to differences in murine and human immunology, and also the differing cell type that predominantly expresses CXCR6: NKT cells in mice and NK cells in humans.

The data presented here supports a paradigm where recruitment of effector NK cells to injured liver and trafficking to inflamed bile ducts is mediated by CXCR6. Primary biliary cirrhosis is a disease typified by inflammation to small bile ductules. The CXCR6/CXCL16 axis is particularly up regulated in this condition, which is characterised by higher frequencies of intrahepatic of CXCR6$^+$ NK cells. This is in contrast to reports of CXCR6-mediated cell trafficking in mice where the major effect of CXCR6 signalling is described on NKT cells (Geissmann *et al.*, 2005) (Wehr *et al.*, 2013). However, these findings are consistent with previous work with human tissue from our laboratory showing a role for CXCR6/CXCL16 in trafficking of lymphocytes to inflamed biliary epithelium (Heydtmann *et al.*, 2005). Targeting this axis may represent a new therapeutic angle in a PBC, which currently has few therapeutic options.

CHAPTER 9: General Discussion

This thesis has focused on a range of chemokine receptors in diverse liver diseases. The principal framework is the study of leukocyte trafficking, a process in which chemokines and their receptors play a significant role. In addition, based on early findings with CXCR6, a non-canonical role of chemokine receptors in hepatocyte regeneration is also described. The common theme linking each of these lines of investigation is the identification of a chemokine receptor/ligand axis associated with a particular liver disease, or the use of murine models incorporating animals in which chemokine receptor expression has been modified genetically to determine the function of particular chemokines in liver disease.

These data represent new insights into the pathogenesis of liver disease and offer potential new therapeutic angles in an area of medicine marked by a lack of effective treatments.

The role of CCR2 in non-alcoholic fatty liver disease

CC-chemokine receptor 2 (CCR2), first identified by Charo *et al.* in 1994 (Charo *et al.*, 1994) mediates the recruitment of monocytes into adipose tissue (Gerhardt *et al.*, 2001) and is associated with adverse consequences of adipose tissue inflammation such as insulin resistance (Weisberg *et al.*, 2006). Patients with NAFLD have higher serum concentrations of CCL2 than healthy, age and gender-matched controls (Haukeland *et al.*, 2006) and levels of CCL2 are greater in advanced NASH and correlate with levels of ALT, a marker of liver injury (Kirovski *et al.*, 2011). Although published human studies NAFLD are confined to

measurements of serum CCL2, experimental murine evidence from provides a rational for studying CCR2 in the pathogenesis of human NAFLD.

In keeping with results from other investigators I found that serum concentrations of CCL2 were significantly higher in patients with NAFLD, and correlated with histological inflammation, and lobular inflammation in particular. Gene expression of CCL2 was higher in liver from patients with all stages of NAFLD compared with normal liver tissue.

In blood classical $CD14^{++}CD16^{-}$ monocytes and to a lesser extent intermediate $CD14^{++}CD16^{+}$ monocytes express CCR2. I focused on a subset of $CD14^{+}$ monocytes that express CD11c and the mannose receptor CD206 because they have recently been associated with insulin resistance in adipose tissue (Wentworth *et al.*, 2010). These monocytes were present in liver tissue at a significantly higher frequency than in blood and their frequency as a percentage of $CD14^{+}$ monocytes, correlated with insulin resistance. A proportion of the $CD14^{+}CD11c^{+}CD206^{+}$ subset expressed CCR2 and levels were particularly high on monocytes isolated from liver tissue from patients with NAFLD.

I detected very few dual positive $CD11c^{+}CD206^{+}$ monocytes in peripheral blood, a finding consistent with previous studies (Bourlier *et al.*, 2008). This suggests that up regulation of $CD206^{+}$ is triggered either during or after transmigration of monocytes across hepatic endothelium into the hepatic parenchyma. A decrease in CCR2 expression on liver-derived monocytes suggests that CCR2 drives recruitment of monocytes but is then down regulated, whilst CD11c and CD206 are expressed after recruitment into liver tissue, a phenomenon recently demonstrated in murine liver injury (Dal-Secco *et al.*, 2015). CD206 is a pattern

recognition receptor that mediates uptake and phagocytosis of a wide range of pathogens and also plays a role in antigen presentation (East and Isacke, 2002). Up-regulation of CD206 by monocytes encountering an area of inflammation is therefore consistent with its known functional properties. This has been demonstrated in principle *in vitro* where treatment of human macrophages, with IL4 and TGF-β induces CD206 expression (Porcheray *et al.*, 2005).

NAFLD is a common disease that may affect between one-third and one-quarter of the UK population. Although only around 10% of patients will develop progressive liver disease this still represents a large number of people. It is this group that require treatment to prevent development of significant hepatic fibrosis, or to reverse established fibrosis. Most trials to date have focused on drugs established in liver or diabetes management, *e.g.* pioglitazone or ursodeoxycholic acid, without compelling evidence of significant benefit (Musso *et al.*, 2010). More recently, early phase trials of novel agents such as obeticholic acid have suggested benefit and will be investigated in phase III trials (Neuschwander-Tetri *et al.*, 2015). Nevertheless these agents are still experimental and there is a need to identify and investigate novel therapeutic angles. There has been considerable interest in targeting CCR2 in the treatment of complications of insulin resistance (Pirow, 2012) (Di Prospero *et al.*, 2014) but only one trial to date has been initiated to investigate CCR2 inhibition in NAFLD, this is a phase II trial using Cencriviroc, a dual CCR2/CCR5 inhibitor initially investigated in HIV (Klibanov *et al.*, 2010) (02217475, 2014).

These experimental data go beyond a simple model of circulating CCR2 monocytes being recruited to liver tissue during NAFLD pathogenesis, but describe a particular subtype of

monocytes that are active in the metabolic syndrome. Recruitment of this CD11c^{+}CD206^{+} subset to liver tissue via CCR2 is associated with greater insulin resistance, a key element in the pathogenesis of NAFLD that prompts the development of NASH from simple steatosis. Animal models show the importance of CCR2 for recruitment of this subset where CCR2 antagonism with a small molecule inhibitor reduced infiltration of an equivalent monocyte subset into both liver and adipose tissue with improvements in liver function and glycaemic control.

The role of CCR9 in acute liver failure

In humans CCR9 is expressed on T lymphocytes (Johansson-Lindbom *et al.*, 2003) and myeloid cells (Schmutz *et al.*, 2010, Linton *et al.*, 2012), and is expressed by a subset of liver-infiltrating lymphocytes in in chronic liver injury most notably PSC (Eksteen *et al.*, 2004) and on subsets of monocytes/macrophages (Linton *et al.*, 2012) (Mizukami *et al.*, 2012). In murine models of ALF CCL25 is up regulated early during injury and CCR9^{+} macrophages were shown to be critical for liver damage (Nakamoto *et al.*, 2012).

I investigated the CCL25/CCR9 axis in human acute liver failure and examined the efficacy of antagonism of CCR9 in mouse models of paracetamol-induced liver failure. Increased serum levels of CCL25 were seen early in human acute liver failure and CCR9^{+} intermediate CD14^{+}CD16^{+} monocytes were detected in liver tissue in a patients undergoing liver transplantation for acute liver failure. In mice, increased CCR9^{+} myeloid cells were observed in the liver early after onset of toxic liver injury, a phenomenon that corresponded to peak serum ALT concentration. Prophylactic antagonism of CCR9 significantly reduced infiltration of liver tissue by CD11b^{+}CD11c^{-} macrophages, and improved liver injury as assessed by

serum AST and ALT concentration. In high dose paracetamol toxicity, CCR9 antagonism caused a trend towards improved mortality although this was not significant.

These data, particularly those described in the mouse models, are consistent with previous reports from Nakamoto et al who reported that CCR9$^+$ macrophages infiltrate the liver early during concanavalin A induced liver injury and exacerbate liver damage. The same group examined blood from human subjects and found increased CCR9 expression on CD14$^+$CD16$^+$ monocytes compared to chronic liver injury or healthy controls. A role for CCR9/CCL25 has been described in the recruitment of T lymphocytes to liver tissue in primary sclerosing cholangitis (PSC) where CCL25 was increased, suggesting that CCL25 is implicated in some chronic as well as acute liver diseases. Whether CCL25 recruits different subsets of leukocytes in acute and chronic disease remains undetermined.

The data from murine models and human data describes an early up regulation of CCL25 leading to recruitment of CCR9$^+$ cells into liver tissue. My data show that this is a transient phenomenon with CCL25 expression and the presence of CCR9$^+$ cells falling away after the initial period of liver injury. This probably corresponds with a transition from pro-inflammatory cellular infiltrate to an anti-inflammatory, pro-resolution infiltrate. CCL25/CCR9 are thus indicated as early drivers of inflammation and injury, in keeping with previous reports of mouse acute liver injury (Nakamoto *et al.*, 2012).

Whilst these data showing a role for CCR9/CCL25 in liver injury shed light on the pathogenesis of ALF, the need for prophylactic dosing to prevent injury in animal models limits their translational potential at present. Clearly in the context of drug-induced liver

injury, especially intentional paracetamol overdose, prophylactic treatment is not feasible although treatment early after poisoning might be Further investigations are required to evaluate the efficacy of therapeutic antagonism of CCR9. Many patients present several hours or even days after an overdose and inhibiting the very early stages of the disease process may therefore not be feasible. An alternative model of predictable acute liver injury is ischaemia-reperfusion injury during liver transplantation. Prophylactic intervention could be of benefit here but no data exist at present to suggest that CCR9/CCL25 might be of importance.

The role of CXCR6 in PBC

CXCR6, identified in 1997 (Deng *et al.*, 1997, Liao *et al.*, 1997, Loetscher *et al.*, 1997) has only one ligand, CXCL16 (Matloubian *et al.*, 2000). CXCL16 is widely expressed in liver by hepatic sinusoidal endothelium, hepatocytes and biliary epithelium (Heydtmann *et al.*, 2005). Most reports on the role of CXCR6 in the liver have been based on murine experiments (Geissmann *et al.*, 2005, Xu *et al.*, 2005). Recently in CCl_4-induced liver injury CXCR6$^{-/-}$ mice had lower serum ALT and demonstrated reduced fibrosis (Wehr *et al.*, 2013). The fibrotic response was restored when CXCR6$^+$ NKT cells were adoptively transferred to CXCR6$^{-/-}$ mice. However there are important differences between humans and mice in the distribution of CXCR6: in mice greater CXCR6 expression is seen on NKT cells (Campbell *et al.*, 2001, Wehr *et al.*, 2013) whereas in humans greatest expression is seen on NK cells (Kim *et al.*, 2001, Boisvert *et al.*, 2003, Heydtmann *et al.*, 2005). In addition, the relevance of CCl_4 and MCD to human disease is debatable: CCl_4 is an acute toxic injury uncommonly seen in humans, and MCD induces steatosis through inhibition of hepatocyte lipid transport and causes marked weight loss, in sharp contrast to common human liver disease. Mouse data

may therefore not accurately reflect the role of CXCR6 in the pathogenesis of human disease. Adhesion of human lymphocytes to biliary epithelial cells in vitro is a CXCL16-dependent process (Heydtmann *et al.*, 2005) and a greater frequency of CXCR6$^+$ lymphocytes in liver tissue has been reported in liver disease, particularly hepatitis C infection (Kim *et al.*, 2001, Heydtmann *et al.*, 2005, Billerbeck *et al.*, 2010).

My data show that CXCR6 is enriched on all lymphoid subsets in the liver compared to peripheral blood, but expression is particularly marked on NK cells, where it is associated with markers of activation. Moreover, CXCR6 expression by T lymphocytes and NKT cells was significantly decreased in cirrhosis, whereas expression tended to increase on NK cells.

CXCR6 expression by NK cells was particularly marked in PBC. In keeping with previous work from our laboratory and others, biliary epithelium was the dominant source of CXCL16. Interestingly, PCR of whole liver tissue showed greatest gene expression of CXCL16 in PBC (**figure 12.2**), although the serum concentration of soluble CXCL16 was low in this disease **(fig 12.5)**. A lower peripheral concentration of CXCL16 may be a consequence of retention in liver tissue allowing for increased trafficking of CXCR6$^+$ cells. CXCL16 is cleaved by the action of ADAM 10, a metalloproteinase (Le Gall *et al.*, 2009) and it would be intriguing to assess the activity of this in the context of PBC.

Antagonism of CXCR6 with a small molecule inhibitor significantly reduced the adhesion and transmigration of isolated NK cells across endothelial cells *in vitro*. This suggests that CXCR6 has a role in the hepatic recruitment of NK cells but may be dispensable for the recruitment of other cells types (**figures 12.14, 12.15**). No role was seen for CXCL16/CXCR6

interaction with regard to survival or proliferation of NK cells in contrast to earlier mouse work showing reduced survival of NKT cells in CXCR6 knockout mice (Geissmann *et al.*, 2005).

Taken together with previous work showing that adhesion to cholangiocytes is mediated by CXCL16 (Heydtmann *et al.*, 2005), this supports a paradigm where CXCR6 directs NK cell recruitment to the liver and positioning around injured bile ducts, and suggests a pathogenic role of CXCR6$^+$ NK cells in PBC.

There are conflicting reports of the actions of NK cells in chronic liver injury: NK cells have been reported to show toxicity to biliary epithelium (Leon *et al.*, 1997, Shimoda *et al.*, 2011, Guo *et al.*, 2012), where biliary epithelial cells isolated from PBC liver tissue are more susceptible to NK cell mediated cytotoxicity than those isolated from HBV, HCV or ALD liver (Shimoda *et al.*, 2011). However NK cells may also have an anti-fibrotic action (Melhem *et al.*, 2006, Radaeva *et al.*, 2006, Abu-Tair *et al.*, 2013). These apparently contrasting activities may be explained in part because reports of NK cell anti-fibrotic properties are shown in mice, whereas human data tends to show on NK cell cytotoxity. In addition, cytotoxic activity of intrahepatic NK cells in hepatitis C varies dependent on the severity of liver inflammation and fibrosis (Fugier *et al.*, 2014).

The role of hepatocyte CXCR6 in hepatocellular carcinoma

Observations made early in my investigation of the role of CXCR6 on immune cells showed that hepatocytes expressed CXCR6. This is consistent with a previous paper reporting

CXCR6 expression in human HCC (Gao *et al.*, 2012). Hepatocytes have been shown to express other CXC chemokine receptors. For example CXCR2 expression has been shown in mice (Hogaboam *et al.*, 1999, Bone-Larson *et al.*, 2001) and was reported to be a regenerative signal although a later manuscript described damaging effects of CXCR2 signalling (Kuboki *et al.*, 2008). There is also evidence that CXCR1 signalling facilitates regeneration of liver tissue after injury in mice (Clarke *et al.*, 2011).

I showed that in human liver tissue, hepatocytes express CXCR6 and in a subset of human HCC CXCR6 is overexpressed. CXCR6 expression in HCC was linked to particular biological phenotypes, for example grade of differentiation and the condition of background liver tissue. Further investigations in hepatoma cells and primary human hepatocytes showed that CXCR6 signalling can influence the proliferation of cells, through down-regulation of pro-apoptotic genes and other genes that regulate the cell cycle. Consistent with previous reports of CXC chemokine receptor expression in murine liver tissue, CXCR6 signalling may exert a protective role in liver injury, allowing regeneration of liver tissue but could become pathological if the regenerative process is unchecked.

My experiments with acute and chronic models of liver injury in mice showed contrasting effects of CXCR6. Mice were protected against liver injury induced by CCl_4 by knockout of CXCR6, whereas in a model of chronic liver injury, mice without functional CXCR6 demonstrated worse liver injury despite reduced infiltration of NKT cells. These apparently contradictory findings correspond to investigations with human tissue that showed a role for CXCR6 in the recruitment of NK cells to liver tissue, but also a pro-proliferative effect of CXCR6 signalling on hepatocytes. My data therefore show CXCR6 as a 'double-edged

sword': contributing to liver injury through the recruitment of inflammatory cells, but also contributing to liver repair through hepatocyte proliferation. This latter process may become pathogenic if hepatocyte proliferation becomes uncontrolled leading to hepatocellular carcinoma.

A recent paper from Wehr et al (Wehr et al., 2013) focussed on CXCR6 in liver injury and explored the underlying immunological mechanisms. The authors report data that in some parts complement my findings and in other contradict them. The found that acute liver injury caused by CCl_4 was ameliorated in CXCR6 knock-out mice: serum ALT concentration 6 hours after injury was significantly lower than in wild type mice, although differences did not appear significant at 12, 24 or 48 hours after injury. The inflammatory infiltrate in liver tissue was characterised by a lack of NKT cells (identified as $CD4^+NK1.1^+$ cells) and a rapid fall in monocyte-macrophages after 12 hours. The authors attributed the lower ALT to the reduction in macrophage-monocyte numbers although the two events were separated by over 24 hours. The authors went on to examine the role of CXCR6 in two models of chronic liver injury: chronic CCl_4 injury and MCD diet. In both models less fibrosis was seen in CXCR6 knock out mice than in wild type controls, as well as fewer NKT cells. Adoptive transfer of wild type NKT cells into CXCR6 knock out mice restored the fibrotic response to 4 weeks of MCD diet.

The findings of Wehr et al in acute liver injury - that knock-out of CXCR6 protected against liver damage - are consistent with my data in a similar injury model and suggest an acute, pro-inflammatory role for CXCR6 through recruitment of inflammatory cells. However in the MCD diet model of chronic liver injury the investigators reported reduced accumulation

of macrophages at eight weeks (but not four weeks) of diet and a reduction in fibrosis in CXCR6 knock out mice. In contrast, after 5 weeks of MCD diet I observed reduced expression of pro-fibrotic genes and greater liver injury, as assessed by serum AST in CXCR6 knock out mice. Wehr and colleagues did not report serum transaminase concentrations in the MCD diet model, and histology images were presented to demonstrate reduced periportal infiltrates although this was not quantified or subjected to a statistical test.

These contradictory findings in CXCR6 knock out mice given MCD may be due to a number of reasons. My data are based on 5 weeks of MCD diet, a limit imposed by Home Office regulations in view of the severe weight loss caused by MCD diet. Wehr *et al* subjected mice to 4 or 8 weeks of diet. However, differences between our results were evident at four weeks. Further, the MCD diet does not cause significant fibrosis, thus Wehr's findings that hydroxyproline content of liver tissue at four and eight weeks was comparable to six weeks of CCl_4 treatment is unusual. In addition, the authors stated categorically that CXCR6 was not expressed on hepatocytes, and ruled out a role for hepatocyte CXCR6 in explaining the differences seen between CXCR6 knockout and wild type mice. However, I detected CXCR6 on hepatocytes. It is possible that there are differences between murine and human hepatocyte expression of chemokine receptors – I have not demonstrated presence of CXCR6 in mouse liver.

There are important differences in the distribution of CXCR6 on lymphoid cells between humans and mice. My data show that in humans intrahepatic $CXCR6^+$ cells are predominantly NK cells, whereas in mice most intrahepatic $CXCR6^+$ cells are $CD4^+$ T

lymphocytes, with roughly equal number of NKT and NK cells (Wehr *et al.*, 2013). A greater percentage of NKT cells are CXCR6$^+$ in both mice and human. These differences are important and limit the applicability of murine data to human disease, particularly as the effect of CXCR6 knock out is ascribed to differences in NKT biology (Wehr *et al.*, 2013) through reduced direct cytotoxicity and also reduced recruitment of macrophages to liver.

Conclusion

Chemokines and their receptors play a critical role in the development of diverse liver diseases through their ability to recruit immune cells and possibly also to deliver signals to injured hepatocytes. My experiments with *ex-vivo* human tissue has shown the role of various chemokine/receptor pairings in liver disease, and pharmacological or genetic manipulation of the chemokine system has been able to ameliorate injury in animal models of liver disease.

NAFLD is a common disease and although most individuals have relatively benign disease a substantial minority will not and treatment is required to prevent liver-related morbidity and mortality. My data show that targeting CCR2 in NAFLD is a rational target in NAFLD moreover the reagent I used to demonstrate efficacy in mice is a clinical grade inhibitor that has been shown to be safe in humans. The extra-hepatic effect of CCR2 inhibition in reducing adipose tissue inflammation and improved glycaemic control are another reason to consider this an attractive therapeutic angle in NAFLD where the risk of cardiovascular disease and diabetes is high (Adams *et al.*, 2005a, Ekstedt *et al.*, 2006, Ekstedt *et al.*, 2014).

The CCR9/CCL25 axis is up regulated in human and mouse acute liver failure die to paracetamol. Whilst fulminant liver failure is a devastating condition, it is thankfully rare.

Although the data presented here show evidence for this axis in human ALF, they do not show a benefit of CCR9 inhibition after administration of paracetamol and as such do not support consideration of this in clinical practice.

Primary Biliary Cirrhosis is much less common than NAFLD but has few effective treatments. Inhibition of CXCR6 can reduce NK recruitment across hepatic endothelium in vitro and might be of benefit in PBC. The potential for translation is limited by the lack of an accurate mouse model of PBC. My finding that CXCR6 can contribute to hepatocyte replication raises the possibility that CXCR6 antagonism in a clinical setting may do more harm than good, if hepatocyte regeneration is compromised. However, this finding raises the possibility of intervention to control hepatocellular carcinoma through CXCR6 antagonism.

In humans, exploration of drugs that target the chemokine system in liver disease remains a relatively new area of therapeutics but may have the potential to deliver new treatments. This is especially important in liver disease where few effective treatments are available.

Appendix 1

Up regulated and down regulated genes in primary hepatocytes treated with CXCL16 (information from entrez gene www.ncbu.nih.gov/gene)

Gene symbol	Relative regulation	Protein	Protein function
CPT2	-254.1	carnitine palmitoyltransferase 2	Nuclear protein which is transported to the mitochondrial inner membrane. Together with carnitine palmitoyltransferase 1, the encoded protein oxidizes long-chain fatty acids in the mitochondria
BAX	-205.0	BCL2-associated X protein	This protein forms a heterodimer with BCL2, and functions as an apoptotic activator
BCL2L1	-166.5	BCL2-like 1	regulate outer mitochondrial membrane channel (VDAC) opening and thus controls production of reactive oxygen species and release of cytochrome C by mitochondria, both of which are potent inducers of apoptosis
GCLC	-88.6	glutamate-cysteine ligase, catalytic subunit	Glutamate-cysteine ligase. First rate-limiting enzyme of glutathione synthesis.
ACTB	-50.5	actin, beta	Actins are highly conserved proteins that are involved in cell motility, structure, and integrity.
CEBPD	-46.2	CCAAT/enhancer binding protein (C/EBP), delta	regulation of genes involved in immune and inflammatory responses, and may be involved in the regulation of genes associated with activation and/or differentiation of macrophages.
BCL2A1	-42.5	BCL2-related protein A1	reduces the release of pro-apoptotic cytochrome c from mitochondria and block caspase activation
ACSL3	-39.7	acyl-CoA synthetase long-chain family member 3	isozyme of the long-chain fatty-acid-coenzyme
ADM	-37.5	adrenomedullin	preprohormone which is cleaved to form two biologically active peptides, adrenomedullin and proadrenomedullin
CDKN1B	-31.5	cyclin-dependent kinase inhibitor 1B	binds to and prevents the activation

			of cyclin E-CDK2 or cyclin D-CDK4 complexes, and thus controls the cell cycle progression at G1
ATF4	-28.0	activating transcription factor 4	transcription factor also isolated and characterized as the cAMP-response element binding protein 2 (CREB-2). belongs to a family of transcription factors involved in protein-protein interactions
CDKN1A	-27.5	cyclin-dependent kinase inhibitor 1A	potent cyclin-dependent kinase inhibitor which binds to and inhibits activity of cyclin-CDK2 or -CDK4 complexes, thus functions as a regulator of cell cycle progression at G1.
EMP1	-18.4	epithelial membrane protein 1	
CCL5	-18.2	chemokine (C-C motif) ligand 5	a chemoattractant for blood monocytes, memory T helper cells and eosinophils.
BBC3	-18.1	BCL2 binding component 3	member of the BH3-only pro-apoptotic subclass. The protein induces mitochondrial outer membrane permeabilization and apoptosis
ACSL5	-14.8	acyl-CoA synthetase long-chain family member 5	isozyme of the long-chain fatty-acid-coenzyme A ligase family
B2M	-13.9	beta-2-microglobulin	serum protein found in association with the major histocompatibility complex (MHC) class I heavy chain on the surface of nearly all nucleated cells
GADD45B	-12.7	growth arrest and DNA-damage-inducible, beta	proteins binding and activating MTK1/MEKK4 kinase, an upstream activator of both p38 and JNK MAPKs. The function of these genes or their protein products is involved in the regulation of growth and apoptosis..
ARNT	-11.8	aryl hydrocarbon receptor nuclear translocator	binds to ligand-bound aryl hydrocarbon receptor and aids in the movement of this complex to the nucleus
ACSL4	-9.9	acyl-CoA synthetase long-chain family member 4	isozyme of the long-chain fatty-acid-coenzyme A ligase family
CCND2	-8.5	cyclin D2	This cyclin forms a complex with CDK4 or CDK6 and functions as a regulatory subunit of the complex, activity is required for cell cycle G1/S transition

GADD45A	-7.9	growth arrest and DNA-damage-inducible, alpha	The protein encoded by this gene responds to environmental stresses by mediating activation of the p38/JNK pathway via MTK1/MEKK4 kinase.
BMP4	-6.8	bone morphogenetic protein 4	member of the bone morphogenetic protein family which is part of the transforming growth factor-beta superfamily.
BTG2	-5.9	BTG family, member 2	member of the BTG/Tob family. This family has structurally related proteins that appear to have antiproliferative properties. This encoded protein is involved in the regulation of the G1/S transition of the cell cycle.
BIRC3	-5.7	aculoviral IAP repeat containing 3	inhibits apoptosis by binding to tumor necrosis factor receptor-associated factors
GSR	-5.3	Glutathione reductase	central enzyme of cellular antioxidant defense: reduces oxidized glutathione disulfide (GSSG) to the sulfhydryl form GSH, an important cellular antioxidant
WISP1	-5.3	WNT1 inducible signaling pathway protein 1	binds to decorin and biglycan, two members of a family of small leucine-rich proteoglycans present in the extracellular matrix of connective tissue, and possibly prevents the inhibitory activity of decorin and biglycan in tumor cell proliferation
WNT5A	-5.1	wingless-type MMTV integration site family, member 5A	member of the WNT family that signals through both the canonical and non-canonical WNT pathways. This protein plays an essential role in regulating developmental pathways during embryogenesis.
RPLP0	-5.1	ribosomal protein, large, P0	ribosomal protein that is a component of the 60S subunit.
BMP2	-4.4	bone morphogenetic protein 2	acts as a disulfide-linked homodimer and induces bone and cartilage formation
FTH1	-4.4	ferritin, heavy polypeptide 1	heavy subunit of ferritin, the major intracellular iron storage protein in prokaryotes and eukaryotes. It is composed of 24 subunits of the heavy and light ferritin chains.
CCND1	-3.6	cyclin D1	This cyclin forms a complex with

			and functions as a regulatory subunit of CDK4 or CDK6, whose activity is required for cell cycle G1/S transition.
STAT1	-3.1	signal transducer and activator of transcription 1	Transcription factors: mediates the expression of a variety of genes, which is thought to be important for cell viability in response to different cell stimuli and pathogens
FOSL1	-3.0	FOS-like antigen 1	implicated as regulators of cell proliferation, differentiation, and transformation.
SQSTM1	-3.0	sequestosome 1	binds ubiquitin and regulates activation of the nuclear factor kappa-B (NF-kB) signaling pathway
BCL2	-2.8	B-cell CLL/lymphoma 2	an integral outer mitochondrial membrane protein that blocks the apoptotic death of some cells
CA9	-2.6	carbonic anhydrase IX	transmembrane protein, one of only two tumor-associated carbonic anhydrase isoenzymes known. It may be involved in cell proliferation and transformation.
EPO	-2.2	erythropoietin	regulates red cell production by promoting erythroid differentiation and initiating hemoglobin synthesis. This protein also antiapoptotic functions in several tissue types
TNF	-2.1	tumor necrosis factor	proinflammatory cytokine that belongs to the tumor necrosis factor (TNF) superfamily.
HPRT1	-2.0	Hypoxanthine phosphoribosyltransferase	Generation of purine nucleotides through purine salvage pathway
MMP7	1.9731	Matrix metalloproteinase 7	Degrades various proteins
HEYL	2.1295	hes-related family bHLH transcription factor with YRPW motif-like	It is thought to be an effector of Notch signaling and a regulator of cell fate decisions.
HES5	2.2353	HES5	Hes family bHLH transcription factor 5
HEY1	2.3141	hes-related family bHLH transcription factor with YRPW motif 1	basic helix-loop-helix (bHLH)-type transcriptional repressors.
WNT3A	3.5813	wingless-type MMTV integration site family, member 3A	These proteins have been implicated in oncogenesis and in several developmental processes

Fold-Change ($2^{\wedge}$(- Delta Delta Ct)) is the normalized gene expression ($2^{\wedge}$(- Delta Ct)) in the

Test Sample divided the normalized gene expression ($2^{\wedge}$(- Delta Ct)) in the Control Sample.

References

Abdelmalek, M. F. et al. Increased fructose consumption is associated with fibrosis severity in patients with nonalcoholic fatty liver disease. Hepatology 2010;51(6):1961-1971.

Abu-Tair, L. et al. Natural killer cell-dependent anti-fibrotic pathway in liver injury via Toll-like receptor-9. PLoS One 2013;8(12):e82571.

Adams, L. A. et al. The histological course of nonalcoholic fatty liver disease: a longitudinal study of 103 patients with sequential liver biopsies. Journal of hepatology 2005a;42(1):132-138.

Adams, L. A. et al. The natural history of nonalcoholic fatty liver disease: a population-based cohort study. Gastroenterology 2005b;129(1):113-121.

Aden, D. P. et al. Controlled synthesis of HBsAg in a differentiated human liver carcinoma-derived cell line. 1979

Afford, S. C. et al. Distinct patterns of chemokine expression are associated with leukocyte recruitment in alcoholic hepatitis and alcoholic cirrhosis. The Journal of pathology 1998;186(1):82-89.

Allen, S. J., Crown, S. E., and Handel, T. M. Chemokine: receptor structure, interactions, and antagonism. Annu. Rev. Immunol. 2007a;25:787-820.

Allen, S. J., Crown, S. E., and Handel, T. M. Chemokine: receptor structure, interactions, and antagonism. Annu. Rev. Immunol. 2007b;25:787-820.

Altekruse, S. F., McGlynn, K. A., and Reichman, M. E. Hepatocellular carcinoma incidence, mortality, and survival trends in the United States from 1975 to 2005. Journal of Clinical Oncology 2009;27(9):1485.

Anstee, Q. M., and Goldin, R. D. Mouse models in non-alcoholic fatty liver disease and steatohepatitis research. International journal of experimental pathology 2006;87(1):1-16.

Antionades, C. G. et al. The importance of immune dysfunction in determining outcome in acute liver failure. Journal of hepatology 2008;49:845 - 861.

Antoniades, C. G. et al. Source and characterization of hepatic macrophages in acetaminophen-induced acute liver failure in humans. Hepatology 2012;56(2):735-746.

Armstrong, M. J. et al. Presence and severity of non-alcoholic fatty liver disease in a large prospective primary care cohort. Journal of Hepatology 2011;21(1):234-240.

Armstrong, M. J. et al. Liraglutide efficacy and action in non-alcoholic steatohepatitis (LEAN): study protocol for a phase II multicentre, double-blinded, randomised, controlled trial. BMJ open 2013;3(11):e003995.

Autschbach, F. et al. Expression of chemokine receptors in normal and inflamed human intestine, tonsil, and liver—an immunohistochemical analysis with new monoclonal antibodies from the 8th international workshop and conference on human leucocyte differentiation antigens. Cellular immunology 2005;236(1):110-114.

Baeck, C. et al. Pharmacological inhibition of the chemokine CCL2 (MCP-1) diminishes liver macrophage infiltration and steatohepatitis in chronic hepatic injury. Gut 2012;61(3):416-426.

Baffy, G. Kupffer cells in non-alcoholic fatty liver disease: the emerging view. Journal of hepatology 2009;51(1):212-223.

Bekker, P. Orally-Administered Chemokine Receptor CCR2 Antagonist CCX140-B in Type 2 Diabetes: A Pilot Double-Blind, Randomized Clinical Trial. Journal of Diabetes & Metabolism 2012

Bekker, P, et al. S0058 Clinical Development Of Ccr2 Antagonists CCX140-B And CCX872-B. Nephrol. Dial. Transplant. 2013;28 (S1):i16-i18.

Bernardini, G. et al. Analysis of the role of chemokines in angiogenesis. Journal of immunological methods 2003;273(1):83-101.

Biassoni, R. et al. Human natural killer cell receptors and co receptors. Immunological reviews 2001;181(1):203-214.

Billerbeck, E. et al. Analysis of CD161 expression on human CD8+ T cells defines a distinct functional subset with tissue-homing properties. Proc Natl Acad Sci U S A 2010;107(7):3006-3011.

Bismuth, H. Revisiting liver anatomy and terminology of hepatectomies. Annals of surgery 2013;257(3):383-386.

Björkland, A. et al. Blood and liver-infiltrating lymphocytes in primary biliary cirrhosis: Increase in activated T and natural killer cells and recruitment of primed memory T cells. Hepatology 1991;13(6):1106-1111.

Blachier, M. et al. The burden of liver disease in Europe: A review of available epidemiological data. Journal of hepatology 2013;58(3):593-608.

Boisvert, J. et al. Liver-infiltrating lymphocytes in end-stage hepatitis C virus: subsets, activation status, and chemokine receptor phenotypes. J Hepatol 2003;38(1):67-75.

Bone-Larson, C. L. et al. IFN-gamma-inducible protein-10 (CXCL10) is hepatoprotective during acute liver injury through the induction of CXCR2 on hepatocytes. J Immunol 2001;167(12):7077-7083.

Bonecchi, R. et al. Chemokine decoy receptors: structure–function and biological properties.

In: The Chemokine System in Experimental and Clinical Hematology, edited by Springer, 2010, 15-36.

Boonstra, K., Beuers, U., and Ponsioen, C. Y. Epidemiology of primary sclerosing cholangitis and primary biliary cirrhosis: a systematic review. Journal of hepatology 2012;56(5):1181-1188.

Boujedidi, H. et al. Housekeeping gene variability in the liver of alcoholic patients. Alcoholism: Clinical and Experimental Research 2012;36(2):258-266.

Bourlier, V. et al. Remodeling phenotype of human subcutaneous adipose tissue macrophages. Circulation 2008;117(6):806-815.

Bower, W. A. et al. Population-based surveillance for acute liver failure. Am J Gastroenterol 2007;102(11):2459-2463.

Brattin, W. J., Glende, E. A. J., and Recknagel, R. O. Pathological mechanisms in carbon tetrachloride hepatotoxicity. J Free Radic Biol Med 1985;1(1):27-38.

Bretherick, A. D. et al. Acute liver failure in Scotland between 1992 and 2009; incidence, aetiology and outcome. QJM 2011;104(11):945-956.

Trust, B. L. Facts about Liver Disease: Liver Deaths 1971-2008. 2008

Browning, J. D. et al. Prevalence of hepatic steatosis in an urban population in the United States: impact of ethnicity. Hepatology 2004;40(6):1387-1395.

Calvisi, D. F. et al. Mechanistic and prognostic significance of aberrant methylation in the molecular pathogenesis of human hepatocellular carcinoma. The Journal of clinical investigation 2007;117(9):2713-2722.

Campbell, J. J. et al. Unique subpopulations of CD56+ NK and NK-T peripheral blood lymphocytes identified by chemokine receptor expression repertoire. The Journal of Immunology 2001;166(11):6477-6482.

Chalasani, N. et al. The diagnosis and management of non-alcoholic fatty liver disease: practice guideline by the American Gastroenterological Association, American Association for the Study of Liver Diseases, and American College of Gastroenterology. Gastroenterology 2012;142(7):1592-1609.

Charo, I. F. et al. Molecular cloning and functional expression of two monocyte chemoattractant protein 1 receptors reveals alternative splicing of the carboxyl-terminal tails. Proceedings of the National Academy of Sciences 1994;91(7):2752-2756.

Chu, P. et al. C-C motif chemokine receptor 9 positive macrophages activate hepatic stellate cells and promote liver fibrosis in mice. Hepatology 2013;58(1):337-350.

Clarke, C. et al. CXC chemokine receptor-1 is expressed by hepatocytes and regulates liver recovery after hepatic ischemia/reperfusion injury. Hepatology 2011;53(1):261-271.

trials.gov, C. Efficacy and Safety Study of Cenicriviroc for the Treatment of NASH in Adult Subjects With Liver Fibrosis (CENTAUR)
. 2014

Colombat, M. et al. Portal lymphocytic infiltrate in alcoholic liver disease. Hum Pathol 2002;33(12):1170-1174.

Cooper, M. A., Fehniger, T. A., and Caligiuri, M. A. The biology of human natural killer-cell subsets. Trends in immunology 2001;22(11):633-640.

Corbisier, J. et al. Biased signaling at chemokine receptors. J Biol Chem 2015;290 (15):9542 - 54.

Crispe, I. N. The liver as a lymphoid organ. Annual review of immunology 2009;27:147-163.

Cullen, R. et al. Enhanced tumor metastasis in response to blockade of the chemokine receptor CXCR6 is overcome by NKT cell activation. The Journal of Immunology 2009;183(9):5807.

Curnock, A. P., Logan, M. K., and Ward, S. G. Chemokine signalling: pivoting around multiple phosphoinositide 3 kinases. Immunology 2002;105(2):125-136.

Cynis, H. et al. Inhibition of Glutaminyl Cyclases alleviates CCL2-mediated inflammation of non-alcoholic fatty liver disease in mice. Int J Exp Pathol 2013;94(3):217-225.

Czaja, A. J. Acute and acute severe (fulminant) autoimmune hepatitis. Dig Dis Sci 2013;58(4):897-914.

Dal-Secco, D. et al. A dynamic spectrum of monocytes arising from the in situ reprogramming of CCR2+ monocytes at a site of sterile injury. Journal of Experimental Medicine 2015;212 (4):447-456.

DeLeve, L. D. Hepatic microvasculature in liver injury. 2007;Seminars in liver disease 27(4):390-400.

Deng, H. K. et al. Expression cloning of new receptors used by simian and human immunodeficiency viruses. Nature 1997;388(6639):296-300.

DeVries, M. E. et al. Defining the origins and evolution of the chemokine/chemokine receptor system. The Journal of Immunology 2006;176(1):401-415.

Di Prospero, N. A. et al. CCR2 antagonism in patients with type 2 diabetes mellitus: a randomized, placebo-controlled study. Diabetes, Obesity and Metabolism 2014;16 (11):1055-1064.

Diehl, A. M., Goodman, Z., and Ishak, K. G. Alcohollike liver disease in nonalcoholics. A clinical and histologic comparison with alcohol-induced liver injury. Gastroenterology 1988;95(4):1056-1062.

Doherty, D. G., and O'Farrelly, C. Innate and adaptive lymphoid cells in the human liver. Immunological reviews 2000;174(1):5-20.

Sherlock's Diseases of the liver and biliary system. 12th Edition. John Wiley & Sons, 2011.

East, L., and Isacke, C. M. The mannose receptor family. Biochimica et Biophysica Acta (BBA)-General Subjects 2002;1572(2):364-386.

Ekstedt, M. et al. Long-term follow-up of patients with NAFLD and elevated liver enzymes. Hepatology 2006;44(4):865-873.

Ekstedt, M. et al. Fibrosis stage is the strongest predictor for disease-specific mortality in NAFLD after up to 33 years of follow-up. Hepatology 2014

Eksteen, B. et al. Hepatic endothelial CCL25 mediates the recruitment of CCR9+ gut-homing lymphocytes to the liver in primary sclerosing cholangitis. J Exp Med 2004;200(11):1511-1517.

Elvevold, K. H. et al. Scavenger properties of cultivated pig liver endothelial cells. Comp Hepatol 2004;3(4)

Esteban, J. I., Sauleda, S., and Quer, J. The changing epidemiology of hepatitis C virus infection in Europe. Journal of hepatology 2008;48(1):148-162.

Liver, E. A. F. S. O. EASL-EORTC clinical practice guidelines: management of hepatocellular carcinoma. European journal of cancer (Oxford, England: 1990) 2012a;48(5):599.

Liver, E. A. F. T. S. O. T. EASL clinical practice guidelines: Management of chronic hepatitis B virus infection. Journal of hepatology 2012b;57(1):167-185.

Liver, E. A. F. T. S. O. T. EASL Clinical Practice Guidelines: Management of hepatitis C virus infection. Journal of Hepatology 2014;60(2):392-420.

Ferenci, P. et al. Hepatocellular carcinoma (HCC): a global perspective. Journal of Clinical Gastroenterology 2010;44 (4):239 - 245.

Fleming, K. M. et al. Incidence and prevalence of cirrhosis in the United Kingdom, 1992-2001: a general population-based study. J Hepatol 2008;49(5):732-738.

Frade, J. M. et al. Characterization of the CCR2 chemokine receptor: functional CCR2 receptor expression in B cells. The Journal of Immunology 1997;159(11):5576-5584.

Fugier, E. et al. Functions of liver natural killer cells are dependent on the severity of liver inflammation and fibrosis in chronic hepatitis C. PLoS One 2014;9(4):e95614.

Furuya, Y. et al. CXCL16-CXCR6 Signaling Accelerates Restitution of the Intestinal Epithelial Cell Layer Through Activation of RAC-1. Gastroenterology 2011;Suppl 1:S836.

Gadd, V. L. et al. The portal inflammatory infiltrate and ductular reaction in human nonalcoholic fatty liver disease. Hepatology 2014;59(4):1393-1405.

Gaida, M. M. et al. Expression of the CXCR6 on polymorphonuclear neutrophils in pancreatic carcinoma and in acute, localized bacterial infections. Clinical & Experimental Immunology 2008;154(2):216-223.

Gao, Q. et al. CXCR6 upregulation contributes to a proinflammatory tumor microenvironment that drives metastasis and poor patient outcomes in hepatocellular carcinoma. Cancer Res 2012;72(14):3546-3556.

Geissmann, F. et al. Intravascular immune surveillance by CXCR6 NKT cells patrolling liver sinusoids. PLoS Biol 2005;3:e113.

Gerhardt, C. C. et al. Chemokines control fat accumulation and leptin secretion by cultured human adipocytes. Mol Cell Endocrinol 2001;175(1-2):81-92.

Gulmez, S. E. et al. Transplantation for acute liver failure in patients exposed to NSAIDs or paracetamol (acetaminophen): the multinational case-population SALT study. Drug Saf 2013;36(2):135-144.

Guo, C. et al. Combinatory effects of hepatic CD8+ and NK lymphocytes in bile duct injury from biliary atresia. Pediatr Res 2012;71(6):638-644.

Hadem, J. et al. Etiologies and outcomes of acute liver failure in Germany. Clinical Gastroenterology and Hepatology 2012;10(6):664-669. e2.

Hashimoto, D. et al. Tissue-resident macrophages self-maintain locally throughout adult life with minimal contribution from circulating monocytes. Immunity 2013;38(4):792-804.

Hata, K. et al. Isolation, phenotyping, and functional analysis of lymphocytes from human liver. Clinical immunology and immunopathology 1990;56(3):401-419.

Hattermann, K. et al. The chemokine CXCL16 induces migration and invasion of glial precursor cells via its receptor CXCR6. Molecular and Cellular Neuroscience 2008;39(1):133-141.

Haukeland, J. W. et al. Systemic inflammation in nonalcoholic fatty liver disease is characterized by elevated levels of CCL2. J Hepatol 2006;44(6):1167-1174.

Hendriks, H. F. J. Moderate alcohol consumption and insulin sensitivity: observations and possible mechanisms. Annals of epidemiology 2007;17(5):S40-S42.

Heydtmann, M. et al. CXC chemokine ligand 16 promotes integrin-mediated adhesion of liver-infiltrating lymphocytes to cholangiocytes and hepatocytes within the inflamed human liver. J Immunol 2005;174(2):1055-1062.

Hogaboam, C. M. et al. Novel CXCR2-dependent liver regenerative qualities of ELR-containing CXC chemokines. FASEB J 1999;13(12):1565-1574.

Holbrook, T. L, Barrett-Connor, E., and Wingard, D. L. A prospective population-based study of alcohol use and non-insulin-dependent diabetes mellitus. American journal of epidemiology 1990;132(5):902-909.

Horuk, R. Physiology: Chemokines beyond inflammation. Nature 1998;393(6685):524-525.

Hoshida, Y. et al. Molecular classification and novel targets in hepatocellular carcinoma: recent advancements. 2010;Seminars in liver disease 30(1):35.

Huang, W. et al. Depletion of liver Kupffer cells prevents the development of diet-induced hepatic steatosis and insulin resistance. Diabetes 2010;59(2):347-357.

Huang, Y. et al. Human trophoblasts recruited T lymphocytes and monocytes into decidua by secretion of chemokine CXCL16 and interaction with CXCR6 in the first-trimester pregnancy. The Journal of Immunology 2008;180(4):2367.

Hvidtfeldt, U. A. et al. Incidence of cardiovascular and cerebrovascular disease in Danish men and women with a prolonged heavy alcohol intake. Alcoholism: Clinical and Experimental Research 2008;32(11):1920-1924.

Itoh, M. et al. Hepatic Crown-Like Structure: A Unique Histological Feature in Non-Alcoholic Steatohepatitis in Mice and Humans. PloS one 2013

Iturriaga, H. et al. Glucose tolerance and the insulin response in recently drinking alcoholic patients: possible effects of withdrawal. Metabolism 1986;35(3):238-243.

Jalan, R. et al. Acute-on chronic liver failure. Journal of Hepatology 2012

Johansson-Lindbom, B. et al. Selective generation of gut tropic T cells in gut-associated lymphoid tissue (GALT) requirement for GALT dendritic cells and adjuvant. The Journal of experimental medicine 2003;198(6):963-969.

Kanda, H. et al. MCP-1 contributes to macrophage infiltration into adipose tissue, insulin resistance, and hepatic steatosis in obesity. Journal of Clinical Investigation 2006;116(6):1494-1505.

Kim, C. H. et al. Bonzo/CXCR6 expression defines type 1-polarized T-cell subsets with extralymphoid tissue homing potential. J Clin Invest 2001;107(5):595-601.

Kinashi, T. Intracellular signalling controlling integrin activation in lymphocytes. Nature Reviews Immunology 2005;5(7):546-559.

Kirovski, G. et al. Elevated systemic monocyte chemoattractrant protein-1 in hepatic steatosis without significant hepatic inflammation. Exp Mol Pathol 2011;91(3):780-783.

Kirovski, G. et al. Hepatic steatosis causes induction of the chemokine RANTES in the absence of significant hepatic inflammation. International Journal of Clinical and Experimental Pathology 2010;3(7):675.

Kita, H. et al. Quantitative and functional analysis of PDC-E2-specific autoreactive cytotoxic T lymphocytes in primary biliary cirrhosis. J Clin Invest 2002;109(9):1231-1240.

Kleiner, D. E. et al. Design and validation of a histological scoring system for nonalcoholic fatty liver disease. Hepatology 2005;41(6):1313-1321.

Klibanov, O. M., Williams, S. H., and Iler, C. A. Cenicriviroc, an orally active CCR5 antagonist for the potential treatment of HIV infection. Curr Opin Investig Drugs 2010;11(8):940-950.

Knolle, P. A., and Gerken, G. Local control of the immune response in the liver. Immunological reviews 2000;174(1):21-34.

Kruszynska, Y. T., Home, P. D., and McIntyre, N. Relationship between insulin sensitivity, insulin secretion and glucose tolerance in cirrhosis. Hepatology 1991;14(1):103-111.

Kubes, P., and Mehal, W. Z. Sterile inflammation in the liver. Gastroenterology 2012;143(5):1158-1172.

Kuboki, S. et al. Hepatocyte signaling through CXC chemokine receptor-2 is detrimental to liver recovery after ischemia/reperfusion in mice. Hepatology 2008;48(4):1213-1223.

Lalor, P. F. et al. Recruitment of lymphocytes to the human liver. Immunology and cell biology 2002;80(1):52-64.

Lalor, P. F. et al. Association between receptor density, cellular activation, and transformation of adhesive behavior of flowing lymphocytes binding to VCAM-1. European journal of immunology 1997;27(6):1422-1426.

Lalor, P. F. et al. Human hepatic sinusoidal endothelial cells can be distinguished by expression of phenotypic markers related to their specialised functions in vivo. World J Gastroenterol 2006;12(34):5429-5439.

Lanthier, N. et al. Kupffer cell depletion prevents but has no therapeutic effect on metabolic and inflammatory changes induced by a high-fat diet. The FASEB Journal 2011;25(12):4301-4311.

Larson, A. M. et al. Acetaminophen-induced acute liver failure: results of a United States multicenter, prospective study. Hepatology 2005;42(6):1364-1372.

Lavanchy, D. Evolving epidemiology of hepatitis C virus. Clinical Microbiology and Infection 2011;17(2):107-115.

Lazennec, G., and Richmond, A. Chemokines and chemokine receptors: new insights into cancer-related inflammation. Trends in molecular medicine 2010;16(3):133-144.

Le Couteur, D. G. et al. The hepatic sinusoid in aging and cirrhosis: effects on hepatic substrate disposition and drug clearance. Clin Pharmacokinet 2005;44(2):187-200.

Le Gall, S. M. et al. ADAMs 10 and 17 represent differentially regulated components of a general shedding machinery for membrane proteins such as transforming growth factor {alpha}, L-selectin, and tumor necrosis factor {alpha}. Molecular Biology of the Cell 2009;20(6):1785.

Lee, W. M., Larson, A. M., and Stravitz, R. T. AASLD position paper: the management of acute liver failure. Update 2011 1-22.

Leifeld, L. et al. Early up-regulation of chemokine expression in fulminant hepatic failure. The Journal of pathology 2003;199(3):335-344.

Leite, N. C. et al. Prevalence and associated factors of non-alcoholic fatty liver disease in patients with type-2 diabetes mellitus. Liver Int 2009;29(1):113-119.

Leon, D. A., and McCambridge, J. Liver cirrhosis mortality rates in Britain from 1950 to 2002: an analysis of routine data. The Lancet 2006;367(9504):52-56.

Leon, M. P. et al. Immunogenicity of biliary epithelium: study of the adhesive interaction with lymphocytes. Gastroenterology 1997;112(3):968-977.

Liao, F. et al. STRL33, A Novel Chemokine Receptor–like Protein, Functions as a Fusion Cofactor for Both Macrophage-tropic and T Cell Line–tropic HIV-1. The Journal of experimental medicine 1997;185(11):2015.

Liaskou, E. et al. Monocyte subsets in human liver disease show distinct phenotypic and functional characteristics. Hepatology 2013;57(1):385-398.

Lindor, K. D. et al. Primary biliary cirrhosis. Hepatology 2009;50(1):291-308.

Linton, L. et al. HLA-DRhi and CCR9 Define a Pro-Inflammatory Monocyte Subset in IBD. Clinical and translational gastroenterology 2012;3(12):e29.

Liu, H. et al. Roles of chemokine receptor 4 (CXCR4) and chemokine ligand 12 (CXCL12) in metastasis of hepatocellular carcinoma cells. Cell Mol Immunol 2008;5(5):373-378.

Loetscher, M. et al. TYMSTR, a putative chemokine receptor selectively expressed in activated T cells, exhibits HIV-1 coreceptor function. Current Biology 1997;7(9):652-660.

Ludwig, A. et al. Enhanced expression and shedding of the transmembrane chemokine CXCL16 by reactive astrocytes and glioma cells. Journal of neurochemistry 2005;93(5):1293-1303.

Lumeng, C. N., Bodzin, J. L., and Saltiel, A. R. Obesity induces a phenotypic switch in adipose tissue macrophage polarization. Journal of Clinical Investigation 2007;117(1):175-184.

Mack, M. et al. Expression and characterization of the chemokine receptors CCR2 and CCR5 in mice. The Journal of Immunology 2001;166(7):4697-4704.

Mandrekar, P. et al. An essential role for monocyte chemoattractant protein-1 in alcoholic liver injury: regulation of proinflammatory cytokines and hepatic steatosis in mice. Hepatology 2011;54(6):2185-2197.

Marques, P. E. et al. Chemokines and mitochondrial products activate neutrophils to amplify organ injury during mouse acute liver failure. Hepatology 2012;56(5):1971-1982.

Marudanayagam, R. et al. Aetiology and outcome of acute liver failure. HPB (Oxford) 2009;11(5):429-434.

Matloubian, M. et al. A transmembrane CXC chemokine is a ligand for HIV-coreceptor Bonzo. Nature Immunology 2000;1(4):298-304.

Mattalia, A. et al. Characterization of antimitochondrial antibodies in healthy adults. Hepatology 1998;27 (3):656 - 661.

McGill, M. R. et al. The mechanism underlying acetaminophen-induced hepatotoxicity in humans and mice involves mitochondrial damage and nuclear DNA fragmentation. J Clin Invest 2012;122(4):1574-1583.

Mehrad, B., Keane, M. P., and Strieter, R. M. Chemokines as mediators of angiogenesis. Thrombosis and Haemostasis 2007;97(5):755.

Melhem, A. et al. Anti-fibrotic activity of NK cells in experimental liver injury through killing of activated HSC. J Hepatol 2006;45(1):60-71.

Michieletti, P. et al. Antimitochondrial antibody negative primary biliary cirrhosis: a distinct syndrome of autoimmune cholangitis. Gut 1994;35(2):260-265.

Miura, K. et al. Hepatic recruitment of macrophages promotes nonalcoholic steatohepatitis through CCR2. Am J Physiol Gastrointest Liver Physiol 2012;302(11):G1310-21.

Mizukami, T. et al. CCR9+ macrophages are required for eradication of peritoneal bacterial infections and prevention of polymicrobial sepsis. Immunology letters 2012;147(1):75-79.

Mora, J. R. et al. Generation of gut-homing IgA-secreting B cells by intestinal dendritic cells. Science 2006;314(5802):1157-1160.

Musso, G. et al. A meta-analysis of randomized trials for the treatment of nonalcoholic fatty liver disease. Hepatology 2010;52(1):79-104.

Myers, R. P. et al. Epidemiology and natural history of primary biliary cirrhosis in a Canadian health region: A population-based study. Hepatology 2009;50(6):1884-1892.

Nakabayashi, H. et al. Growth of human hepatoma cell lines with differentiated functions in chemically defined medium. Cancer research 1982;42(9):3858-3863.

Nakamoto, N. et al. CCR9+ macrophages are required for acute liver inflammation in mouse models of hepatitis. Gastroenterology 2012;142(2):366-376.

02217475, N. C. T. Efficacy and Safety Study of Cenicriviroc for the Treatment of NASH in Adult Subjects With Liver Fibrosis (CENTAUR)
. 2014

Neuschwander-Tetri, B. A. et al. Farnesoid X nuclear receptor ligand obeticholic acid for non-cirrhotic, non-alcoholic steatohepatitis (FLINT): a multicentre, randomised, placebo-controlled trial. The Lancet 2015;385(9972):956-965.

Nio, Y. et al. Monocyte chemoattractant protein-1 (MCP-1) deficiency enhances alternatively activated M2 macrophages and ameliorates insulin resistance and fatty liver in lipoatrophic diabetic A-ZIP transgenic mice. Diabetologia 2012;55(12):3350-3358.

Norris, S. et al. Resident human hepatitis lymphocytes are phenotypically different from circulating lymphocytes. Journal of hepatology 1998;28(1):84-90.

Norris, S. et al. Natural T cells in the human liver: cytotoxic lymphocytes with dual T cell and natural killer cell phenotype and function are phenotypically heterogenous and include V [alpha] 24-J [alpha] Q and [gamma][delta] T cell receptor bearing cells. Human immunology 1999;60(1):20-31.

Northfield, J. W. et al. CD161 expression on hepatitis C virus-specific CD8+ T cells suggests a distinct pathway of T cell differentiation. Hepatology 2008;47(2):396-406.

Obstfeld, A. E. et al. CC chemokine receptor 2 (CCR2) regulates the hepatic recruitment of myeloid cells that promote obesity-induced hepatic steatosis. Diabetes 2010;59(4):916-925.

Ogilvie, P. et al. Eotaxin-3 is a natural antagonist for CCR2 and exerts a repulsive effect on human monocytes. Blood 2003;102(3):789-794.

Oo, Y. H., and Adams, D. H. The role of chemokines in the recruitment of lymphocytes to the liver. Journal of autoimmunity 2010;34(1):45-54.

Ouyang, X. et al. Fructose consumption as a risk factor for non-alcoholic fatty liver disease. Journal of hepatology 2008;48(6):993-999.

Patsouris, D. et al. Ablation of CD11c-positive cells normalizes insulin sensitivity in obese insulin resistant animals. Cell metabolism 2008;8(4):301-309.

Pende, D. et al. Identification and molecular characterization of NKp30, a novel triggering receptor involved in natural cytotoxicity mediated by human natural killer cells. J Exp Med 1999;190(10):1505-1516.

Poli, A. et al. CD56bright natural killer (NK) cells: an important NK cell subset. Immunology 2009;126(4):458-465.

Porcheray, F. et al. Macrophage activation switching: an asset for the resolution of inflammation. Clinical & Experimental Immunology 2005;142(3):481-489.

Porta, C. A. M. L. CXCR6: The Role of Environment in Tumor Progression. Challenges for Therapy. Stem Cell Reviews and Reports 2012

Promrat, K. et al. Randomized controlled trial testing the effects of weight loss on nonalcoholic steatohepatitis. Hepatology 2010;51(1):121-129.

Racanelli, V., and Rehermann, B. The liver as an immunological organ. Hepatology 2006;43(S1):S54-S62.

Radaeva, S. et al. Natural Killer Cells Ameliorate Liver Fibrosis by Killing Activated Stellate Cells in NKG2D-Dependent and Tumor Necrosis Factor–Related Apoptosis-Inducing Ligand–Dependent Manners. Gastroenterology 2006;130(2):435-452.

Raz, E., and Mahabaleshwar, H. Chemokine signaling in embryonic cell migration: a fisheye view. Development 2009;136(8):1223-1229.

Recknagel, R. O. et al. Mechanisms of carbon tetrachloride toxicity. Pharmacol Ther 1989;43(1):139-154.

Reha, J. L., Lee, S., and Hofmann, L. J. Prevalence and predictors of nonalcoholic steatohepatitis in obese patients undergoing bariatric surgery: a Department of Defense experience. Am Surg 2014;80(6):595-599.

Reid D et al. Hepatic Expression of CCL25 Mediates Recruitment of Plasmacytoid Dendritic Cells to Limit Liver Injury. Gut 2013;62:A23-A24.

Rinella, M. E. et al. Mechanisms of hepatic steatosis in mice fed a lipogenic methionine choline-deficient diet. Journal of lipid research 2008;49(5):1068-1076.

Rinella, M. E., and Green, R. M. The methionine-choline deficient dietary model of steatohepatitis does not exhibit insulin resistance. Journal of hepatology 2004;40(1):47-51.

Rohlfing, C. L. et al. Defining the relationship between plasma glucose and HbA1c analysis of glucose profiles and HbA1c in the Diabetes Control and Complications Trial. Diabetes care 2002;25(2):275-278.

Rot, A., and von Andrian, U. H. Chemokines in innate and adaptive host defense: basic chemokinese grammar for immune cells. Annu. Rev. Immunol. 2004;22:891-928.

Ruth, J. H. et al. CXCL16-mediated cell recruitment to rheumatoid arthritis synovial tissue and murine lymph nodes is dependent upon the MAPK pathway. Arthritis & Rheumatism 2006;54(3):765-778.

Santodomingo-Garzon, T., and Swain, M. G. Role of NKT cells in autoimmune liver disease. Autoimmunity reviews 2011;10(12):793-800.

Schaffner, F., and Poper, H. Capillarization of hepatic sinusoids in man. Gastroenterology 1963;44:239-242.

Schall, T. J., and Proudfoot, A. E. I. Overcoming hurdles in developing successful drugs targeting chemokine receptors. Nature Reviews Immunology 2011;11(5):355-363.

Schmutz, C. et al. Monocytes/macrophages express chemokine receptor CCR9 in rheumatoid arthritis and CCL25 stimulates their differentiation. Arthritis research & therapy 2010;12(4):R161.

Seki, E. et al. CCR2 promotes hepatic fibrosis in mice. Hepatology 2009;50(1):185-197.

Selmi, C. et al. Primary biliary cirrhosis. The Lancet 2011;377(9777):1600-1609.

Sgro, C. et al. Incidence of drug-induced hepatic injuries: A French population-based study. Hepatology 2002;36(2):451-455.

Shields, P. L. et al. Chemokine and chemokine receptor interactions provide a mechanism for selective T cell recruitment to specific liver compartments within hepatitis C-infected liver. The Journal of Immunology 1999;163(11):6236-6243.

Shimoda, S. et al. Interaction between Toll-like receptors and natural killer cells in the destruction of bile ducts in primary biliary cirrhosis. Hepatology 2011;53(4):1270-1281.

Spring, H. et al. Chemokines direct endothelial progenitors into tumor neovessels. Proceedings of the National Academy of Sciences of the United States of America 2005;102(50):18111-18116.

Susca, M. et al. Liver inflammatory cells, apoptosis, regeneration and stellate cell activation in non-alcohol steatohepatitis. Digestive and liver disease 2001;33(9):768-777.

Svensson, M. et al. CCL25 mediates the localization of recently activated CD8αβ+ lymphocytes to the small-intestinal mucosa. The Journal of clinical investigation 2002;110(8):1113-1121.

Tabata, S. et al. Distribution and kinetics of SR-PSOX/CXCL16 and CXCR6 expression on human dendritic cell subsets and CD4+ T cells. Journal of leukocyte biology 2005;77(5):777.

Tacke, F., and Zimmermann, H. W. Macrophage heterogeneity in liver injury and fibrosis. Journal of hepatology 2014;60(5):1090-1096.

Tamura, Y. et al. CC chemokine receptor 2 inhibitor improves diet-induced development of insulin resistance and hepatic steatosis in mice. Journal of atherosclerosis and thrombosis 2010;17(3):219-228.

Tamura, Y. et al. Inhibition of CCR2 ameliorates insulin resistance and hepatic steatosis in db/db mice. Arteriosclerosis, thrombosis, and vascular biology 2008;28(12):2195-2201.

Targher, G. et al. Nonalcoholic fatty liver disease is independently associated with an increased incidence of cardiovascular events in type 2 diabetic patients. Diabetes Care 2007;30(8):2119-2121.

Tay, S. S. et al. Intrahepatic Activation of Naive CD4+ T Cells by Liver-Resident Phagocytic Cells. The Journal of Immunology 2014;193(5):2087-2095.

Tetri, L. H. et al. Severe NAFLD with hepatic necroinflammatory changes in mice fed trans fats and a high-fructose corn syrup equivalent. American Journal of Physiology-Gastrointestinal and Liver Physiology 2008;295(5):G987-G995.

Thelen, M., and Stein, J. V. How chemokines invite leukocytes to dance. Nature immunology 2008;9:953-959.

Tiegs, G., Hentschel, J., and Wendel, A. AT cell-dependent experimental liver injury in mice inducible by concanavalin A. Journal of Clinical Investigation 1992

Tiegs, G., and Lohse, A. W. Immune tolerance: what is unique about the liver. Journal of autoimmunity 2010;34(1):1-6.

Tuncer, C. et al. The regulation of T-cell recruitment to the human liver during acute liver failure. Liver International 2013;33(6):852-863.

Unutmaz, D. et al. The primate lentiviral receptor Bonzo/STRL33 is coordinately regulated with CCR5 and its expression pattern is conserved between human and mouse. The Journal of Immunology 2000;165(6):3284.

Urashima, S. et al. Studies on capillarization of the hepatic sinusoids in alcoholic liver disease. Alcohol Alcohol Suppl 1993;1B:77-84.

Vernon, G., Baranova, A., and Younossi, Z. M. Systematic review: the epidemiology and natural history of non-alcoholic fatty liver disease and non-alcoholic steatohepatitis in adults. Alimentary pharmacology & therapeutics 2011;34(3):274-285.

Vivier, E. et al. Functions of natural killer cells. Nature immunology 2008;9(5):503-510.

Wehr, A. et al. Chemokine Receptor CXCR6-Dependent Hepatic NK T Cell Accumulation Promotes Inflammation and Liver Fibrosis. Journal of Immunology 2013

Wehr, A. et al. Pharmacological Inhibition of the Chemokine CXCL16 Diminishes Liver Macrophage Infiltration and Steatohepatitis in Chronic Hepatic Injury. PloS one 2014

Weisberg, S. P. et al. CCR2 modulates inflammatory and metabolic effects of high-fat feeding. Journal of Clinical Investigation 2006;116(1):115-124.

Wentworth, J. M. et al. Pro-inflammatory CD11c+CD206+ adipose tissue macrophages are associated with insulin resistance in human obesity. Diabetes 2010;59(7):1648-1656.

Whittaker, S., Marais, R., and Zhu, A. X. The role of signaling pathways in the development and treatment of hepatocellular carcinoma. Oncogene 2010;29(36):4989-5005.

Williams, C. D. et al. Prevalence of nonalcoholic fatty liver disease and nonalcoholic steatohepatitis among a largely middle-aged population utilizing ultrasound and liver biopsy: a prospective study. Gastroenterology 2011;140(1):124-131.

Williams, R. et al. Addressing liver disease in the UK: a blueprint for attaining excellence in health care and reducing premature mortality from lifestyle issues of excess consumption of alcohol, obesity, and viral hepatitis. The Lancet 2014;384(9958):1953-1997.

Xu, B. et al. Capillarization of hepatic sinusoid by liver endothelial cell-reactive autoantibodies in patients with cirrhosis and chronic hepatitis. Am J Pathol 2003;163(4):1275-1289.

Xu, H. et al. Involvement of up-regulated CXC chemokine ligand 16/scavenger receptor that binds phosphatidylserine and oxidized lipoprotein in endotoxin-induced lethal liver injury via regulation of T-cell recruitment and adhesion. Infection and immunity 2005;73(7):4007.

Yang, S. J. et al. Inhibition of the chemokine (C–C motif) ligand 2/chemokine (C–C motif) receptor 2 pathway attenuates hyperglycaemia and inflammation in a mouse model of hepatic steatosis and lipoatrophy. Diabetologia 2009;52(5):972-981.

Yona, S. et al. Fate mapping reveals origins and dynamics of monocytes and tissue macrophages under homeostasis. Immunity 2013;38(1):79-91.

Zaballos, A. et al. Cutting edge: identification of the orphan chemokine receptor GPR-9-6 as CCR9, the receptor for the chemokine TECK. The Journal of Immunology 1999;162(10):5671-5675.

Ziegler-Heitbrock, L., Ancuta, P., and Crowe, S. Nomenclature of monocytes and dendritic cells in blood. Blood 2010;116 (16):74-80.

Zimmermann, H. W. et al. Bidirectional transendothelial migration of monocytes across hepatic sinusoidal endothelium shapes monocyte differentiation and regulates the balance between immunity and tolerance in liver. Hepatology 2015

Zlotnik, A., and Yoshie, O. Chemokines: A New Classification Review System and Their Role in Immunity. Immunity 2000;12:121-127.

Zlotnik, A., Yoshie, O., and Nomiyama, H. The chemokine and chemokine receptor superfamilies and their molecular evolution. Genome biology 2006;7(12):243.